

# Supporting Information

## Impact of the acceptor units on optoelectronic and photovoltaic properties of (XDADAD)<sub>n</sub>-type copolymers: computational and experimental study

Irina V. Klimovich,<sup>a,b</sup> Fedor A. Prudnov,<sup>b</sup> Olga Mazaleva,<sup>a</sup> Nikita V. Tukachev,<sup>a</sup> Alexander V. Akkuratov,<sup>b</sup> Ilya V. Martynov,<sup>b</sup> Alexander S. Peregudov,<sup>c</sup> Alexander F. Shestakov,<sup>b</sup> Andriy Zhugayevych<sup>a</sup> and Pavel A. Troshin<sup>a,b</sup>

a. Skolkovo Institute of Science and Technology, Bolshoy Boulevard 30, bld. 1, Moscow, Russian Federation 121205;

b. Institute of Problems of Chemical Physics of Russian Academy of Sciences Academician Semenov avenue 1, Chernogolovka, Moscow region, Russian Federation 142432;

c. A.N.Nesmeyanov Institute of Organoelement Compounds of Russian Academy of Sciences, Vavilova St. 28, Moscow, Russian Federation 119991

## Contents

Extended computational details .....	4
The calculation of optical bandgap .....	4
Calculation of ionization potential and electron affinity .....	5
Figure S1. Highest occupied molecular orbitals (HOMO) for a set of P1-P10 conjugated polymers in vacuum .....	6
Figure S2. Lowest vacant molecular orbitals (LUMO) for a set of P1-P10 conjugated polymers in vacuum .....	7
Figure S3. Correlation between the vertical transition energy to the lowest excited singlet electronic state (CAM-B3LYP/6-31G*) and optical absorption energy .....	8
Figure S4. Correlations between the HOMO-LUMO gap (a) and vertical transition energy to the lowest excited singlet electronic state (b) in chloroform (CPCM solvation model) and in vacuum .....	9
Figure S5. Correlation plot between calculated (HOMO energy, ionization potential both in vacuum and in solution) and measured (cyclic voltammetry, photoelectron spectroscopy in air) ionization potential for P1-P10 polymers. ....	10
Figure S6. Comparison of calculated ionization potential (IP) and electron affinity (EA) using different calculation schemes (P1-P10 polymers). ....	11

Figure S7. Four types of oligomers used in calculations are illustrated here for P9 system.....	12
Figure S8. Electronic absorption spectra for different fragments of P1-P10 conjugated polymers computed by TD-DFT CAM-B3LYP/6-31G* in vacuum.....	13
Table S1. PCE parameters: measurements and analysis (extended version of Table 2 in the main text). .....	14
Table S2. Experimental and calculated (CAM-B3LYP /6-31G* for different oligomers) absolute values of energy gap and frontier orbital energies.....	15
Table S3. Experimental and calculated (CAM-B3LYP /6-31G* for different oligomers) trends for energy gap and frontier orbital energies.....	16
Table S4. Conformational properties of dimers of acceptor unit andthiophene calculated by CAM-B3LYP/6-31G*. .....	17
Figure S9. HOMO energy levels estimated by CV and calculated values.....	18
Figure S10. Comparison of HOMO and LUMO with hole and electron NTOs for longer oligomer of P2 polymer.....	19
Figure S11. LMO interaction diagram for possible interconnections between the building blocks.....	20
Figure S12. Some important LMOs sampled in the P1 polymer.....	21
Table S5. MO energies and electronic couplings between MOs participating in intramolecular charge transfer for P1-10 systems for occupied orbitals of acceptor unit and adjacent thiophene units.....	22
Figure S13. Hole NTOs computed for a set of similar oligomers.....	23
Figure S14. <sup>1</sup> H NMR spectrum of <b>A3</b> .....	24
Figure S15. <sup>13</sup> C NMR spectrum of <b>A3</b> .....	25
Figure S16. <sup>1</sup> H NMR spectrum of <b>B3</b> .....	26
Figure S17. <sup>13</sup> C NMR spectrum of <b>B3</b> .....	27
Figure S18. <sup>1</sup> H NMR spectrum of <b>C3</b> .....	28
Figure S19. <sup>13</sup> C NMR spectrum of <b>C3</b> .....	29
Figure S20. <sup>1</sup> H NMR spectrum of <b>D3</b> .....	30
Figure S21. <sup>13</sup> C NMR spectrum of <b>D3</b> .....	31
Figure S22. <sup>1</sup> H NMR spectrum of <b>A4</b> .....	32
Figure S23. <sup>13</sup> C NMR spectrum of <b>A4</b> .....	33
Figure S24. <sup>1</sup> H NMR spectrum of <b>B4</b> .....	34
Figure S25. <sup>13</sup> C NMR spectrum of <b>B4</b> .....	35
Figure S26. <sup>1</sup> H NMR spectrum of <b>C4</b> .....	36
Figure S27. <sup>13</sup> C NMR spectrum of <b>C4</b> .....	37

Figure S28. $^1\text{H}$ NMR spectrum of <b>D4</b> .....	38
Figure S29. $^{13}\text{C}$ NMR spectrum of <b>D4</b> .....	39
Figure S30. $^1\text{H}$ NMR spectrum of <b>A5</b> .....	40
Figure S31. $^{13}\text{C}$ NMR spectrum of <b>A5</b> .....	41
Figure S32. $^1\text{H}$ NMR spectrum of <b>B5</b> .....	42
Figure S33. $^{13}\text{C}$ NMR spectrum of <b>B5</b> .....	43
Figure S34. $^1\text{H}$ NMR spectrum of <b>C5</b> .....	44
Figure S35. $^{13}\text{C}$ NMR spectrum of <b>C5</b> .....	45
Figure S36. $^1\text{H}$ NMR spectrum of <b>D5</b> .....	46
Figure S37. $^{13}\text{C}$ NMR spectrum of <b>D5</b> .....	47
Figure S38. $^1\text{H}$ NMR spectrum of <b>C6</b> .....	48
Figure S39. $^{13}\text{C}$ NMR spectrum of <b>C6</b> .....	49
Figure S40. $^1\text{H}$ NMR spectrum of <b>D6</b> .....	50
Figure S41. $^{13}\text{C}$ NMR spectrum of <b>D6</b> .....	51
Figure S42. $^1\text{H}$ NMR spectrum of <b>A7</b> .....	52
Figure S43. $^1\text{H}$ NMR spectrum of <b>B7</b> .....	54
Figure S44. $^{13}\text{C}$ NMR spectrum of <b>B7</b> .....	54
Figure S45. $^1\text{H}$ NMR spectrum of <b>C7</b> .....	55
Figure S46. $^{13}\text{C}$ NMR spectrum of <b>C7</b> .....	56
Figure S47. $^1\text{H}$ NMR spectrum of <b>D7</b> .....	57
Figure S48. $^{13}\text{C}$ NMR spectrum of <b>D7</b> .....	58
Figure S49. $^1\text{H}$ NMR spectrum of <b>A8</b> .....	59
Figure S50. $^1\text{H}$ NMR spectrum of <b>B8</b> .....	60
Figure S51. $^{13}\text{C}$ NMR spectrum of <b>B8</b> .....	61
Figure S52. $^1\text{H}$ NMR spectrum of <b>C8</b> .....	62
Figure S53. $^{13}\text{C}$ NMR spectrum of <b>C8</b> .....	63
Figure S54. $^1\text{H}$ NMR spectrum of <b>D8</b> .....	64
Figure S55. $^{13}\text{C}$ NMR spectrum of <b>D8</b> .....	65
<b>Figure S56.</b> IR spectrum of <b>A6</b> .....	66
<b>Figure S57.</b> MS spectrum of <b>A6</b> .....	67
<b>Figure S58.</b> IR spectrum of <b>A7</b> .....	68

## **Extended computational details**

To minimize conformational uncertainty compared to excitation energy for different polymers, the main set of calculations is performed for oligomers with planar conjugated backbone. Keeping planarity for oligomers **P7-8** during geometry optimization was non-trivial. In order to keep the nuclei of molecular backbone in plane, allowing all other parts to move freely, Z-matrix representation of molecular geometry was used:

- Firstly, the structure of oligomer without any "deplanarizing" substituents was optimized.
- Then, by means of either molecular editor (i.e. Avogadro) tools or script, these substituents were added to planar structure.
- Finally, in Gaussian job involving geometry optimization, Z-matrix representation for previously obtained structure with all the dihedrals equal strictly to 0 or 180 degrees fixed was used.

## **The calculation of optical bandgap**

The main idea behind the theoretical part of present investigation was to find out whether linear correlations for two molecular descriptors, e.g. experimentally measured optical absorption energy and ionizaton potential and its theoretical counterparts, could be established (at least, for this series of similar polymers with different acceptor unit). Indeed, using the approach described in Computational Details section of the article, we succeeded, as shown on Figure 3 and Figs. S1-S2, to correctly reproduce experimentally observed trends for energy gap (Table S3). Solid correlations for experimental results and HOMO-LUMO differences (DFT) as well as vertical transition energies (TD DFT) have been obtained.

Since it is known that natural transition orbitals (NTOs) give the best representation of a single-electron transition density matrix in terms of molecular orbitals, irrespective of the quantum chemistry method used, we would like to compare HOMO/LUMO energies computed for our systems with corresponding NTOs for  $S_0$ - $S_1$  transition. NTOs for **P2** polymer fragment are presented on Fig. 5 as an example. They are very similar to frontier orbitals (Fig.S5-S6), supporting the idea that  $S_0$ - $S_1$  electronic transition for investigated polymers could indeed be understood in terms of just frontier orbitals.

### **Calculation of ionization potential and electron affinity**

One can note that the difference for IP of **P7** and **P8** structures obtained by means of cyclic voltammetry is equal to 0.11 eV, while in our computational procedure they are treated as effectively the same (since, according to Fig. S5-S6, HOMO and LUMO orbitals are localized mainly on the conduction backbone, OR substituents should probably not influence IP and EA considerably).

Both experimentally and theoretically predicted values of IP are quite similar for different systems under consideration, especially in comparison with bandgaps (Fig. S3, Table S2). These variations in IP obtained by either CV or PESA could be comparable to experimental errors. Thus, in order to establish a linear correlation using our computational approach, we believe that polymer series with larger differences in IP should be studied. Alternatively, more sophisticated and computationally demanding theoretical schemes (i.e. those taking into account of not only electrostatic effects on intermolecular interactions) could be tried to reproduce experimental values. Calculated values for ionization potential and electron affinity show good correlation with HOMO and LUMO energies for the polymer fragments under consideration (Fig.S4); moreover, trends for the larger fragments correspond to shorter well-centered ones.

Figure S1. Highest occupied molecular orbitals (HOMO) for a set of P1-P10 conjugated polymers in vacuum.

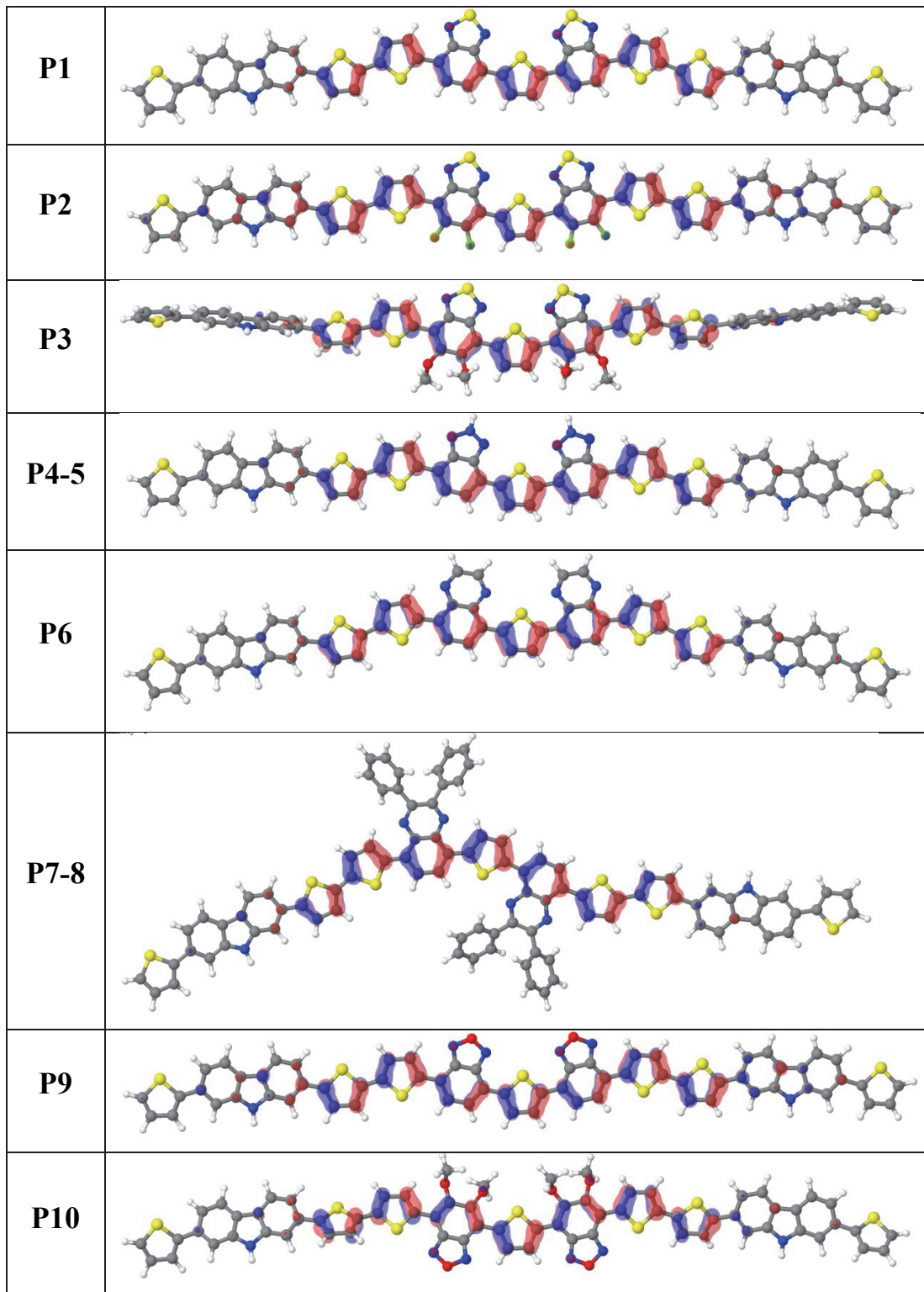
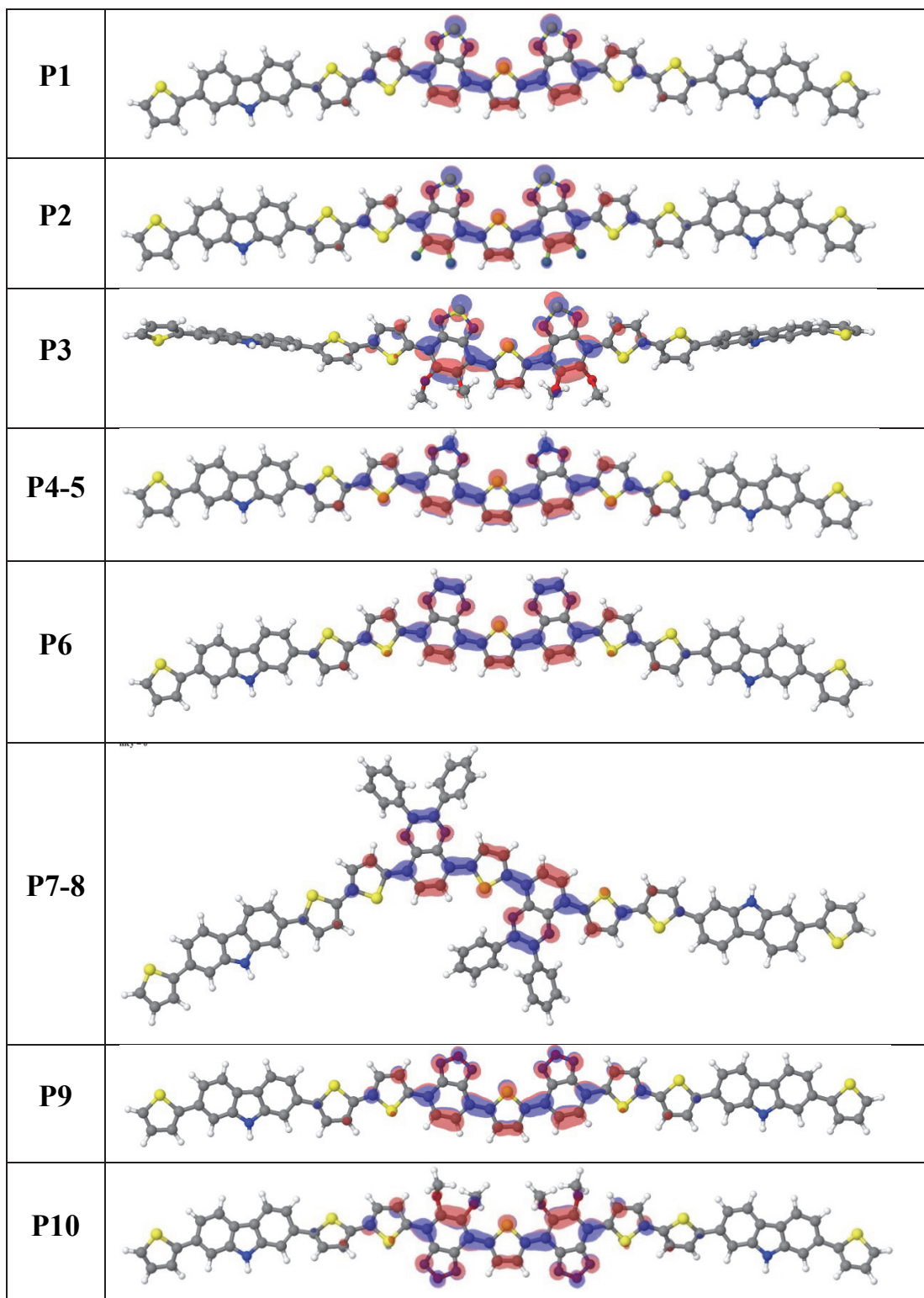


Figure S2. Lowest vacant molecular orbitals (LUMO) for a set of P1-P10 conjugated polymers in vacuum.



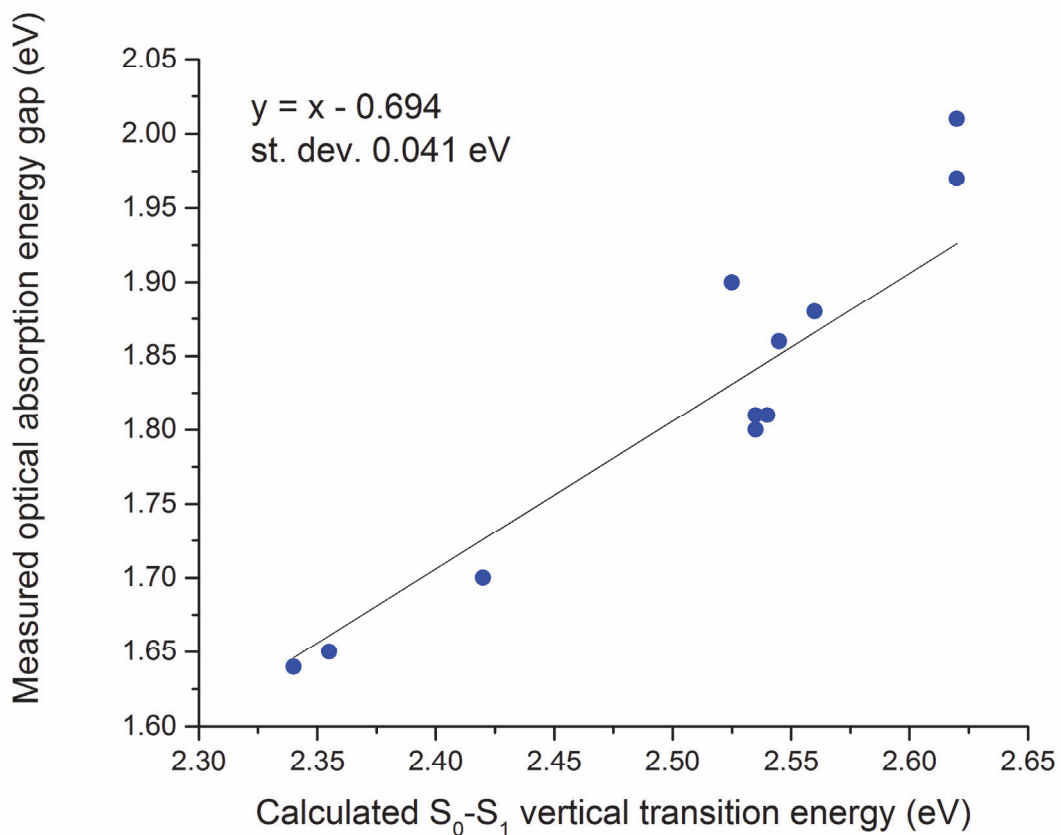


Figure S3. Correlation between the vertical transition energy to the lowest excited singlet electronic state (CAM-B3LYP/6-31G\*) and optical absorption energy. Blue dots correspond to data for different polymers (P1-P10 and PCDTBT); solid black line is a linear fit with a constraint (slope must be equal to 1) for this data set. Linear regression equation, as well as standard deviation, are given in the top-left corner.

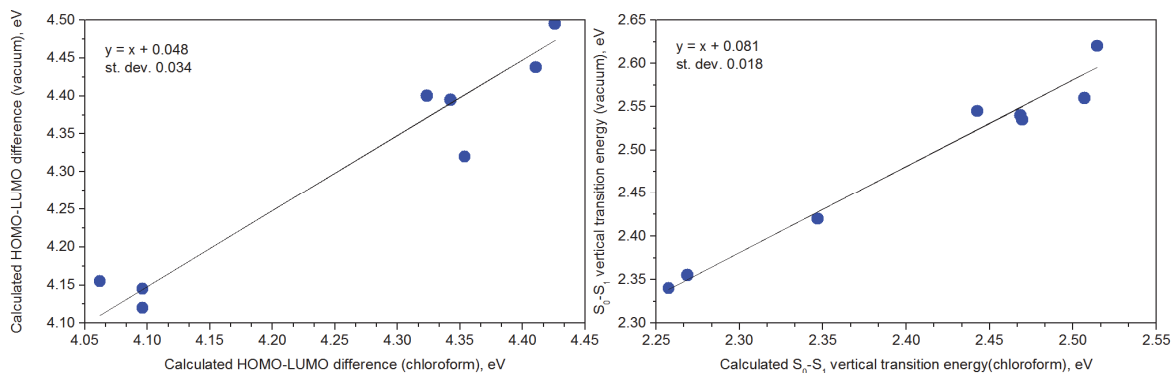


Figure S4. Correlations between the HOMO-LUMO gap (a) and vertical transition energy to the lowest excited singlet electronic state (b) in chloroform (CPCM solvation model) and in vacuum. Blue dots correspond to data for different polymers (**P1-P10**); solid black line is a linear fit with a constraint (slope must be equal to 1) for this data set. Linear regression equations, as well as standard deviations, are given in the top-left corner.

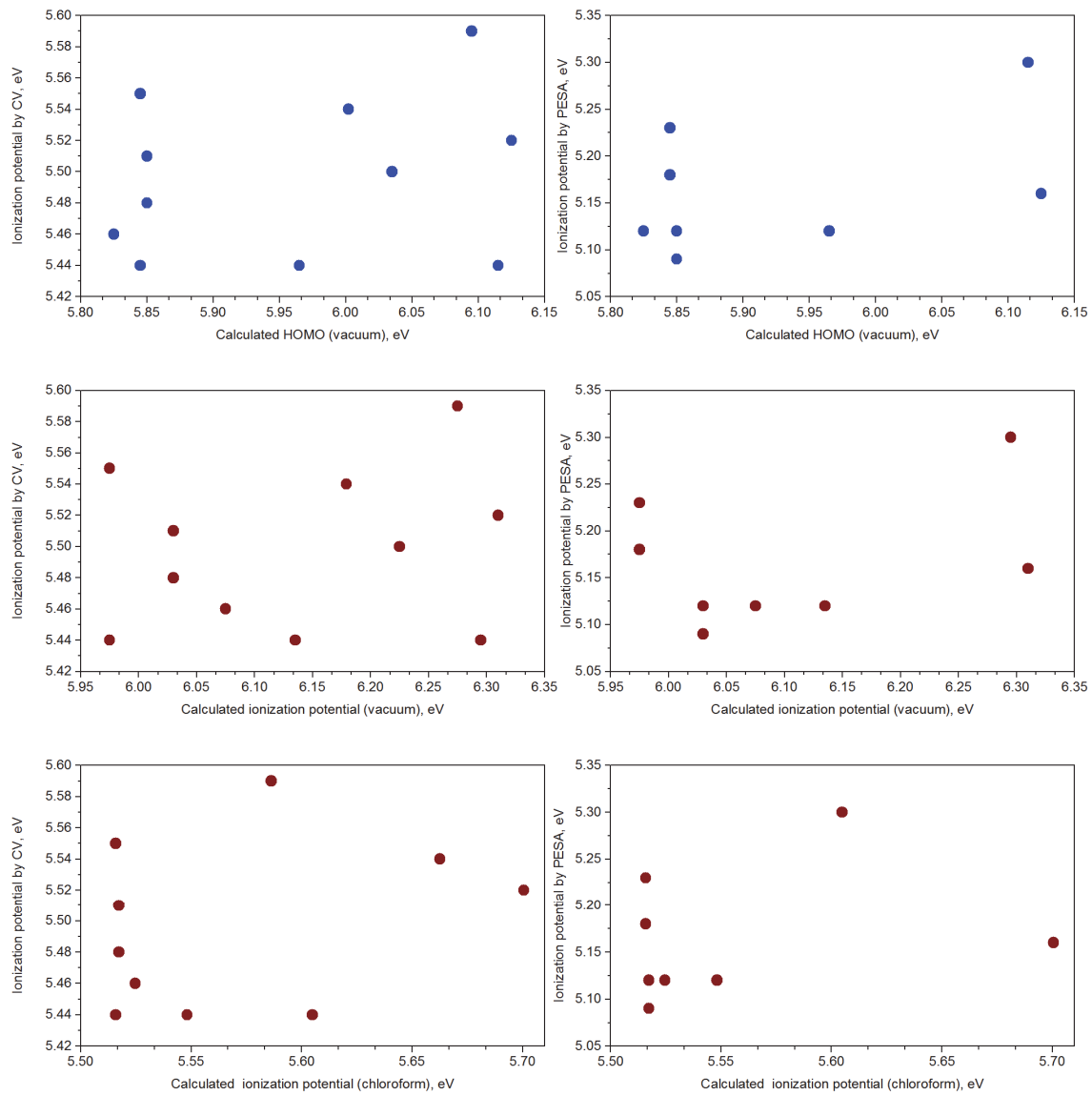
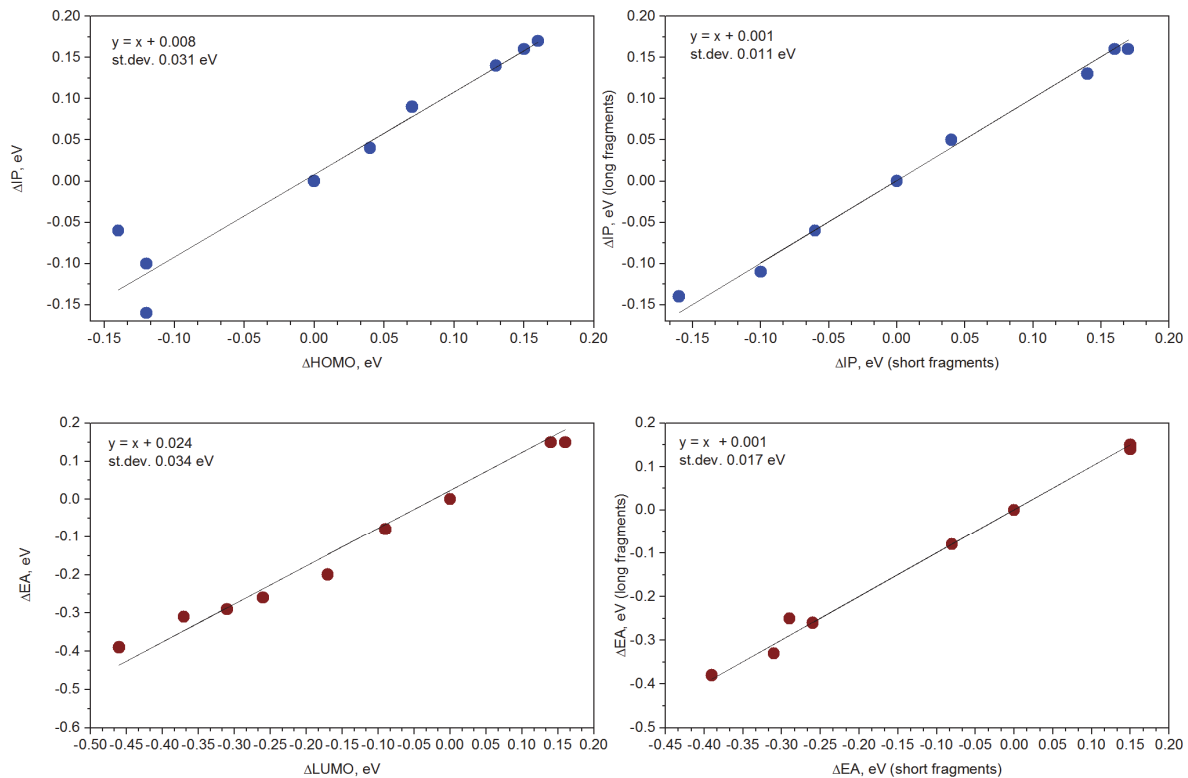


Figure S5. Correlation plot between calculated (HOMO energy, ionization potential both in vacuum and in solution) and measured (cyclic voltammetry, photoelectron spectroscopy in air) ionization potential for P1-P10 polymers. Note that experimental PESA data for **P2-3** are not available.

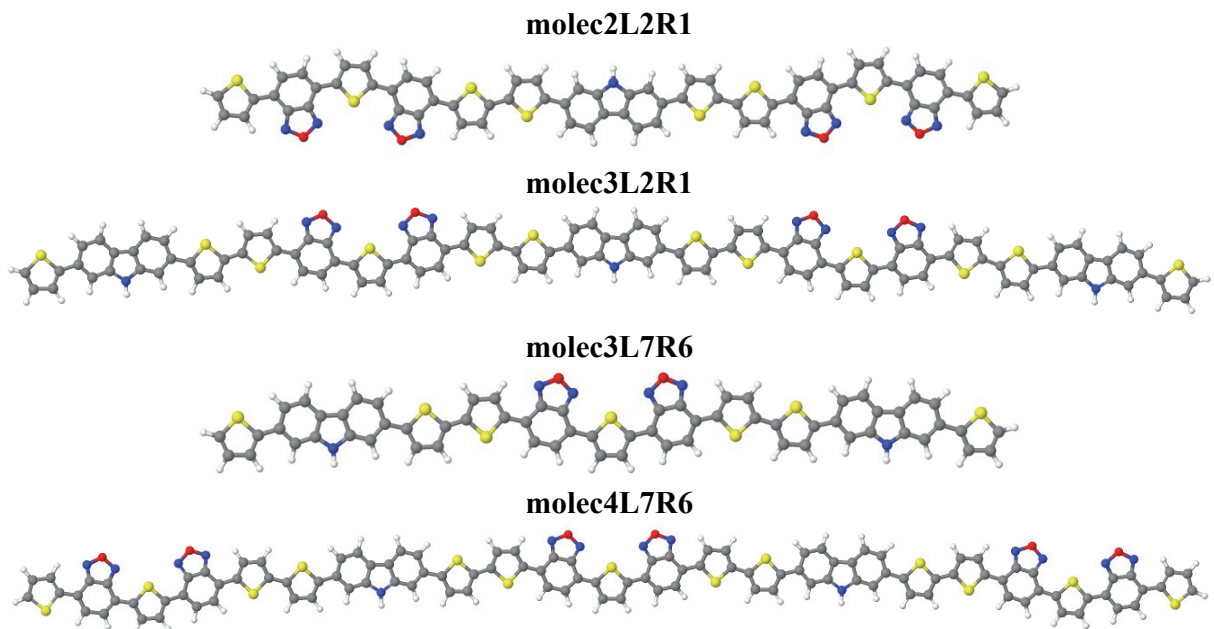


**Figure S6.** Comparison of calculated ionization potential (IP) and electron affinity (EA) using different calculation schemes (P1-P10 polymers). **P1** was chosen as a reference system.

In this work we aimed to predict not absolute values of bandgap, IP and EA of investigated polymers, but rather *relative quantities* for these values. Thus, for some quantity X,  $\Delta X = X(\text{Pn}) - X(\text{P0})$ .

IP could be evaluated as either HOMO energy or by definition as a energy difference between cation and neutral molecule; same for EA. Two plots on the left show the discrepancy between these two ways to estimate IP and EA. Two plots on the right show the discrepancy for IP and EA estimated for oligomers of different length (see Fig. S7 below).

Figure S7. Four types of oligomers used in calculations are illustrated here for P9 system. Since conjugation length in real conjugated polymers is relatively (compared to molecule size) small, modeling of electronic properties of a polymer calculating them for oligomer of sufficient size is used. In order to verify how these properties correlate with the length of the fragment used we made calculations for oligomers of different length. "Short" is referred to oligomers containing 15 aromatic rings - molec2L2R1 ("donor"-centered) and molec3L7R6 ("acceptor"-centered); "long" is for oligomers containing 25 aromatic rings.



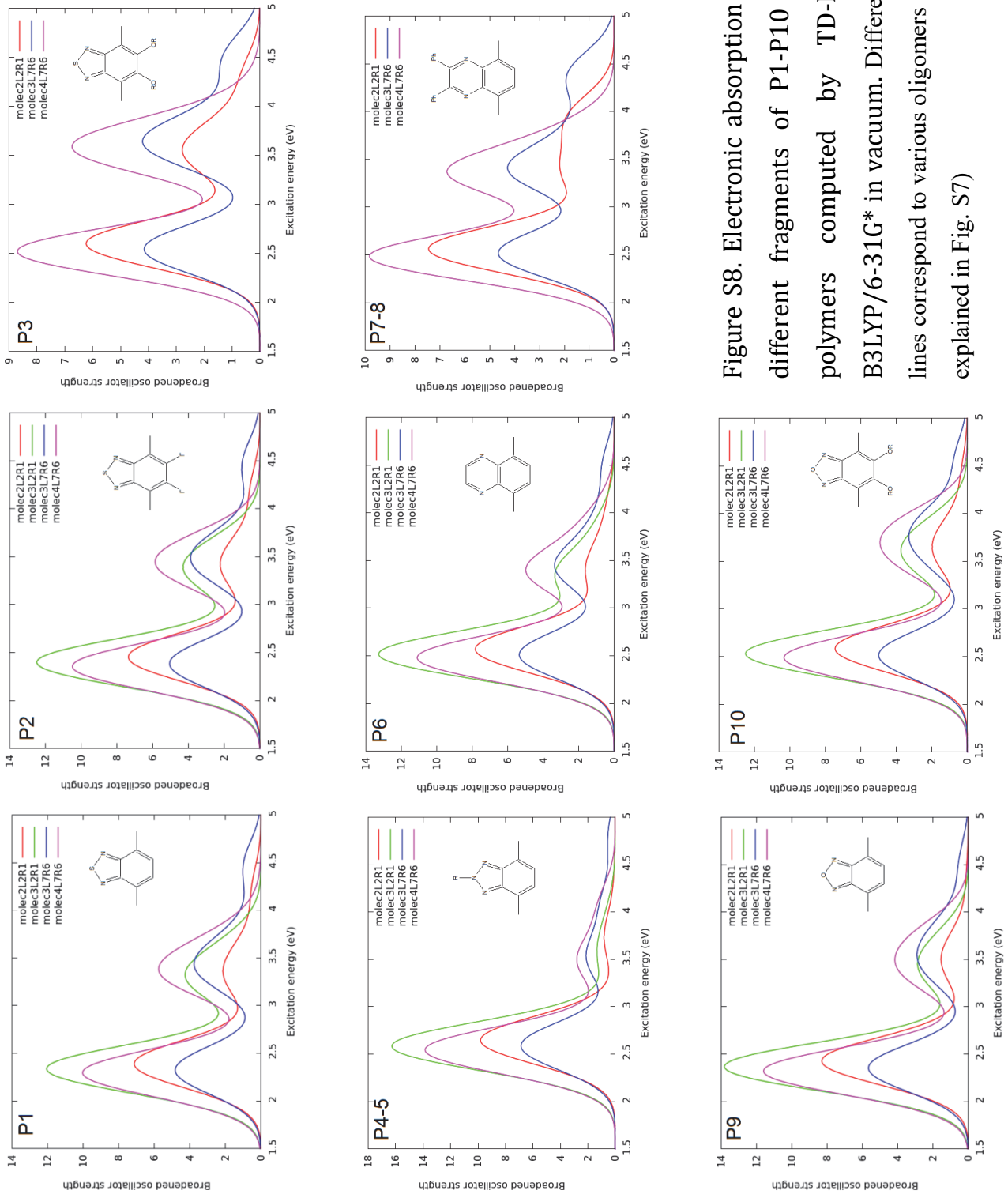


**Figure S8.** Electronic absorption spectra for different fragments of P1-P10 conjugated polymers computed by TD-DFT CAM-B3LYP/6-31G\* in vacuum. Differently coloured lines correspond to various oligomers (notations are explained in Fig. S7)

**Table S1. PCE parameters: measurements and analysis (extended version of Table 2 in the main text).**

Voc stands for open circuit voltage, Jsc - short circuit current, FF- field factor, PCE - power conversion efficiency,  $\lambda_{\max}(\text{sol})$  - absorption maximum for a polymer in solution. All these data are experimental and given here for comparison (corresponding cells in the table are coloured by gray). Analyzing different cells it could be convenient to compare not only absolute values, but also meaningful relative quantities: voltage loss -  $V_{\text{OC}}/E_{\text{gap}}$ , current loss  $J_{\text{SC}}/J_{\text{SC}}^{\max}$  where  $J_{\text{SC}}^{\max} = P_{\max} / E_g$ , and energy loss  $\text{PCE}_{\max} = P_{\max} / P_{\text{inc}}$ , where  $P_{\text{inc}}$  is an incident power derived from solar spectrum and  $P_{\max}$  is a power estimated in approximation that all light below bandgap is absorbed (too simplistic approximation compared to Shockley and Queisser theory that could however be used as a descriptor to rank different cells). The difference LUMO(acceptor) - LUMO(donor) is frequently used as a descriptor for intermolecular charge transfer probability between donor (Pn) and acceptor (PCBM, hence LUMO(acceptor) $\approx 4.15$ ) molecules.

	PCE <sub>max</sub>	PCE	V <sub>oc</sub>	V <sub>OC</sub> /E <sub>gap</sub>	J <sub>SC</sub>	J <sub>SC</sub> /J <sub>SC</sub> <sup>max</sup>	FF	4.15-LUMO,	$\lambda_{\max}(\text{sol})$
<b>units</b>	%	%	V	%	mA/cm <sup>2</sup>	%	%	eV	nm
<b>P1</b>	40	6.4	0.775	47	13.6	57	62	0.36	610
<b>P2</b>	38	5.2	0.743	44	11.4	51	61	0.26	n/a
<b>P3</b>	34	2.6	0.8	43	7.6	41	43	0.49	n/a
<b>P4</b>	29	1.6	0.651	32	3.6	25	33	0.68	480
<b>P5</b>	30	1.8	0.655	33	3.2	21	38	0.67	492
<b>P6</b>	35	3.6	0.717	40	11.2	58	45	0.5	570
<b>P7</b>	35	3.3	0.846	47	8.5	44	45	0.52	550
<b>P8</b>	35	4.9	0.802	45	11.4	58	53	0.41	567
<b>P9</b>	40	4.9	0.8	49	12.6	52	49	0.35	634
<b>P10</b>	34	5.5	0.862	46	10.7	59	59	0.46	571

Table S2. Experimental and calculated (CAM-B3LYP /6-31G\* for different oligomers) absolute values of energy gap and frontier orbital energies.

	$E_{gap\ opt\ exp}$ , eV	$E(S_0-S_1)$ calc	$HOMO_{exp}$ , eV	$HOMO_{calc}$ , eV	$IP_{calc\ in\ vac}$ , eV	$V_{OC}$ , mV	$LUMO_{exp}$ , eV	$LUMO_{calc}$ , eV	$EA_{calc\ in}$ vac
<b>P1</b>	1.65	2.32-2.39	5.44	5.95-5.98	6.11-6.16	775	3.79	1.81-1.83	1.63-1.66
<b>P2</b>	1.7	2.38-2.45	5.59	6.09-6.10	6.27-6.28	743	3.89	1.97-1.98	1.79-1.80
<b>P3</b>	1.88	2.54-2.58	5.54	6.00	6.17-6.19	800	3.66	1.55-1.58	1.38-1.40
<b>P4</b>	2.01	2.59-2.65	5.48	5.84-5.86	6.01-6.05	650	3.47	1.33-1.38	1.21-1.29
<b>P5</b>	1.97	2.59-2.65	5.51	5.84-5.86	6.01-6.05	629	3.48	1.33-1.38	1.21-1.29
<b>P6</b>	1.81	2.51-2.57	5.46	5.75-5.90	6.06-6.09	717	3.65	1.49-1.52	1.35-1.37
<b>P7</b>	1.81	2.51-2.56	5.44	5.84-5.85	5.95-6.00	846	3.63	1.43-1.47	1.30-1.37
<b>P8</b>	1.8	2.51-2.56	5.55	5.84-5.85	5.95-6.00	802	3.74	1.43-1.47	1.30-1.37
<b>P9</b>	1.64	2.33-2.35	5.44	6.09-6.14	6.27-6.32	800	3.8	1.96	1.78-1.80
<b>P10</b>	1.86	2.51-2.58	5.52	6.11-6.14	6.29-6.33	862	3.69	1.71-1.74	1.55-1.59

$LUMO_{exp}$  was estimated as ( $E_{gap}$ - $HOMO_{exp}$ )

Table S3. Experimental and calculated (CAM-B3LYP /6-31G\* for different oligomers) trends for energy gap and frontier orbital energies. Here "solv" means that solvent (namely, chloroform) effects were taken into account using CPCM solvation model, whereas "vac" means that calculations were made for isolated molecule. In this work we aimed to predict not absolute values of bandgap, IP and EA of investigated polymers, but rather relative quantities for these values. Thus, for some quantity  $X$ ,  $\Delta X = X(Pn) - X(P0)$ .

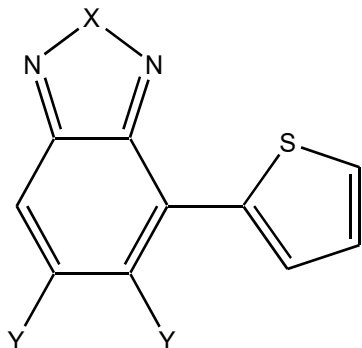
	$\Delta E_{\text{gap}}$	$\Delta E(S_0-S_1)$ , vac	$\Delta E(S_0-S_1)$ , solv	$\Delta HOMO$ , CV	$\Delta HOMO$ , vac	$\Delta IP$ , vac	$\Delta IP$ , solv (exp)	$\Delta LUMO$ , vac	$\Delta LUMO$ , vac	$\Delta EA$ , vac
<b>P1</b>	0	0	0	0	0	0	0	0	0	0
<b>P2</b>	0.05	0.06(7)	0.08	0.15	0.13(1)	0.14(1)	0.04	0.10	0.16(1)	0.15(1)
<b>P3</b>	0.23	0.20(4)	0.24	0.10	0.04(0)	0.04(1)	0.11	-0.13	-0.26(4)	-0.26(2)
<b>P4</b>	0.36	0.27(6)	0.25	0.04	-0.12(2)	-0.10(4)	-0.03	-0.32	-0.46(3)	-0.39(5)
<b>P5</b>	0.32	0.27(6)	0.25	0.07	-0.12(2)	-0.10(4)	-0.03	-0.31	-0.46(3)	-0.39(5)
<b>P6</b>	0.16	0.19(6)	0.20	0.02	-0.14(9)	-0.06(4)	-0.02	-0.14	-0.31(2)	-0.29(2)
<b>P7</b>	0.16	0.18(5)	0.20	0	-0.12(1)	-0.16(5)	-0.03	-0.16	-0.37(4)	-0.31(7)
<b>P8</b>	0.15	0.18(5)	0.20	0.11	-0.12(1)	-0.16(5)	-0.03	-0.05	-0.37(4)	-0.31(7)
<b>P9</b>	-0.01	-0.02(4)	-0.01	0	0.15(4)	0.16(5)	0.06	0.01	0.14(1)	0.15(2)
<b>P10</b>	0.21	0.19(7)	0.17	0.08	0.16(3)	0.17(4)	0.15	-0.1	-0.09(2)	-0.08(3)

Table S4. Conformational properties of dimers of acceptor unit and thiophene calculated by CAM-B3LYP/6-31G\*. One can see that for all considered dimers the lowest energy conformer corresponds to planar conformation **II** except for the case with quinoxaline derivatives (**P6-P8**) for which DFT CAM-B3LYP calculations predict non-planar conformers with the one close to conformation **I** slightly lower in energy. However, corresponding planarization energies are quite low, i.e. these dimers are likely effectively planar at room temperature (because of the population of vibrational levels higher than the barrier to planar structure).

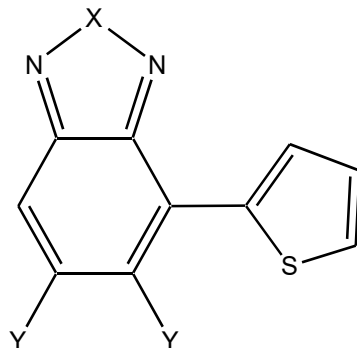
	Conformation I (dihedral = 0)		Conformation II (dihedral = 180)		$\Delta E$ (I - II)
	Dihedral (min)	E, meV (planarization)	Dihedral (min)	E, meV (planarization)	meV
P1	23	8	170	0	43
P2	0	0	180	0	27
P3	22	34	170	14	58
P4-5	25	7	180	0	49
P6-8	23	7	153	16	-24
P9	23	8	180	0	68
P10	21	30	173	11	95

Here, dihedral angles are in degrees.

Conformation I



Conformation II



P1: X = S, Y = H

P2: X = S, Y = F

P3: X = S, Y = OCH<sub>3</sub>

P4-5: X = NH, Y = H

P6-8: X = CH=CH, Y = H

P9: X = O, Y = H

P10: X = O, Y = OCH<sub>3</sub>

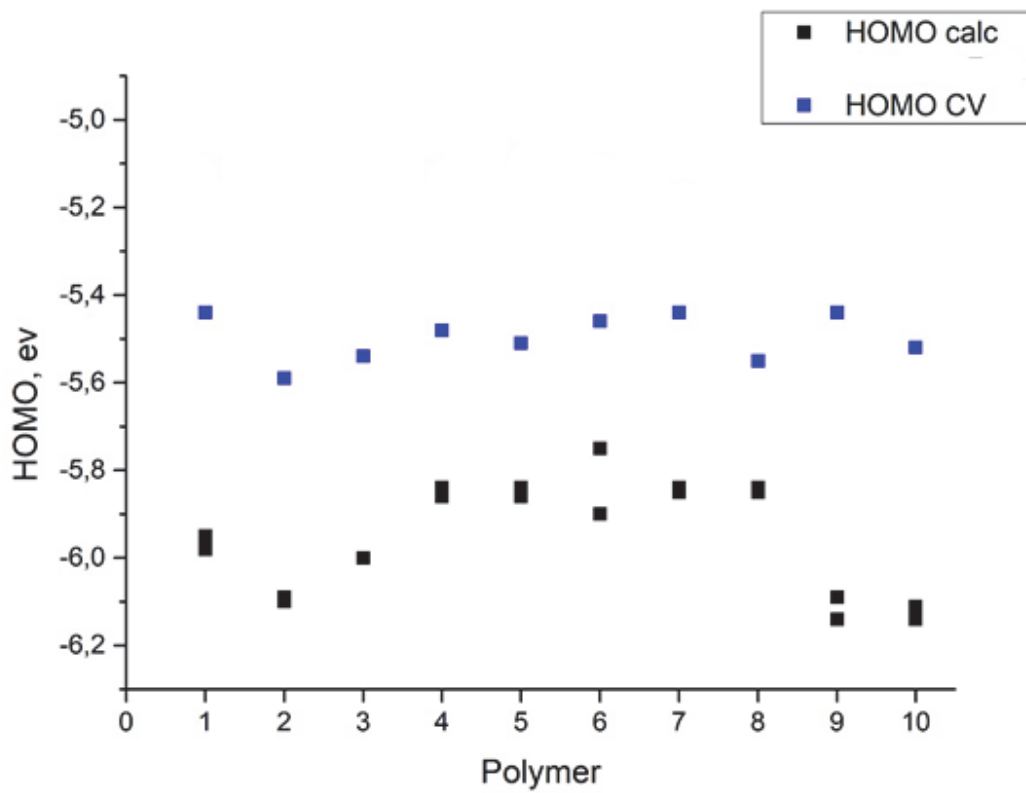


Figure S9. HOMO energy levels estimated by CV and calculated values.

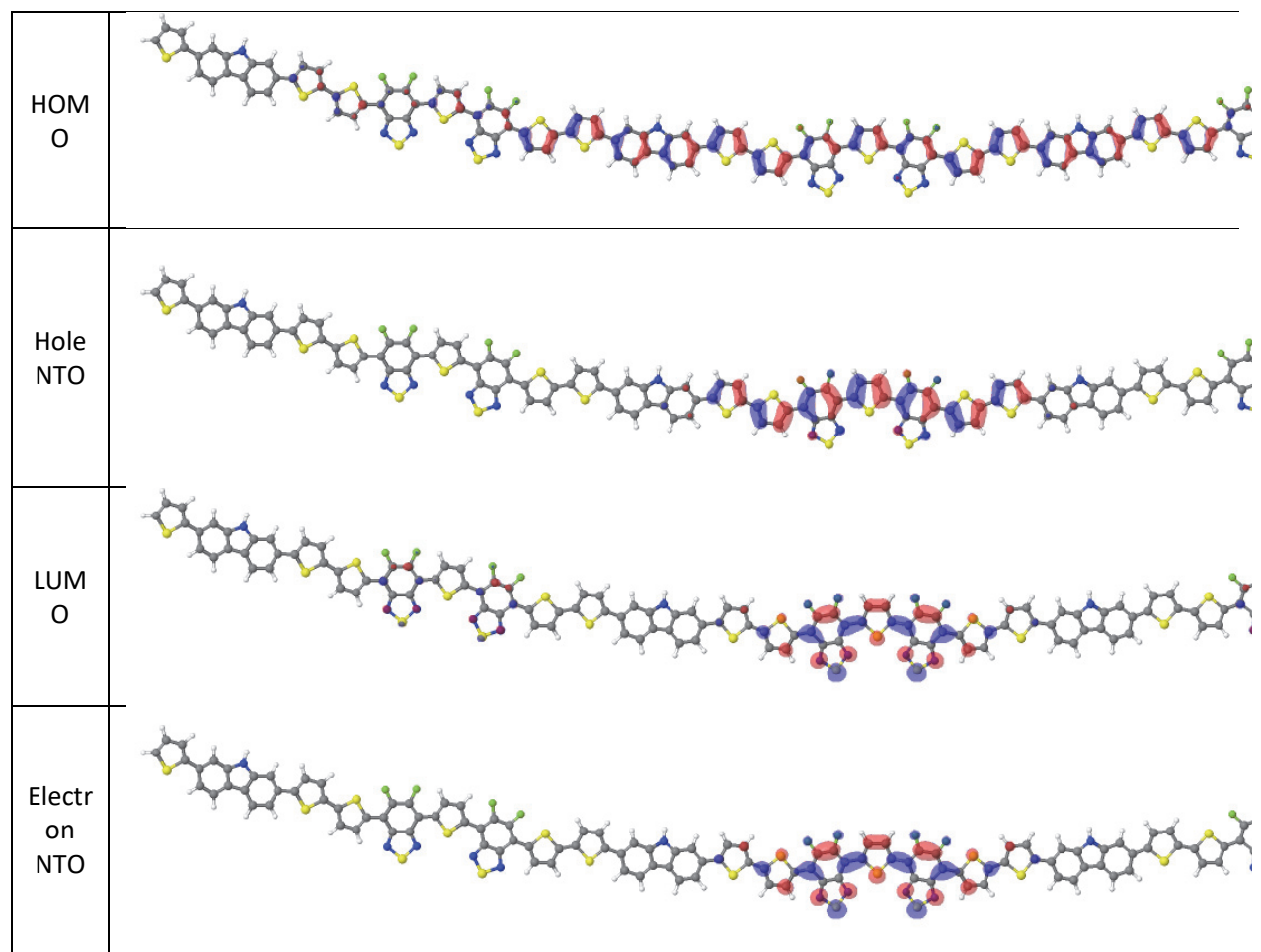


Figure S10. Comparison of HOMO and LUMO with hole and electron NTOs for longer oligomer of P2 polymer.

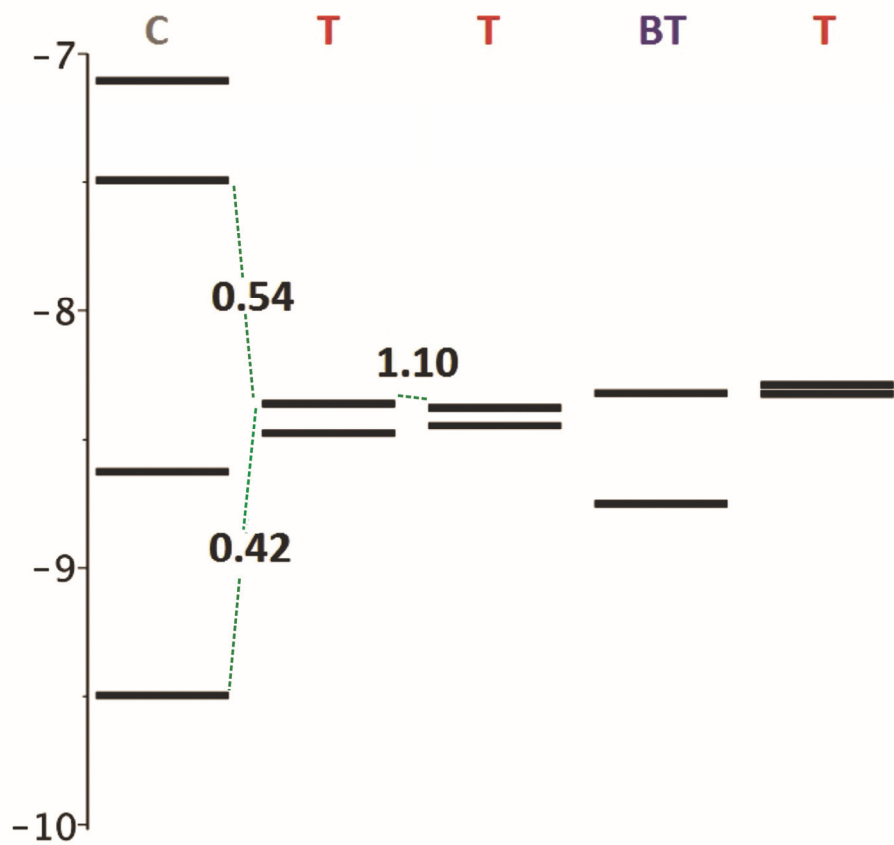


Figure S11. LMO interaction diagram for possible interconnections between the building blocks sampled in the P1 polymer ("C" stands for carbazole, "T" for thiophene, "BT" for benzothiadiazole units). Numbers indicate renormalized electronic couplings (in eV) for holes between orbitals facilitating intramolecular charge transfer (green puncture lines). Electronic coupling  $t$  between a pair of orbitals with energy difference  $\varepsilon$  are renormalized according to the formula  $t' = t \cdot \sqrt{1 - 1/\sqrt{1 + 4t^2/\varepsilon^2}}$ , which gives exact level shifts  $t'$  for the two-level system.

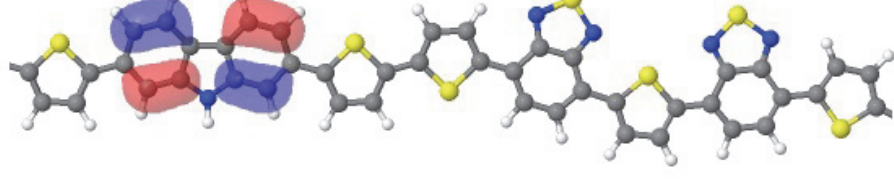
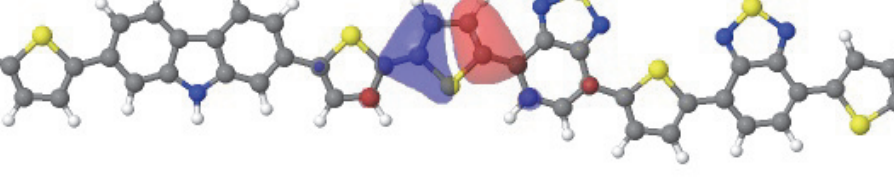
LMO energy, eV	LMO
-9.50	
-8.62	
-7.49	
-8.36	
-8.38	

Figure S12. Some important LMOs sampled in the P1 polymer.

Table S5. MO energies and electronic couplings between MOs participating in intramolecular charge transfer for P1-10 systems for occupied orbitals of acceptor unit and adjacent thiophene units.

polymer	MO energy, eV	LMO energy in polymer, eV	Electronic coupling	
<b>P1</b>	-8.02	-8.32	0.91	-0.88
<b>P2</b>	-8.37	-8.65	0.84	0.84
<b>P3</b>	-7.47	-8.22	0.82	0.67
<b>P4-5</b>	-7.66	-8.04	-0.85	-0.79
<b>P6-8</b>	-8.09	-8.43	0.89	0.88
<b>P9</b>	-8.28	-8.50	-0.88	-0.86
<b>P10</b>	-7.75	-8.43	0.85	0.79

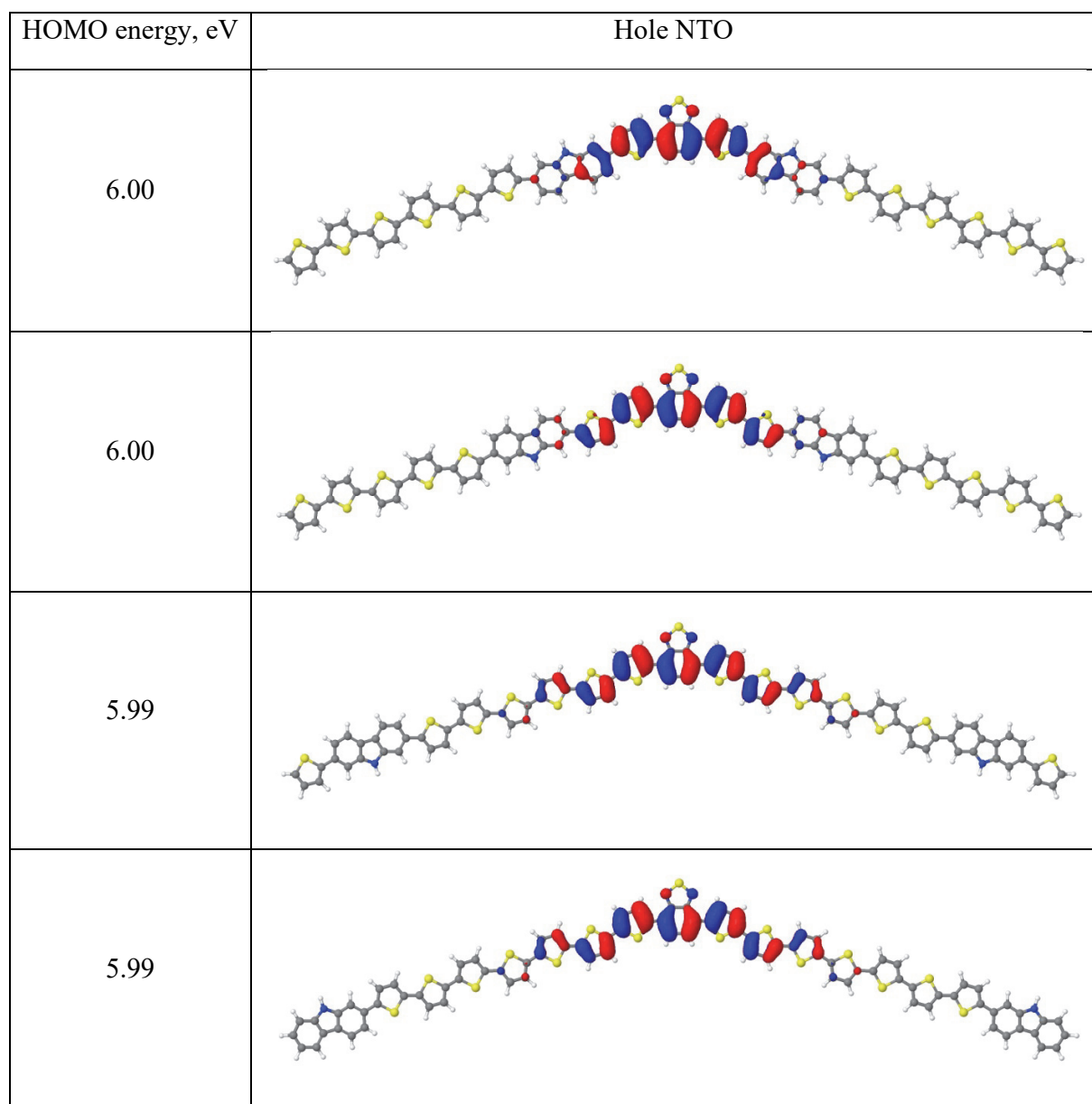


Figure S13. Hole NTOs computed for a set of similar oligomers.

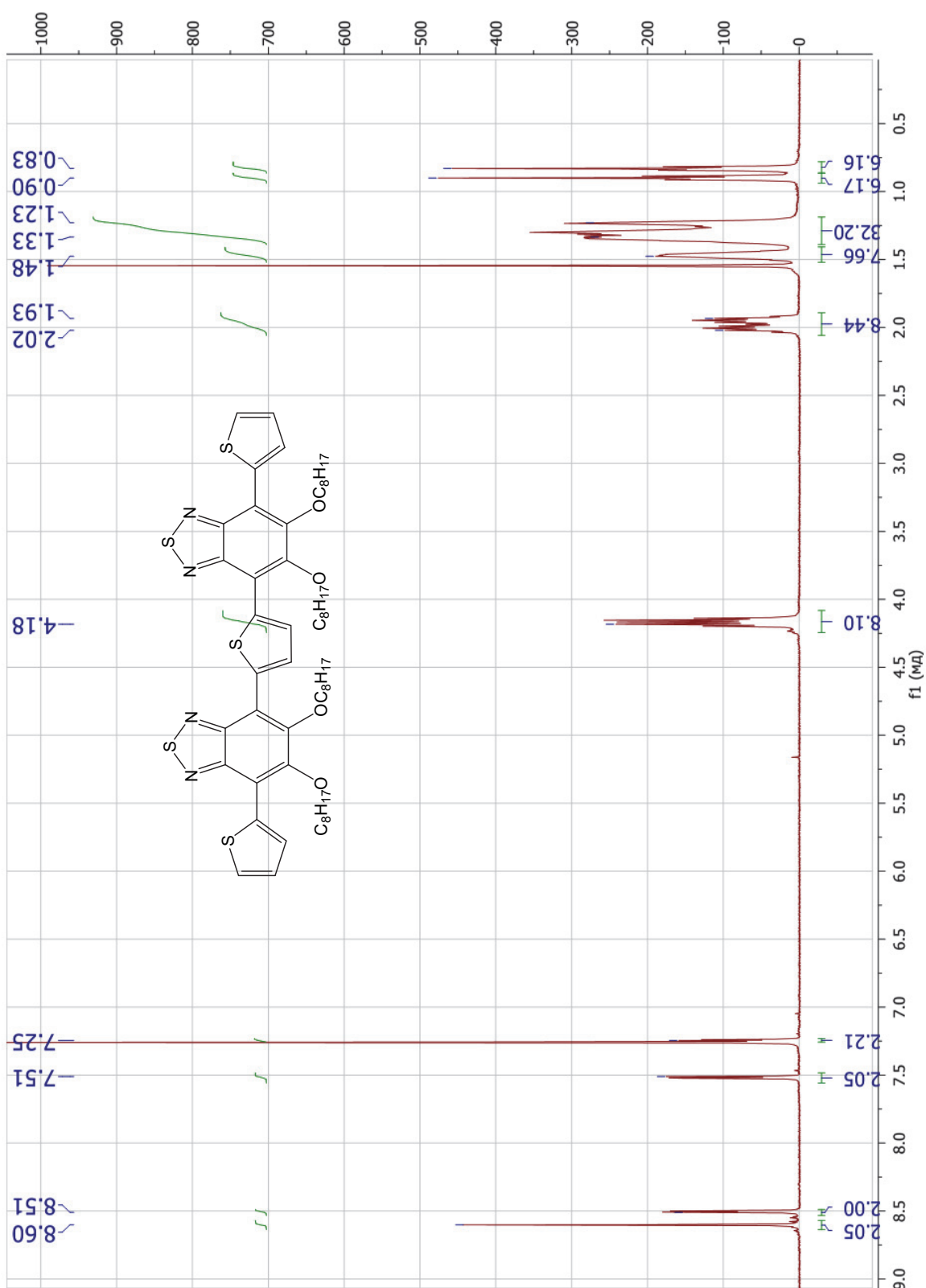


Figure S14.  $^1\text{H}$  NMR spectrum of A3

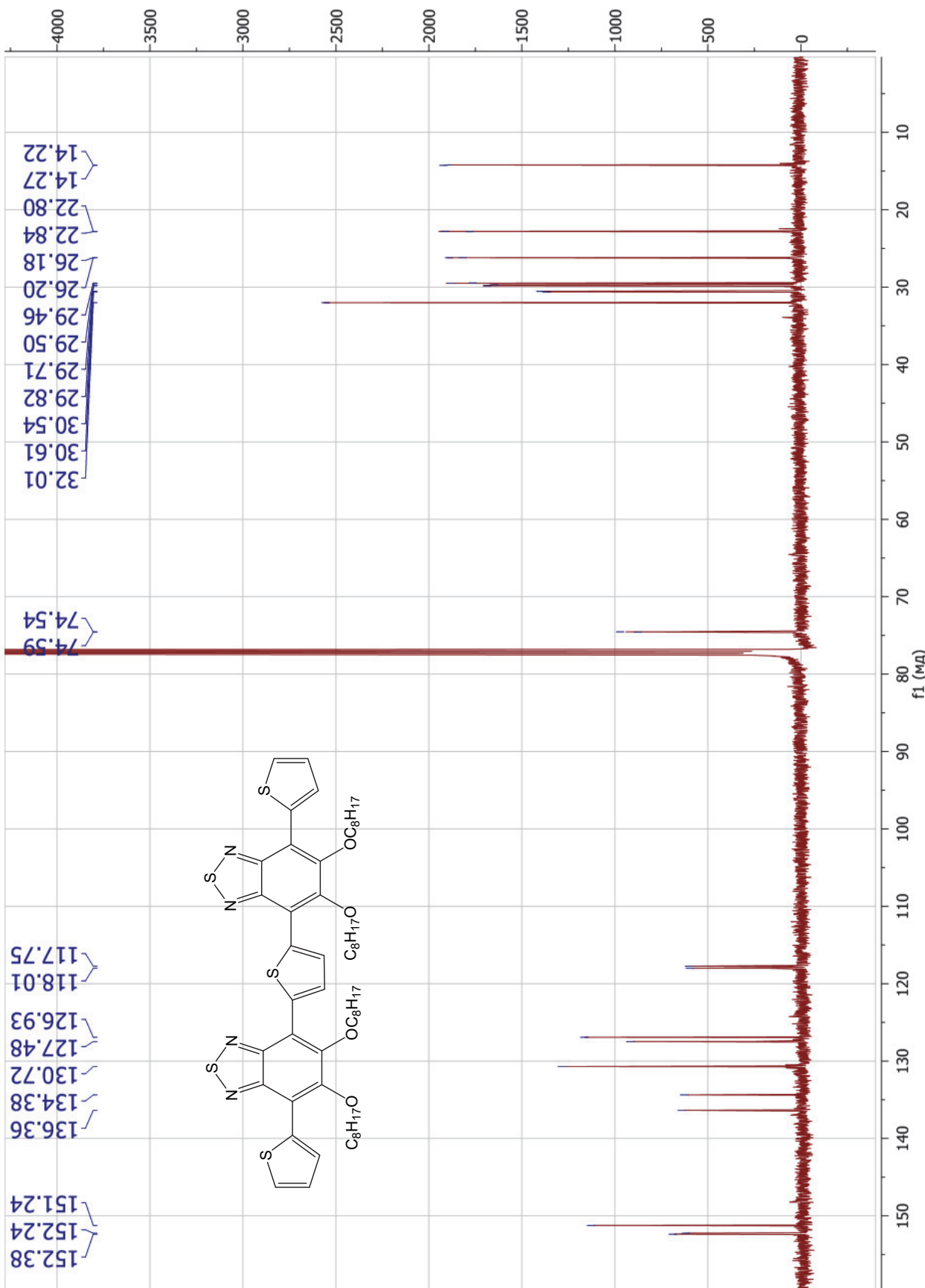


Figure S15.  $^{13}\text{C}$  NMR spectrum of A3

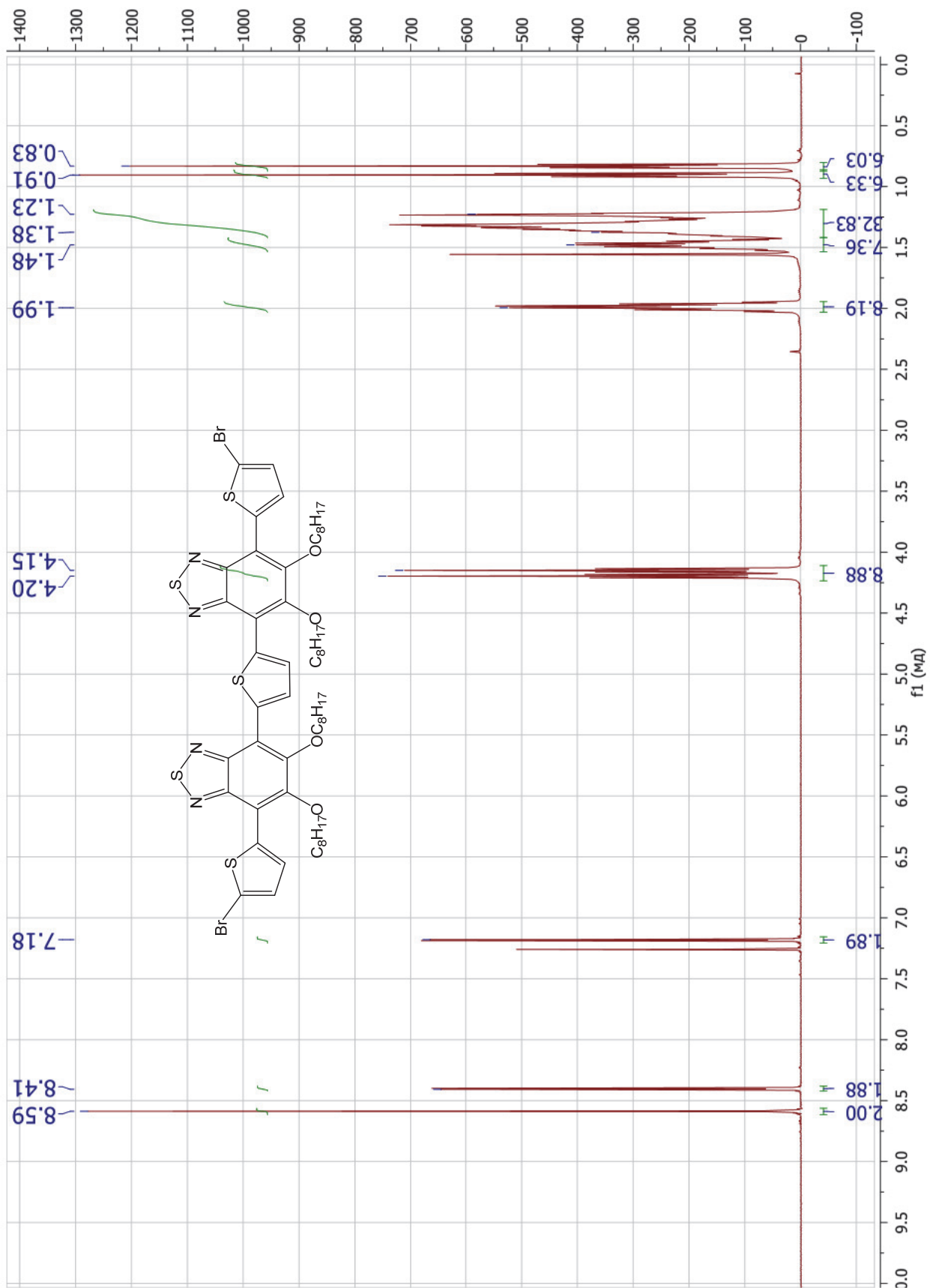


Figure S16.  $^1\text{H}$  NMR spectrum of B3

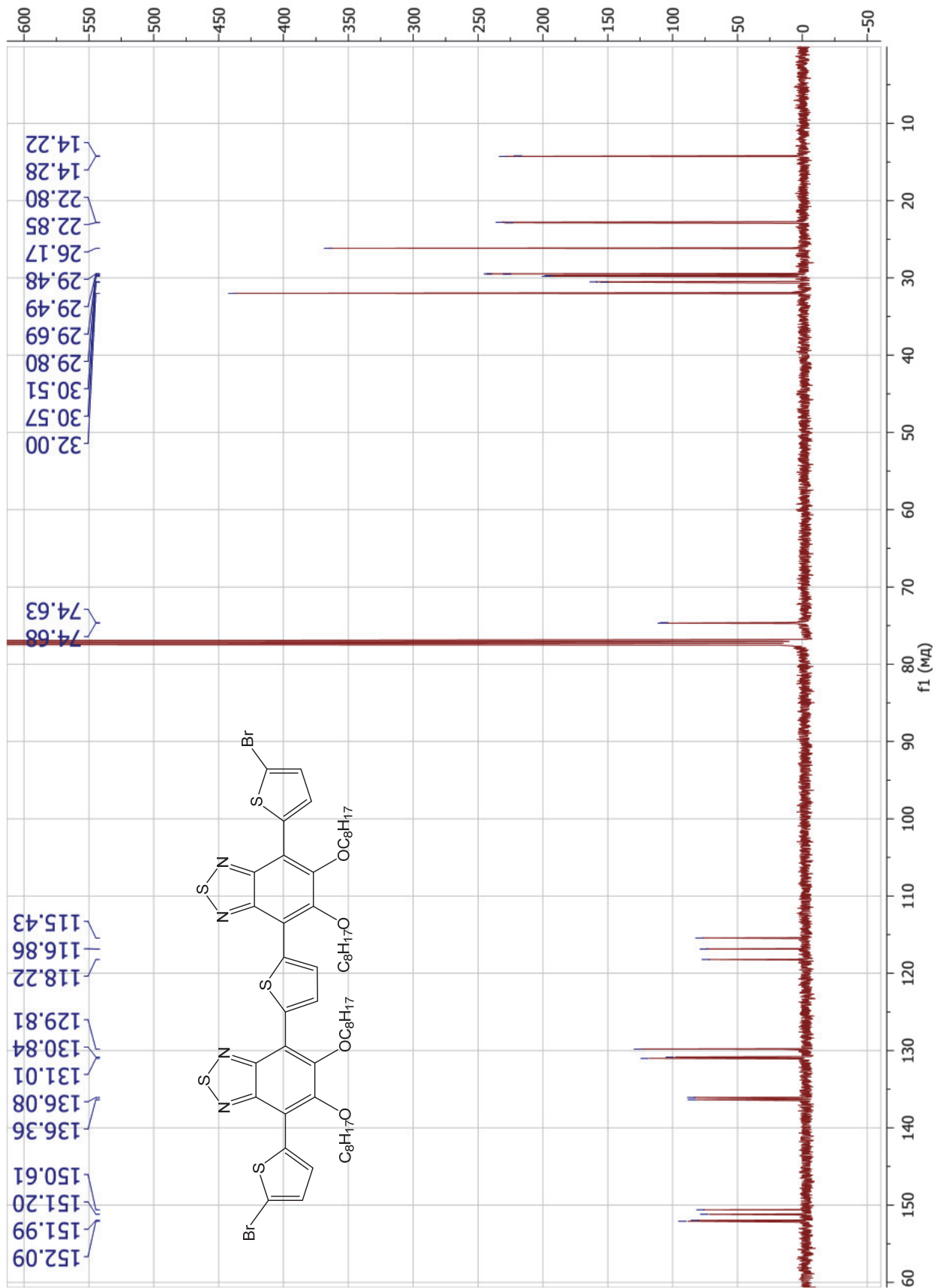


Figure S17.  $^{13}\text{C}$  NMR spectrum of B3

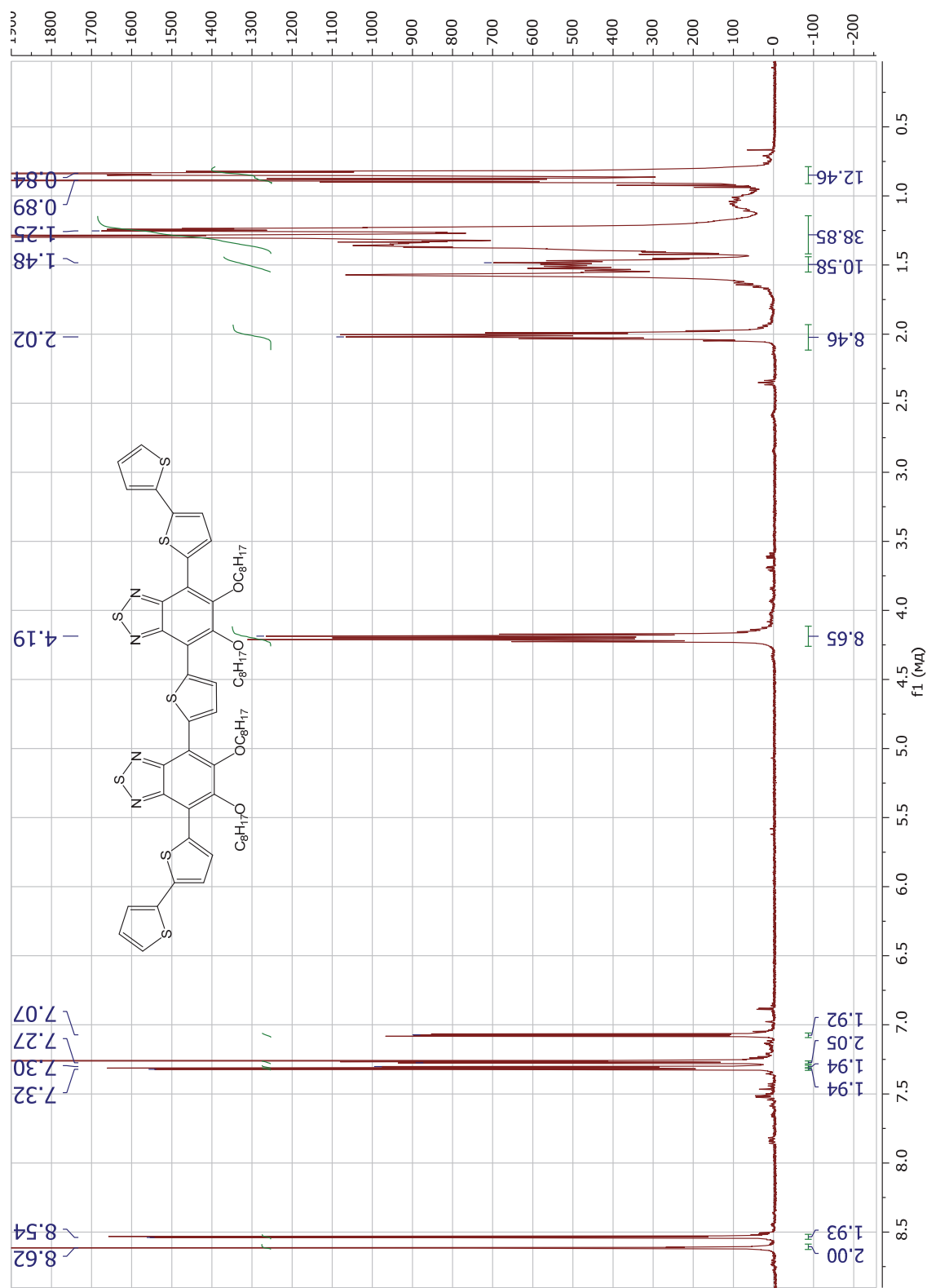


Figure S18.  $^1\text{H}$  NMR spectrum of C3

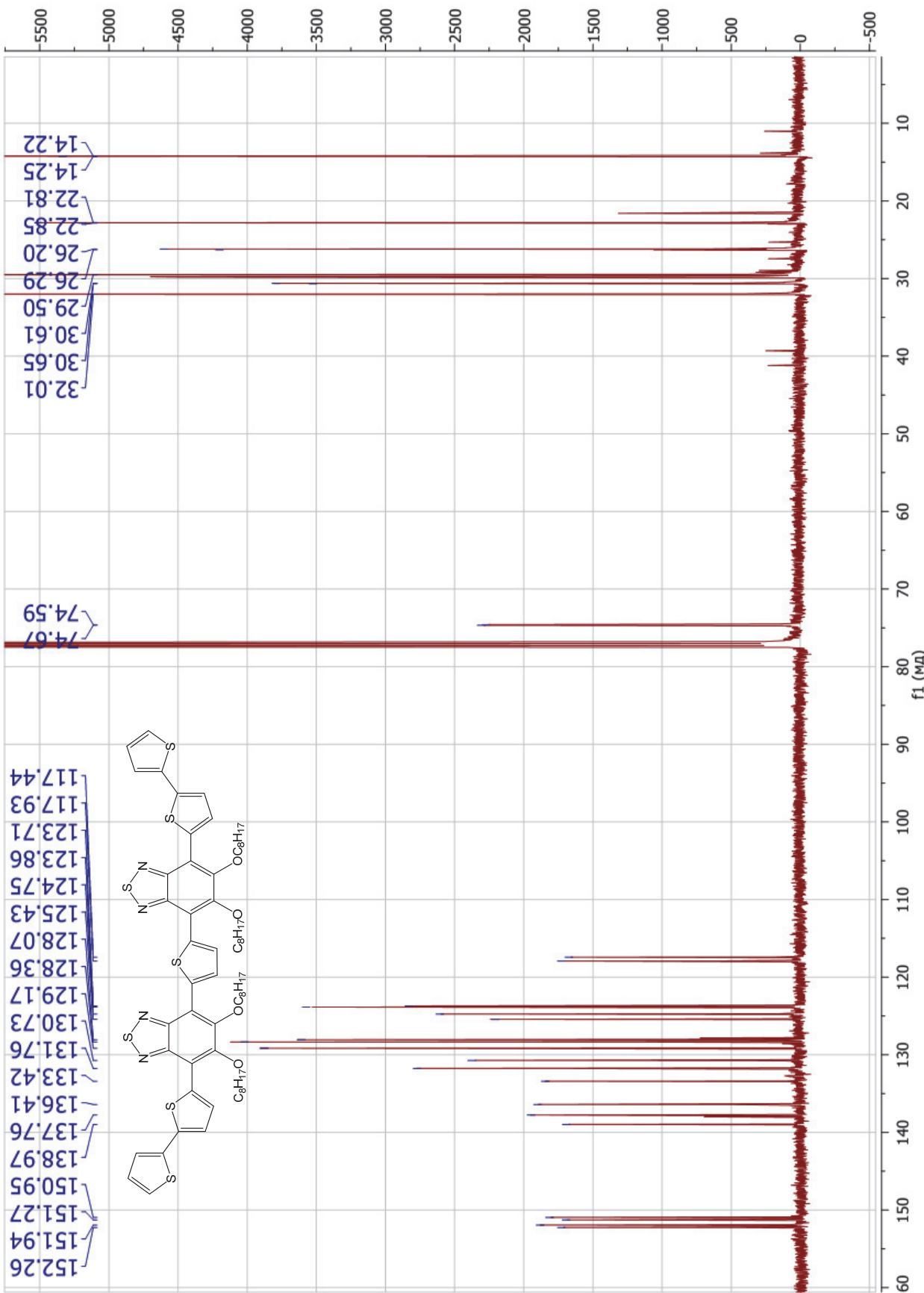


Figure S19.  $^{13}\text{C}$  NMR spectrum of C3

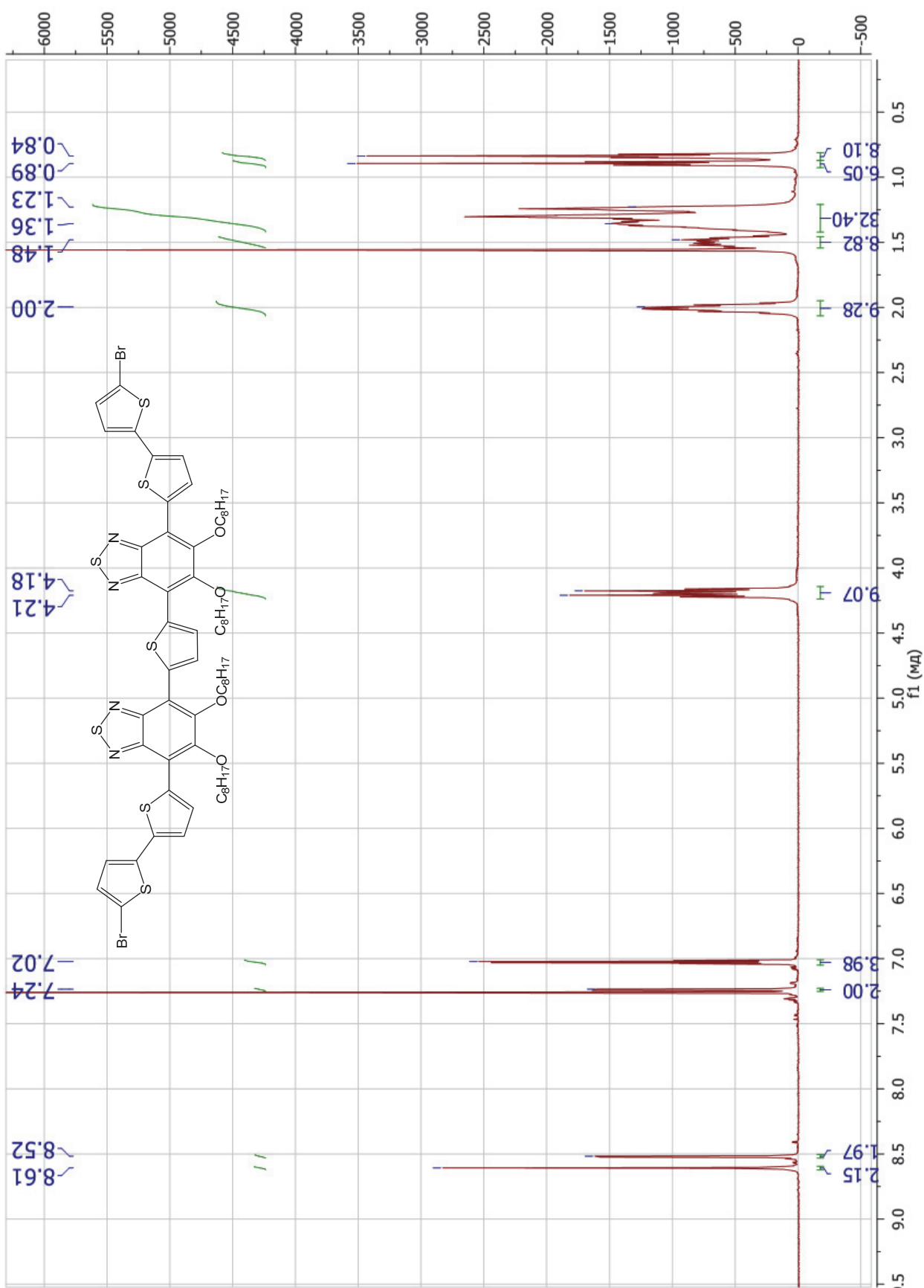


Figure S20.  $^1\text{H}$  NMR spectrum of D3

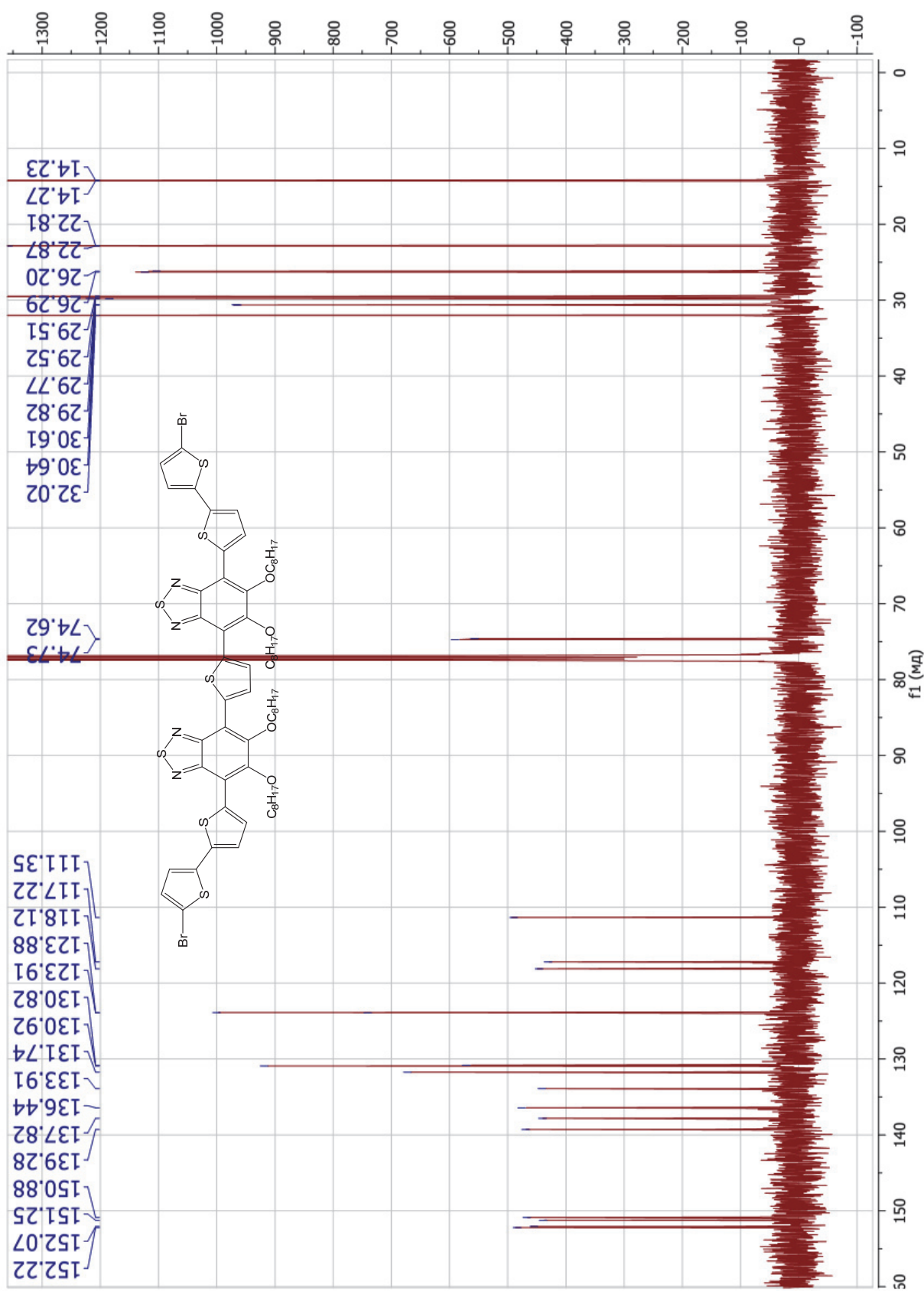


Figure S21.  $^{13}\text{C}$  NMR spectrum of D3

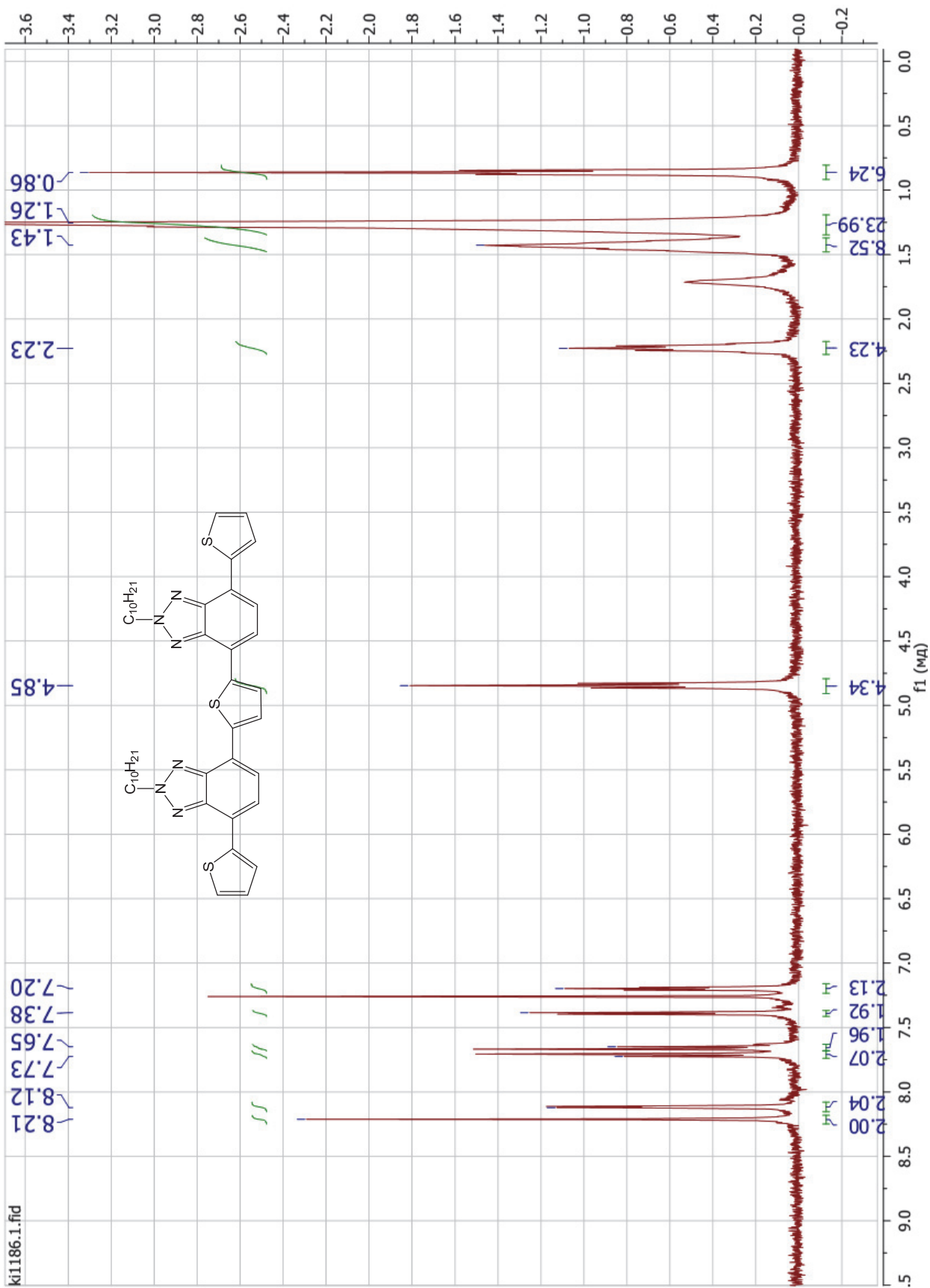


Figure S22.  $^1\text{H}$  NMR spectrum of A4

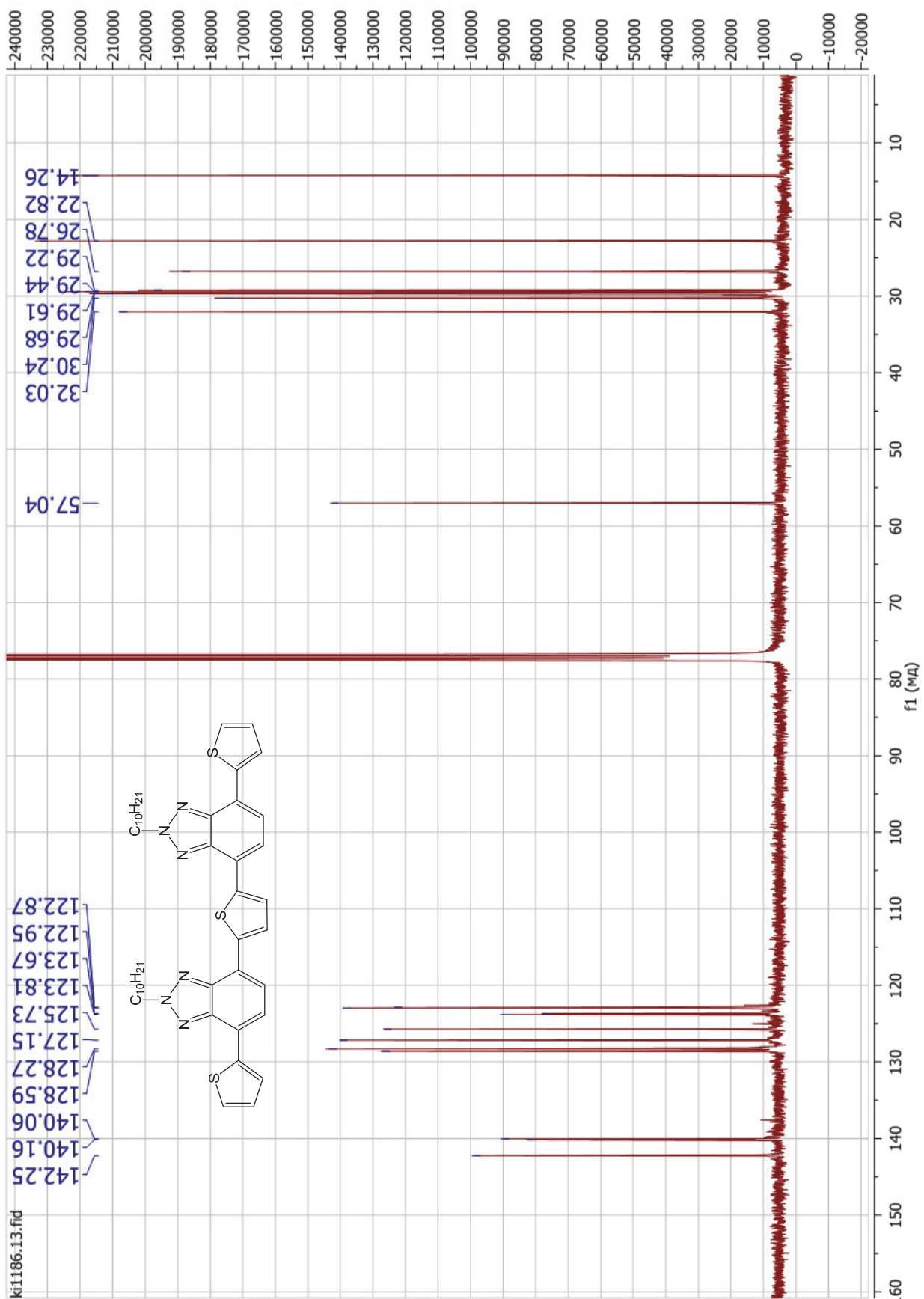


Figure S23.  $^{13}\text{C}$  NMR spectrum of A4

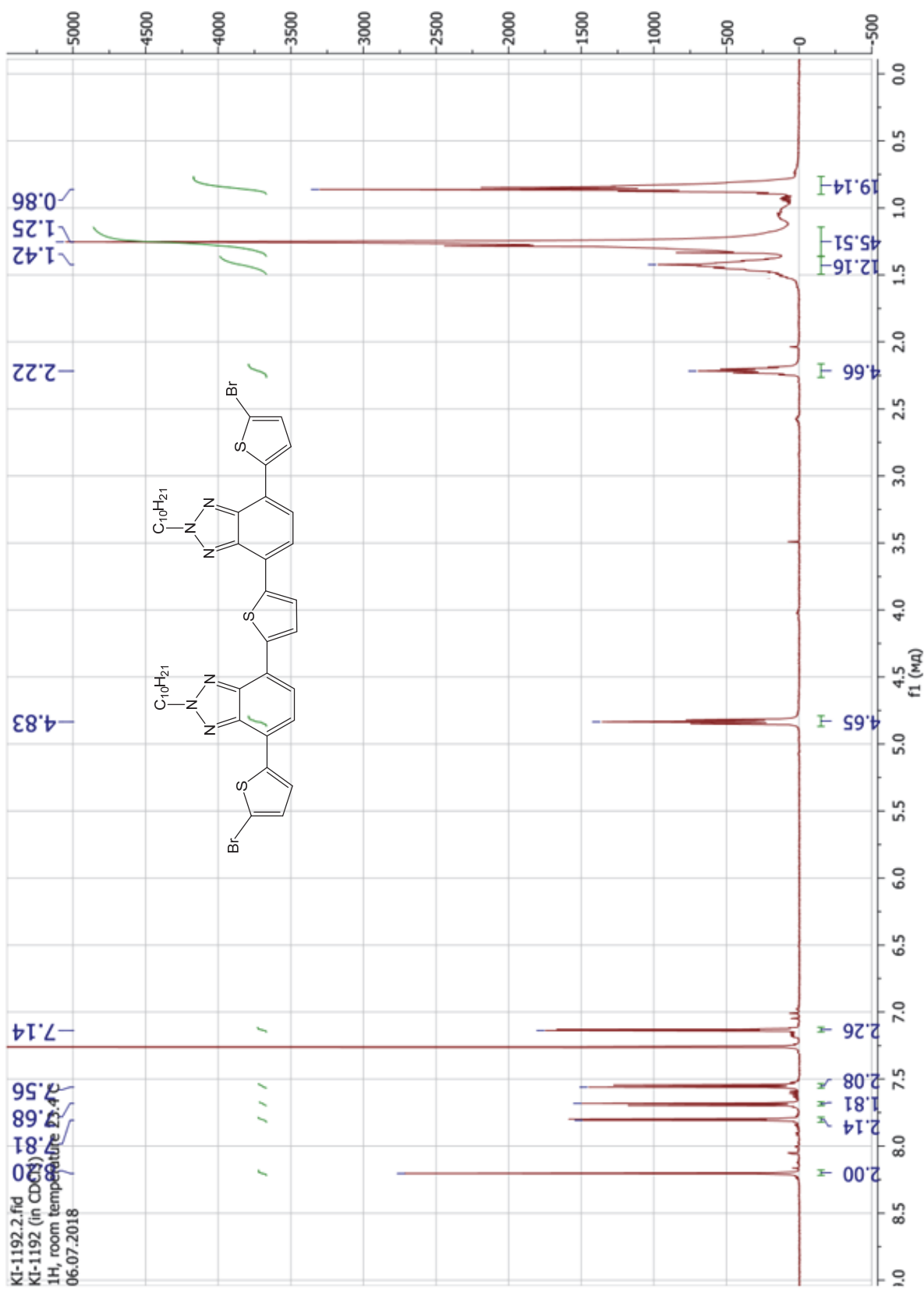


Figure S24. <sup>1</sup>H NMR spectrum of B4

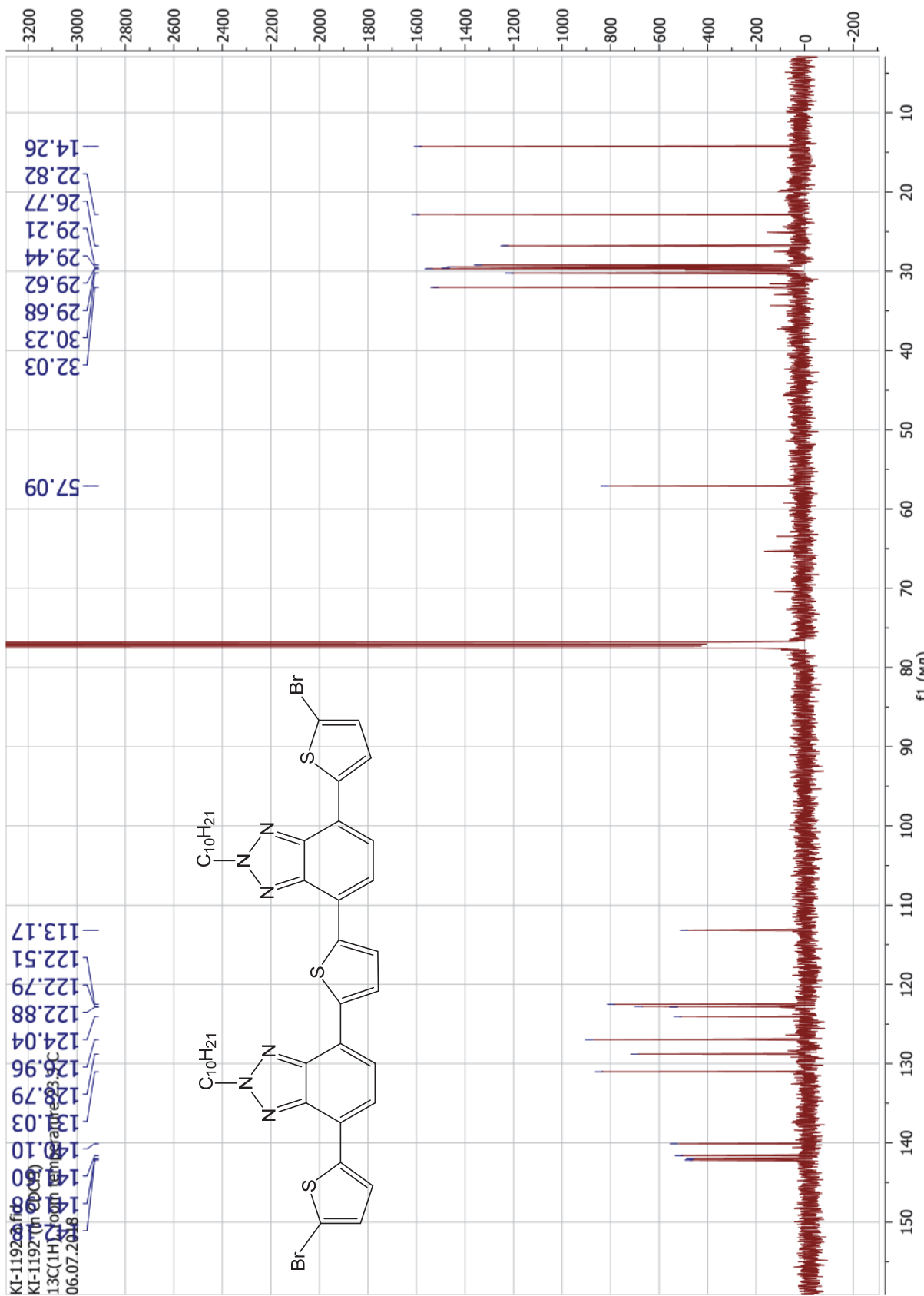


Figure S25.  $^{13}\text{C}$  NMR spectrum of B4

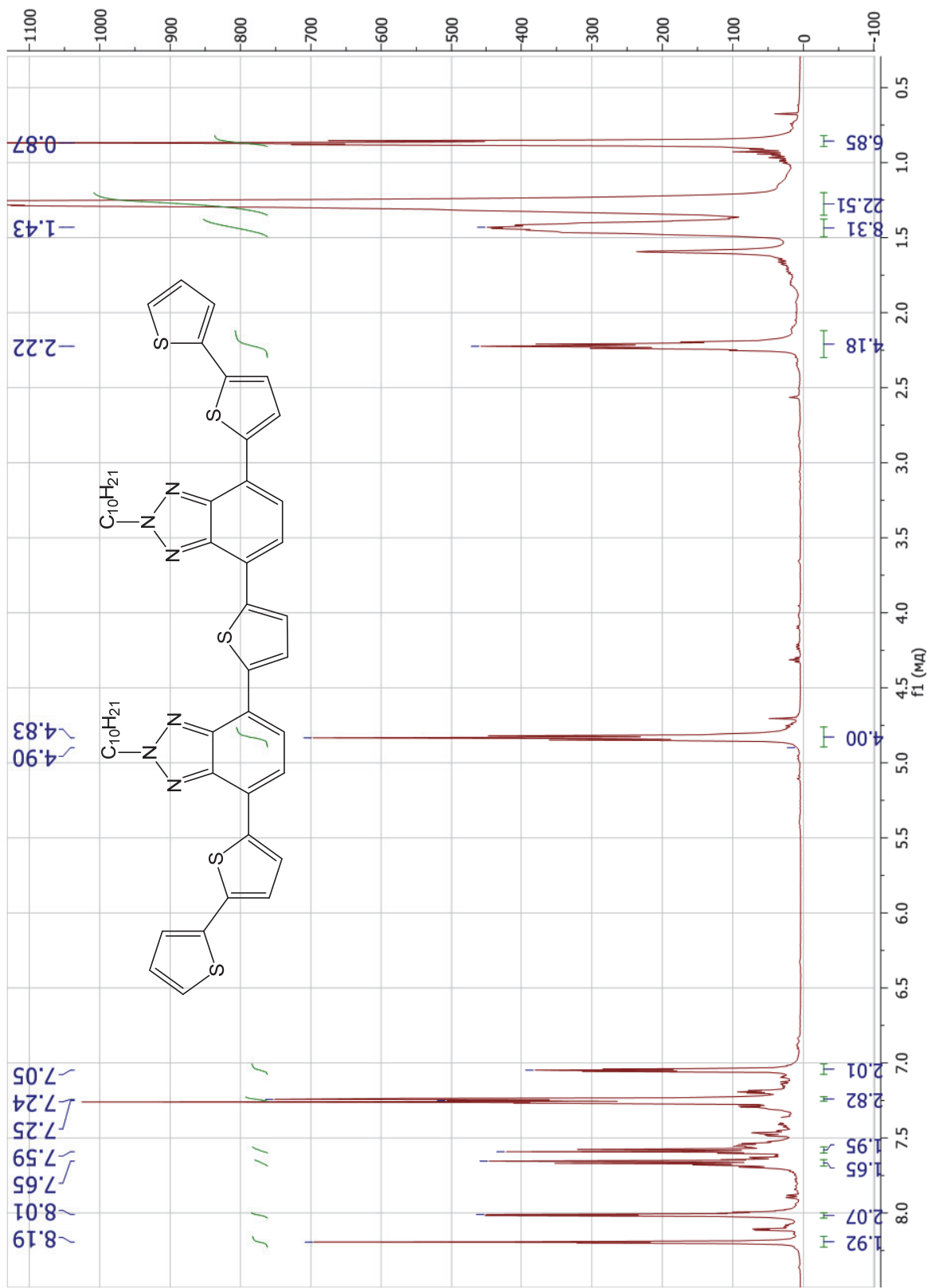


Figure S26.  $^1\text{H}$  NMR spectrum of C4

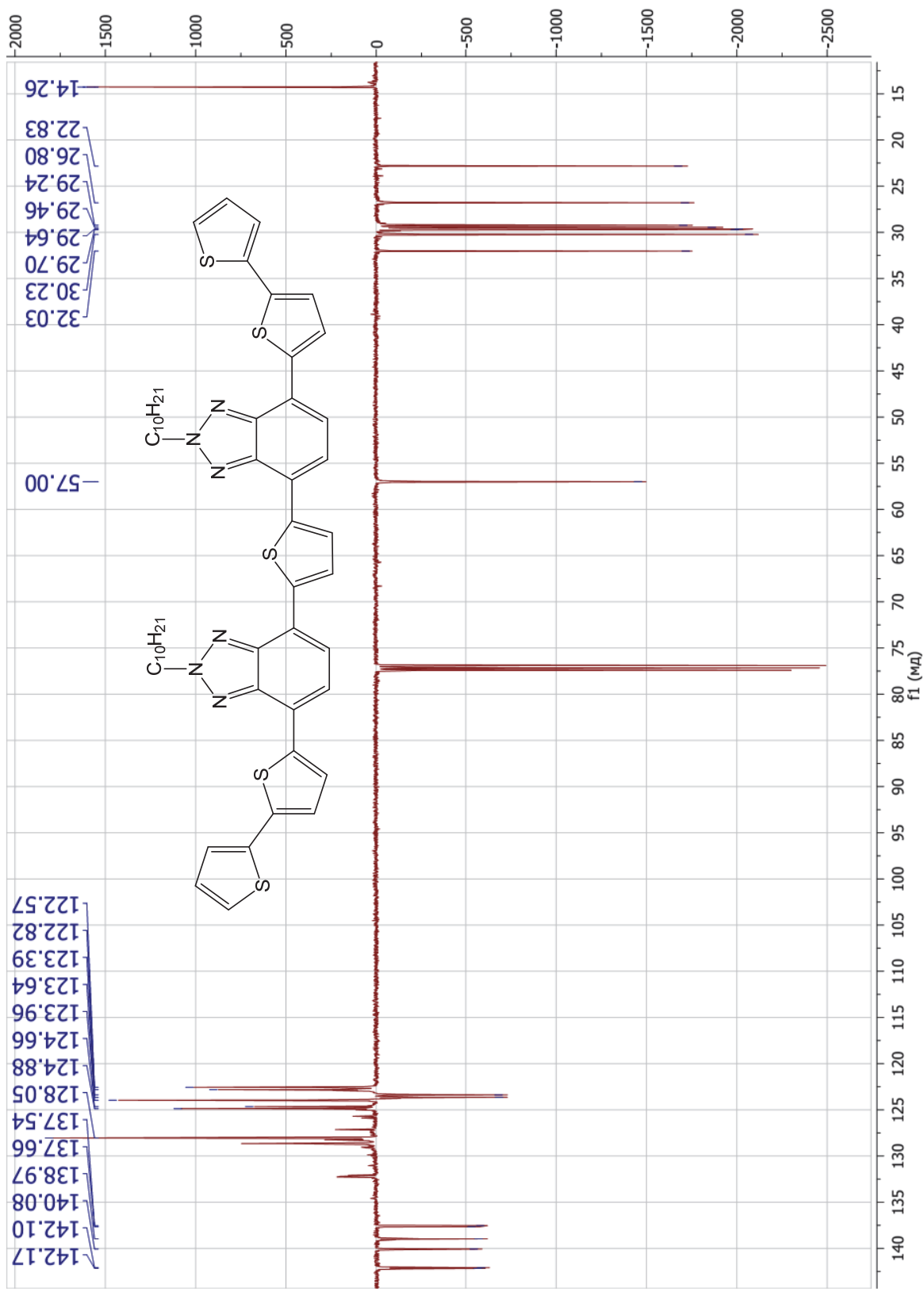


Figure S27.  $^{13}\text{C}$  NMR spectrum of C4

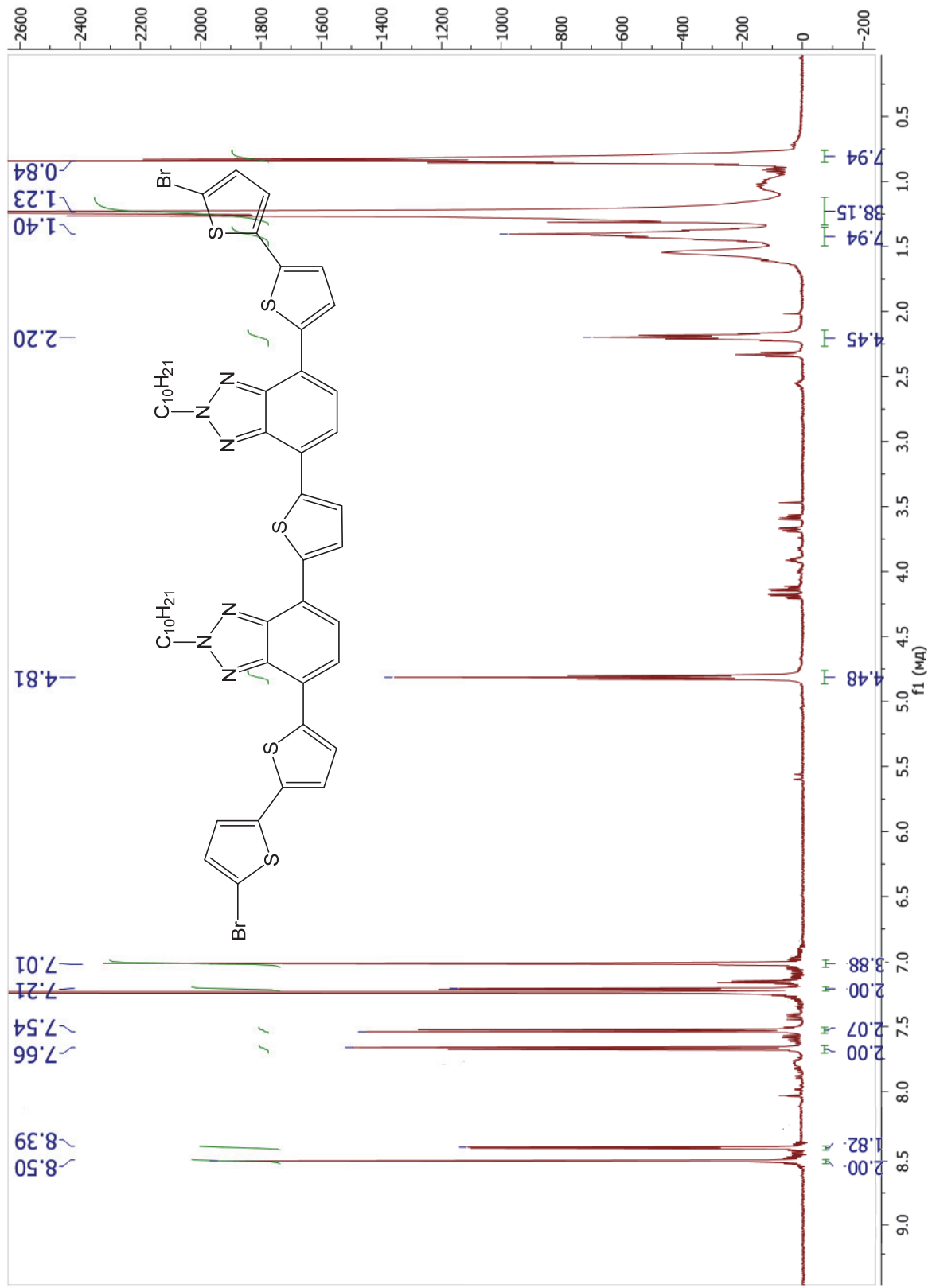


Figure S28.  $^1\text{H}$  NMR spectrum of D4

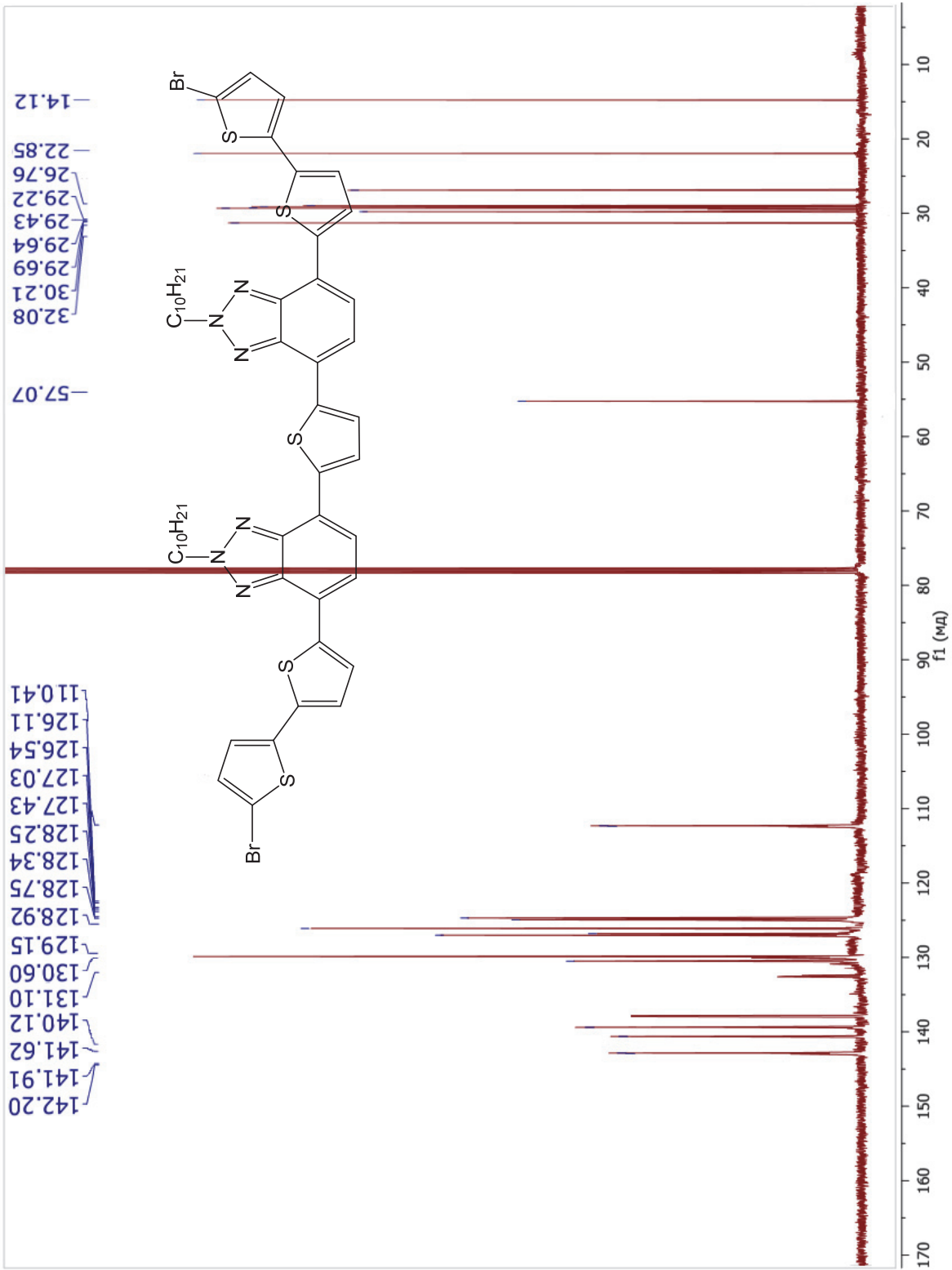


Figure S29.  $^{13}\text{C}$  NMR spectrum of D4

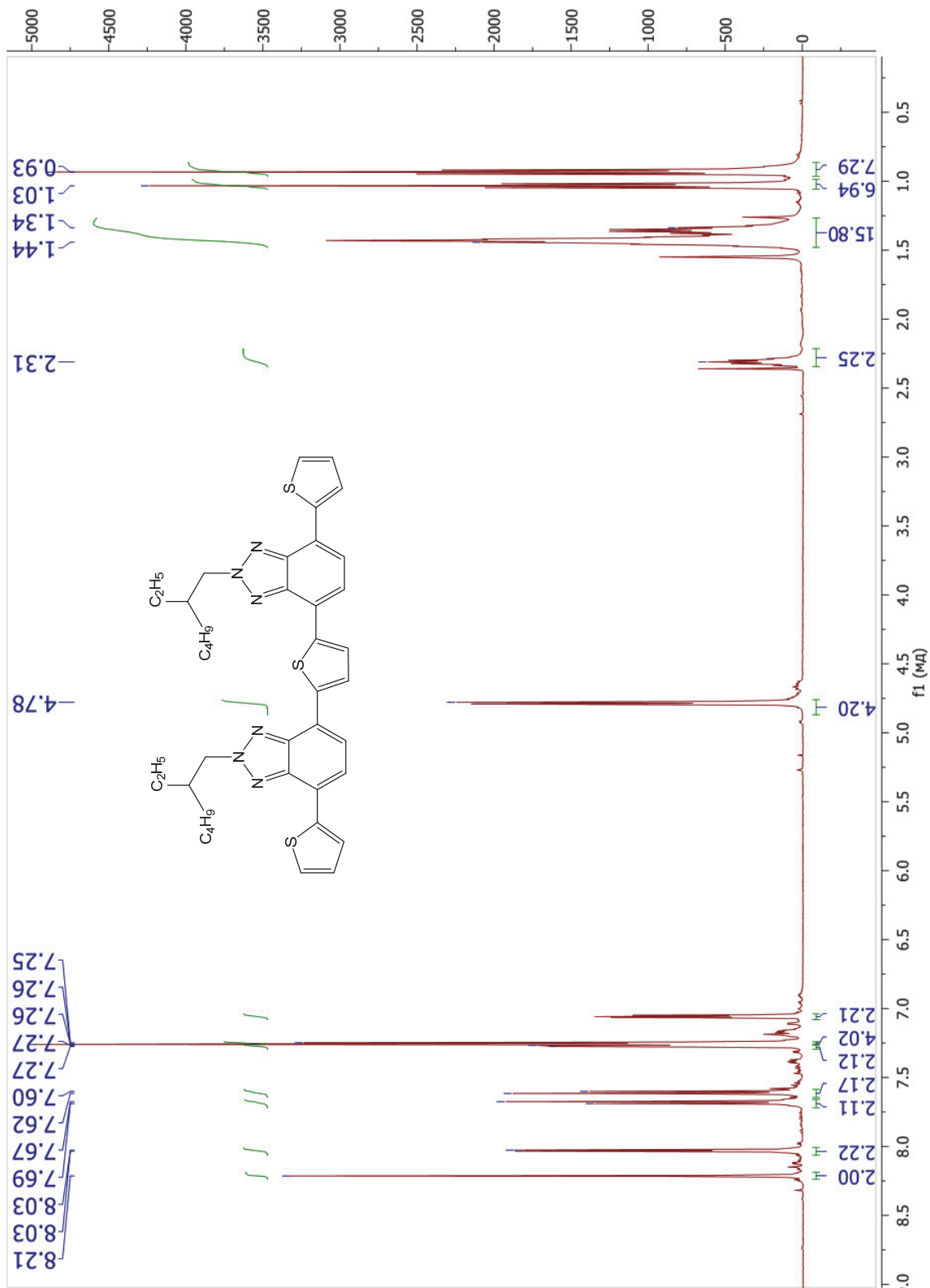


Figure S30.  $^1\text{H}$  NMR spectrum of A5

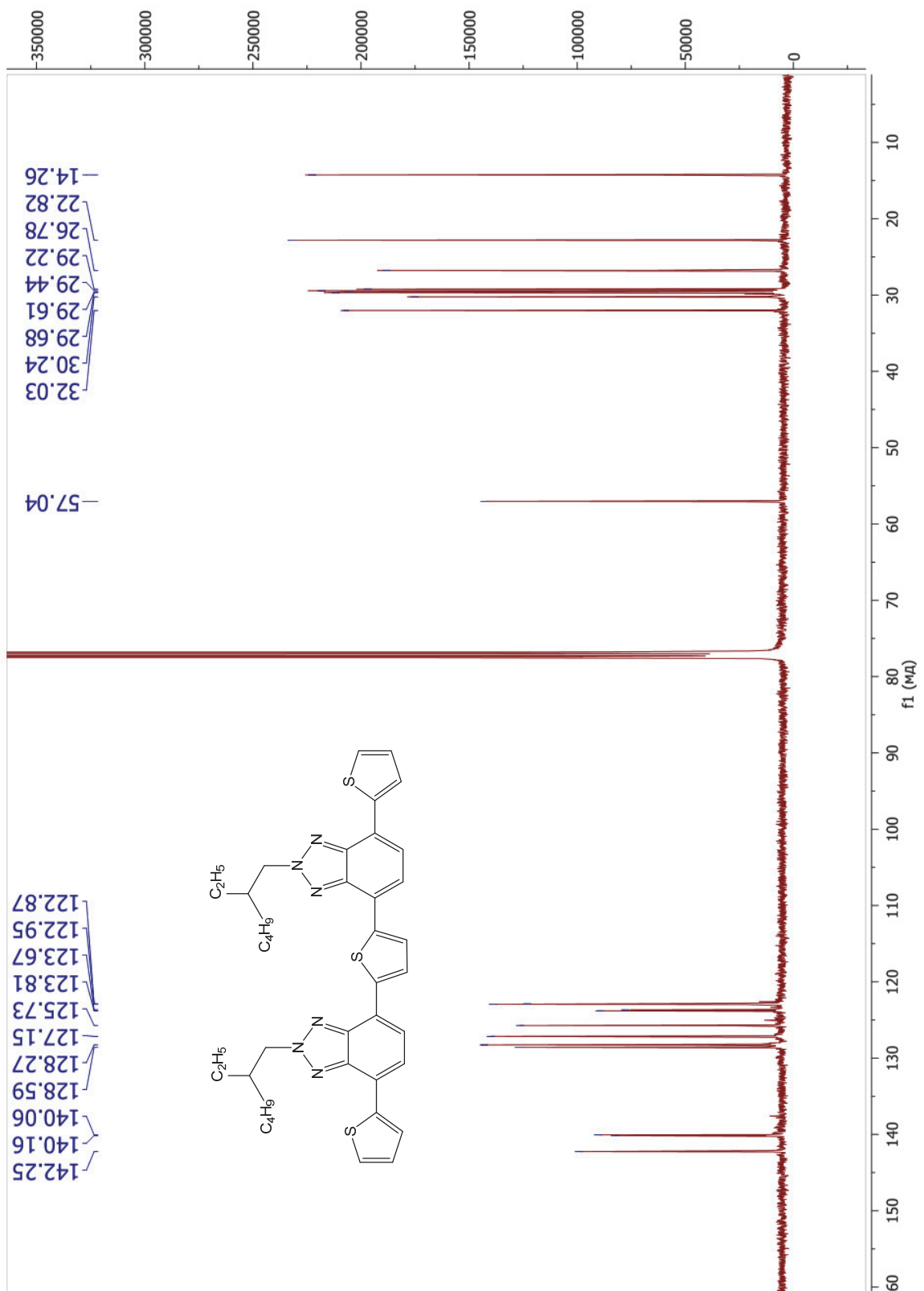


Figure S31.  $^{13}\text{C}$  NMR spectrum of A5

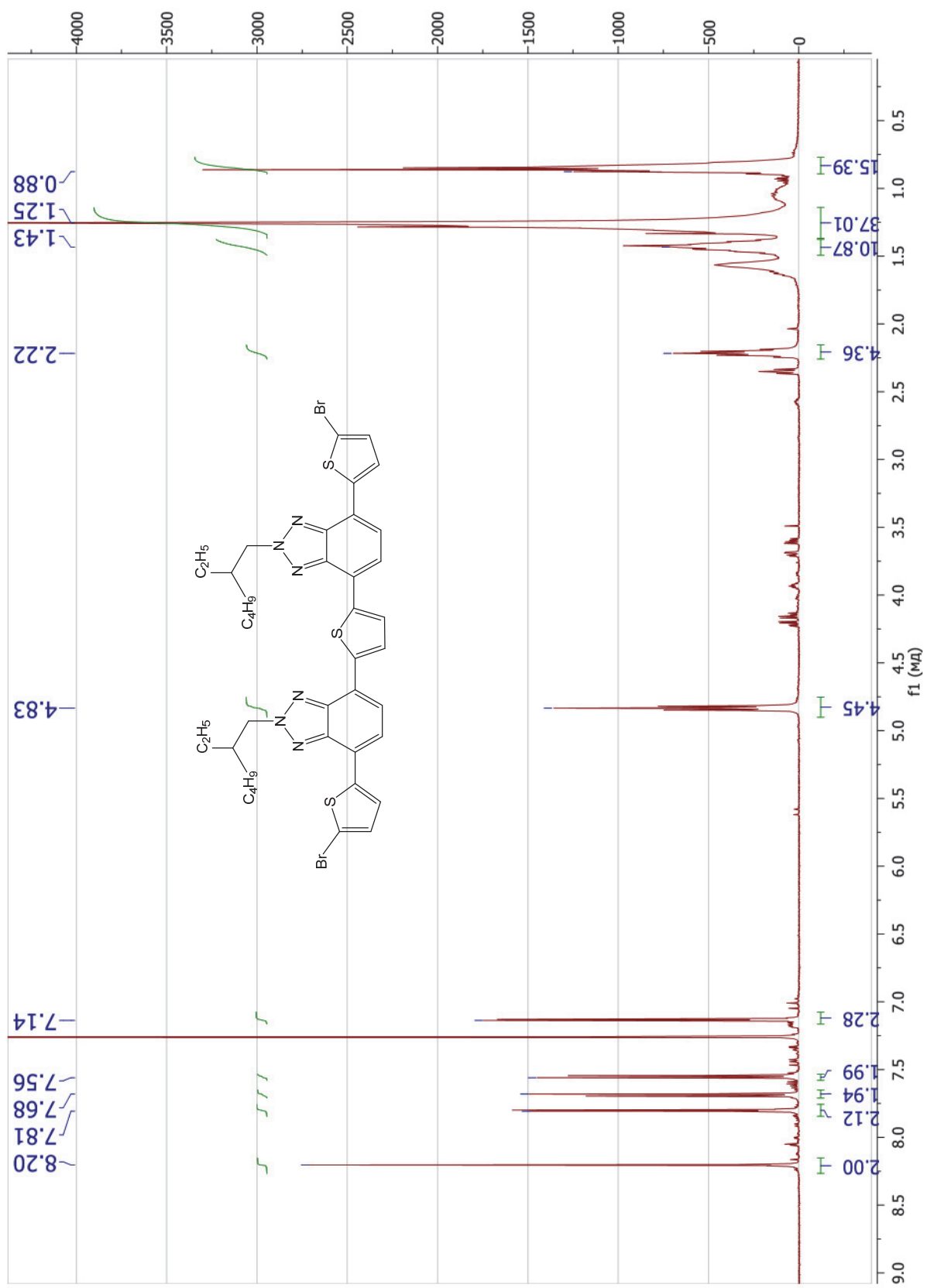


Figure S32.  $^1\text{H}$  NMR spectrum of B5

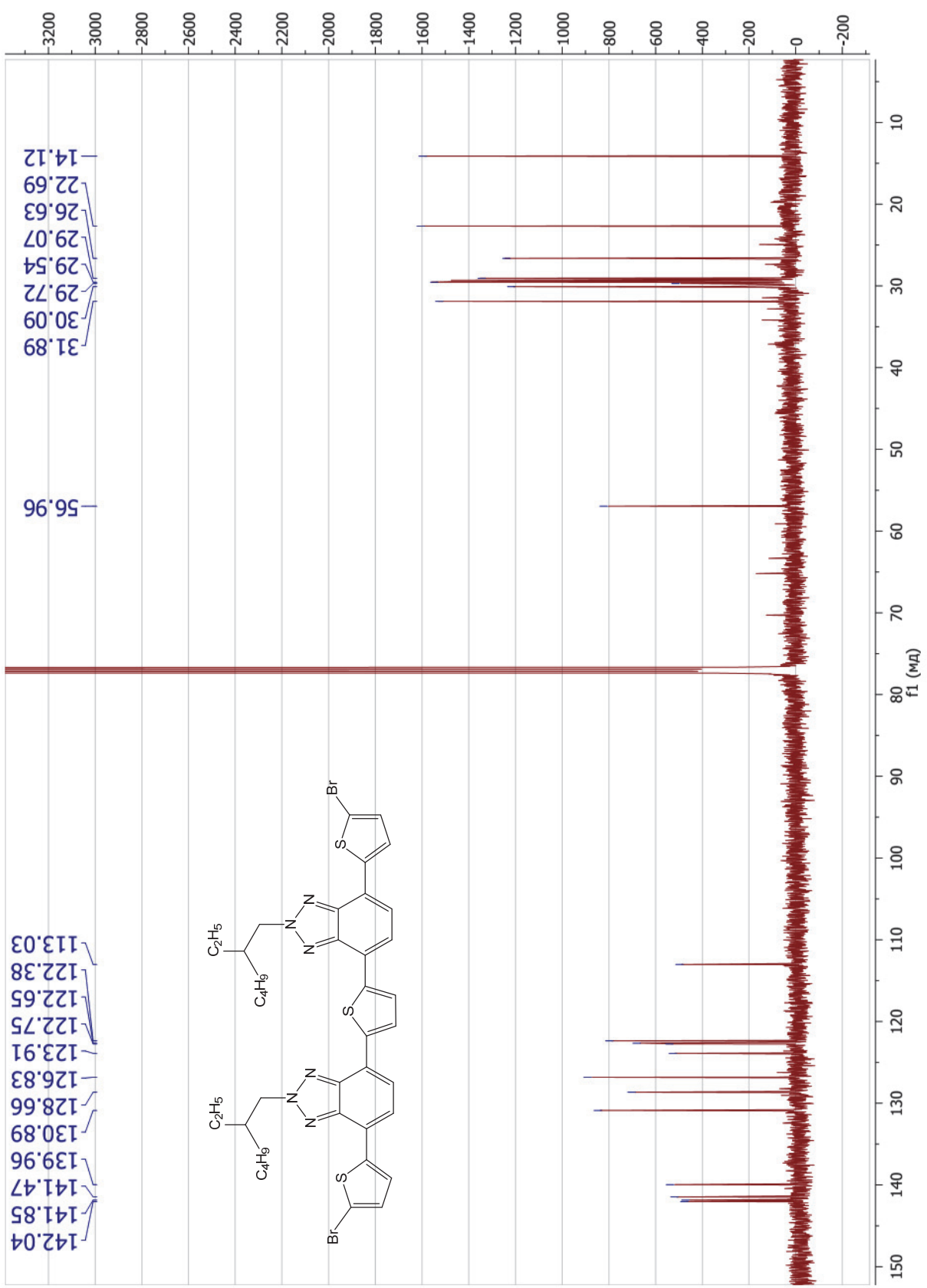


Figure S33.  $^{13}\text{C}$  NMR spectrum of B5

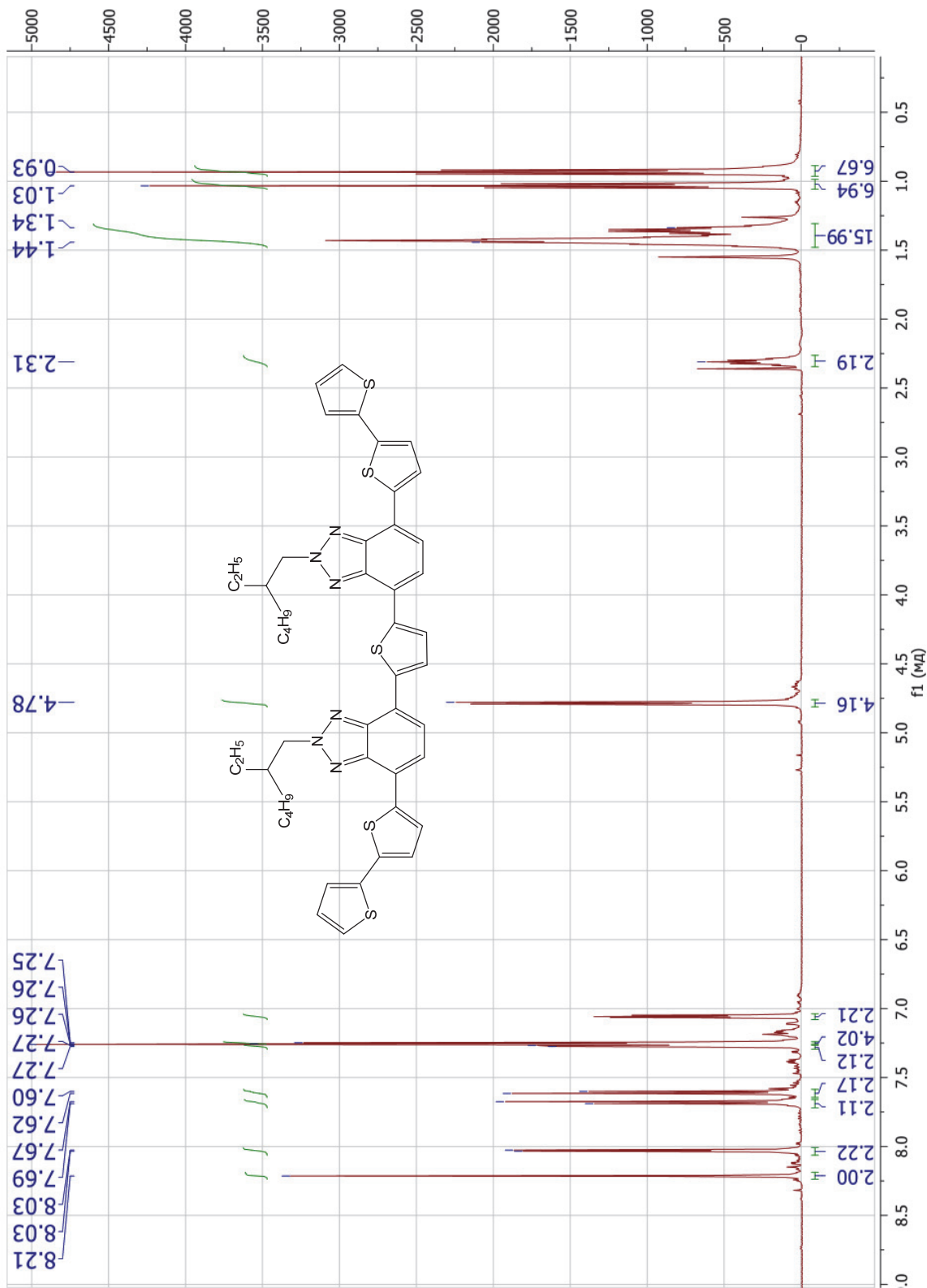


Figure S34.  $^1\text{H}$  NMR spectrum of C5

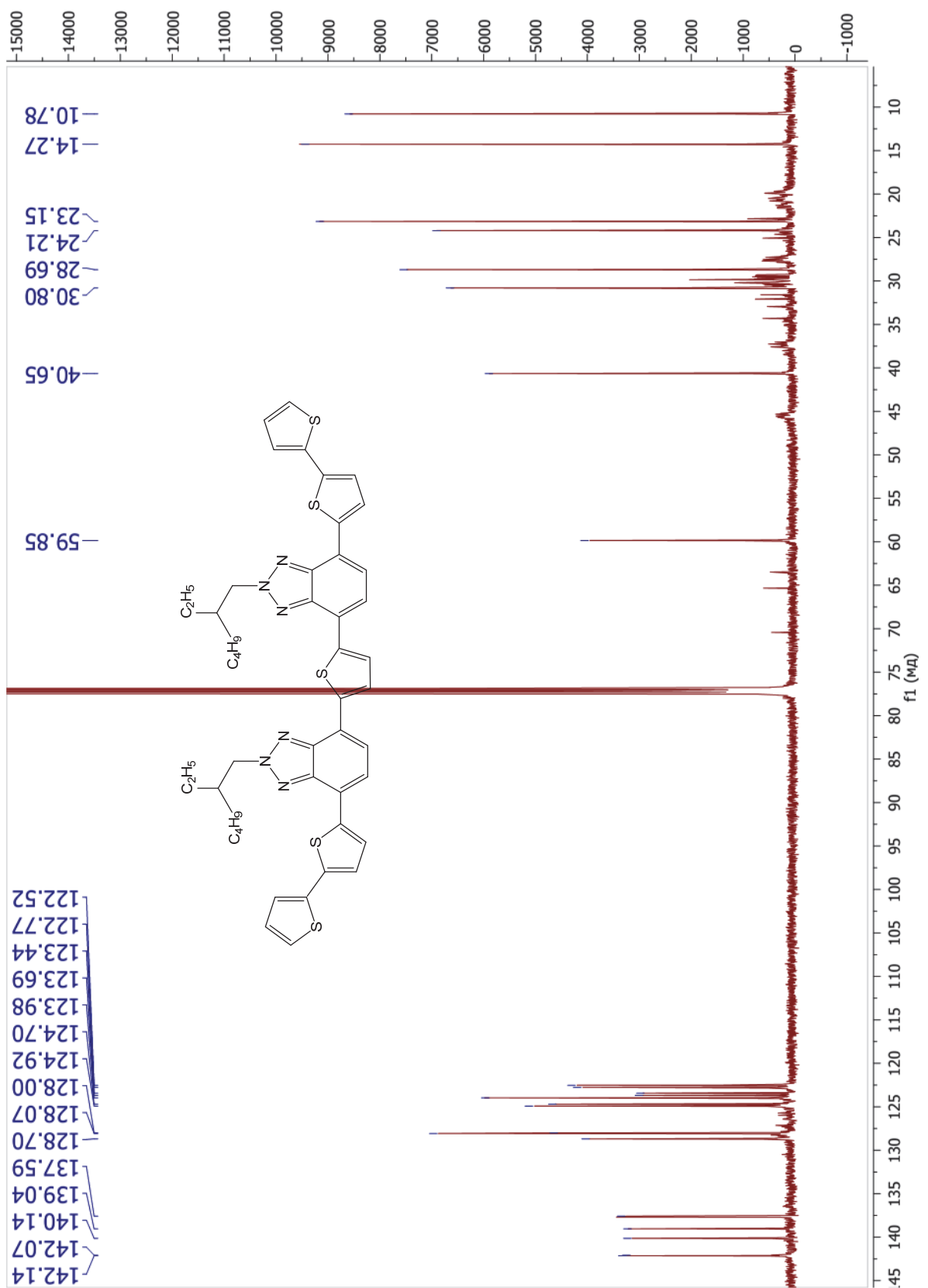


Figure S35.  $^{13}\text{C}$  NMR spectrum of C5

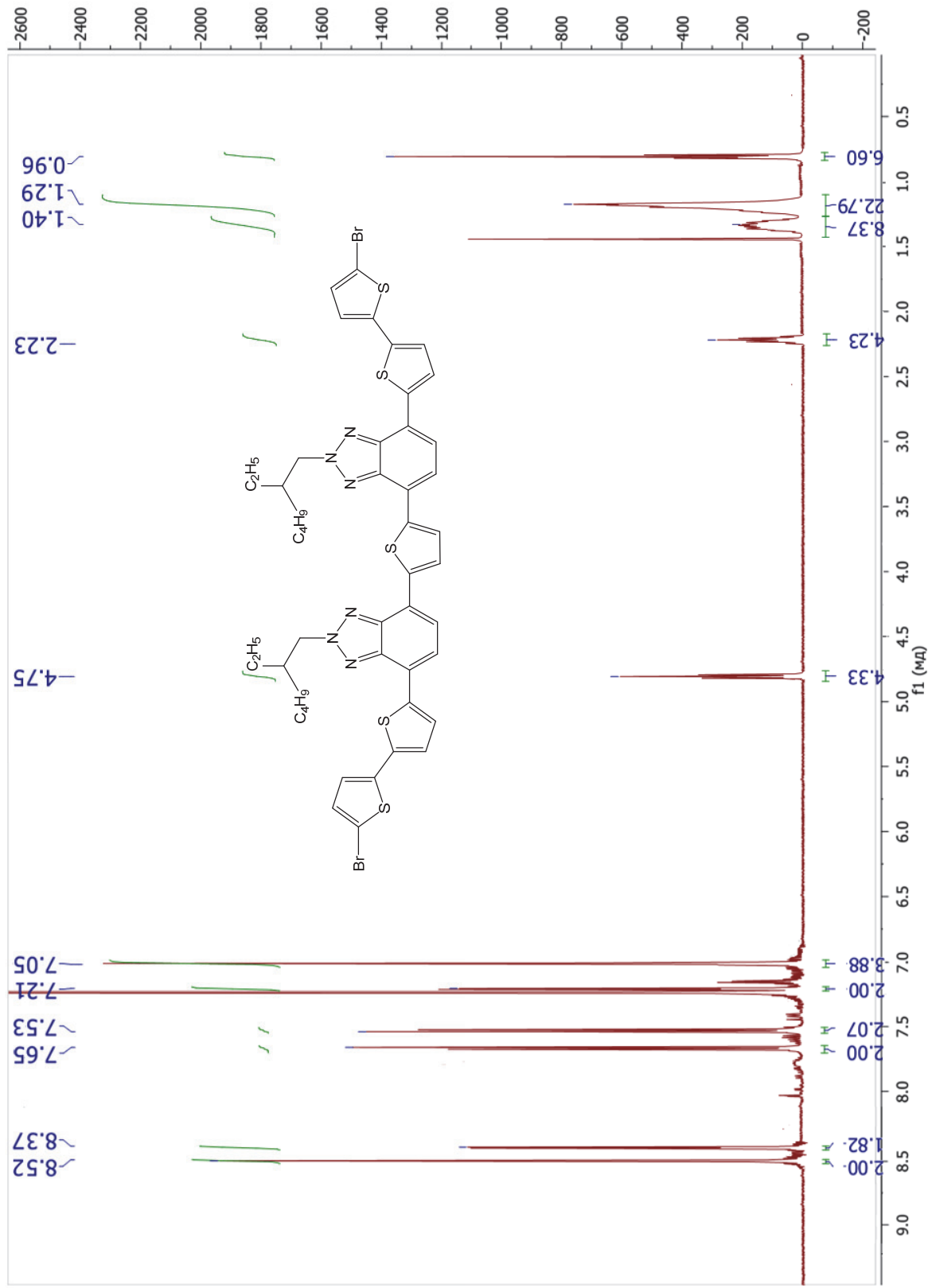


Figure S36.  $^1\text{H}$  NMR spectrum of D5

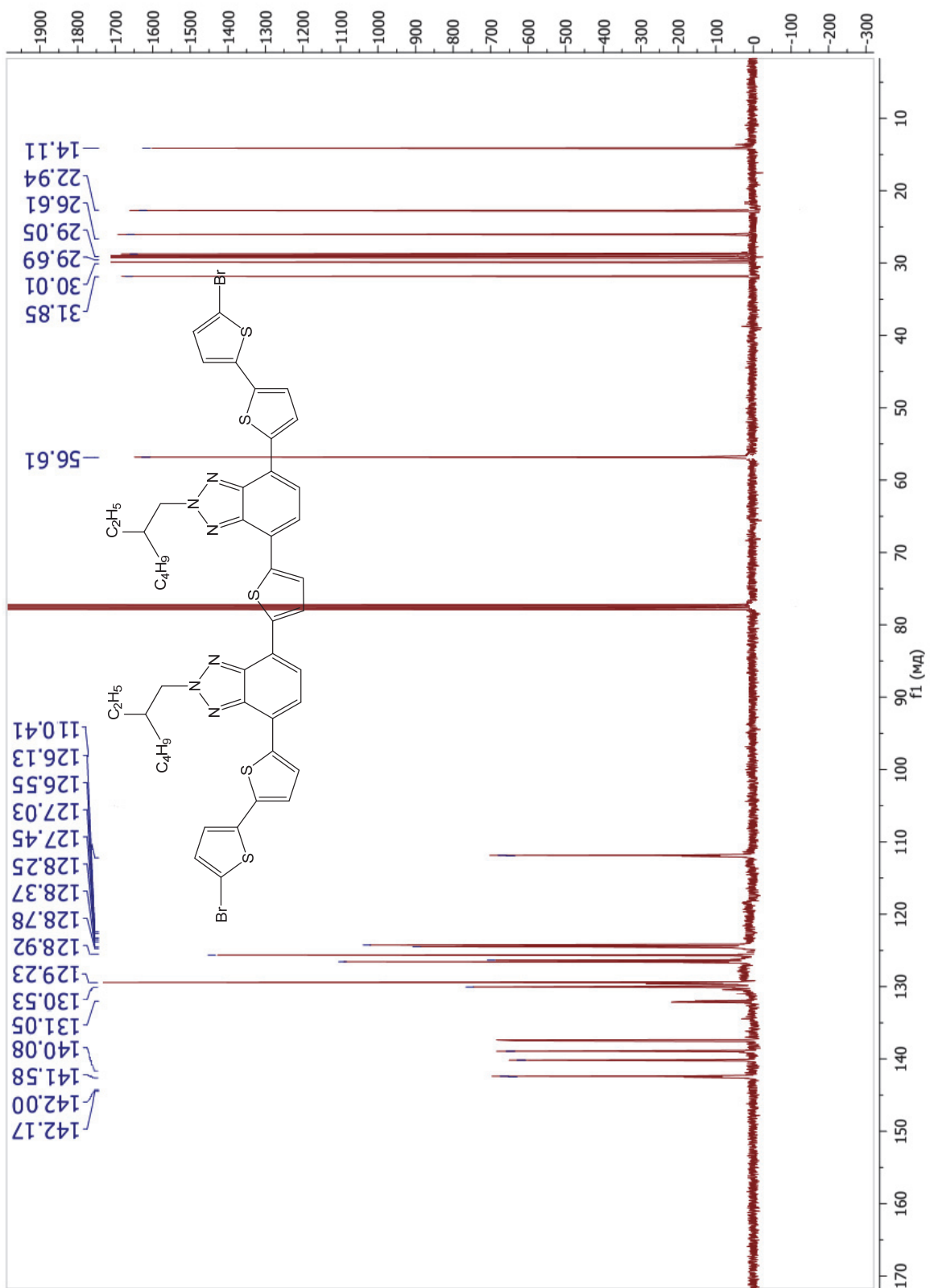


Figure S37.  $^{13}\text{C}$  NMR spectrum of D5

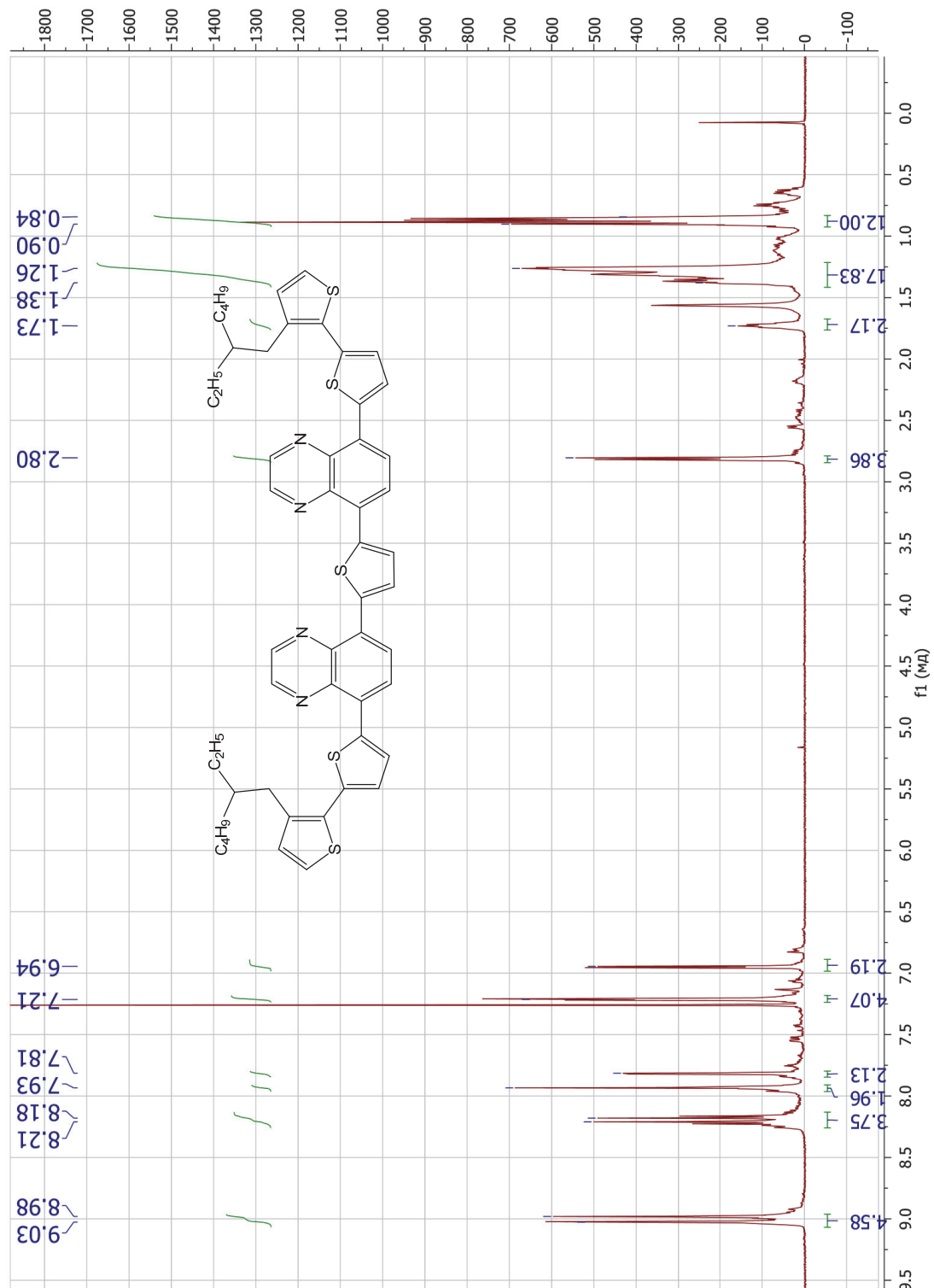


Figure S38.  $^1\text{H}$  NMR spectrum of C6

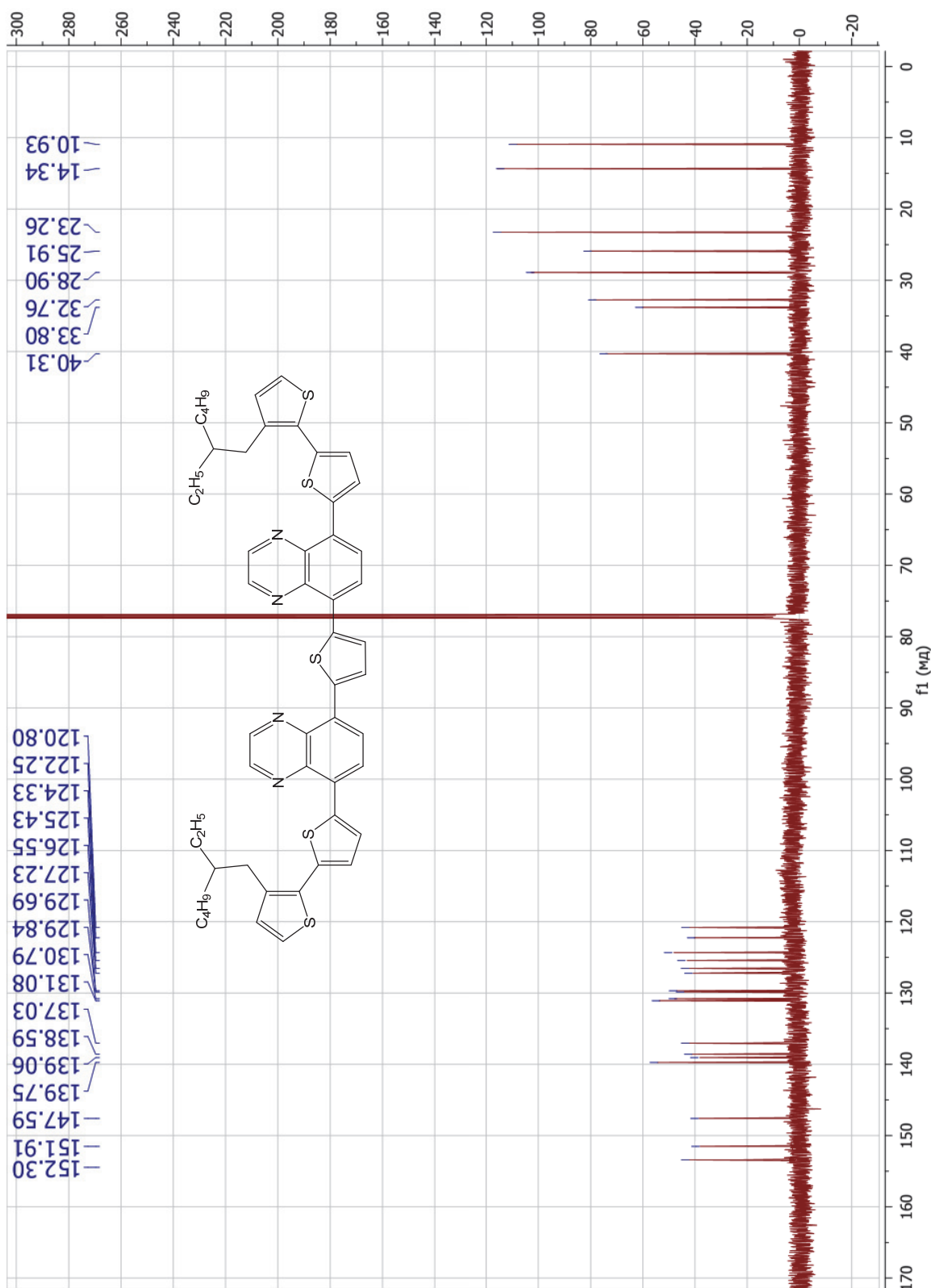


Figure S39.  $^{13}\text{C}$  NMR spectrum of C6

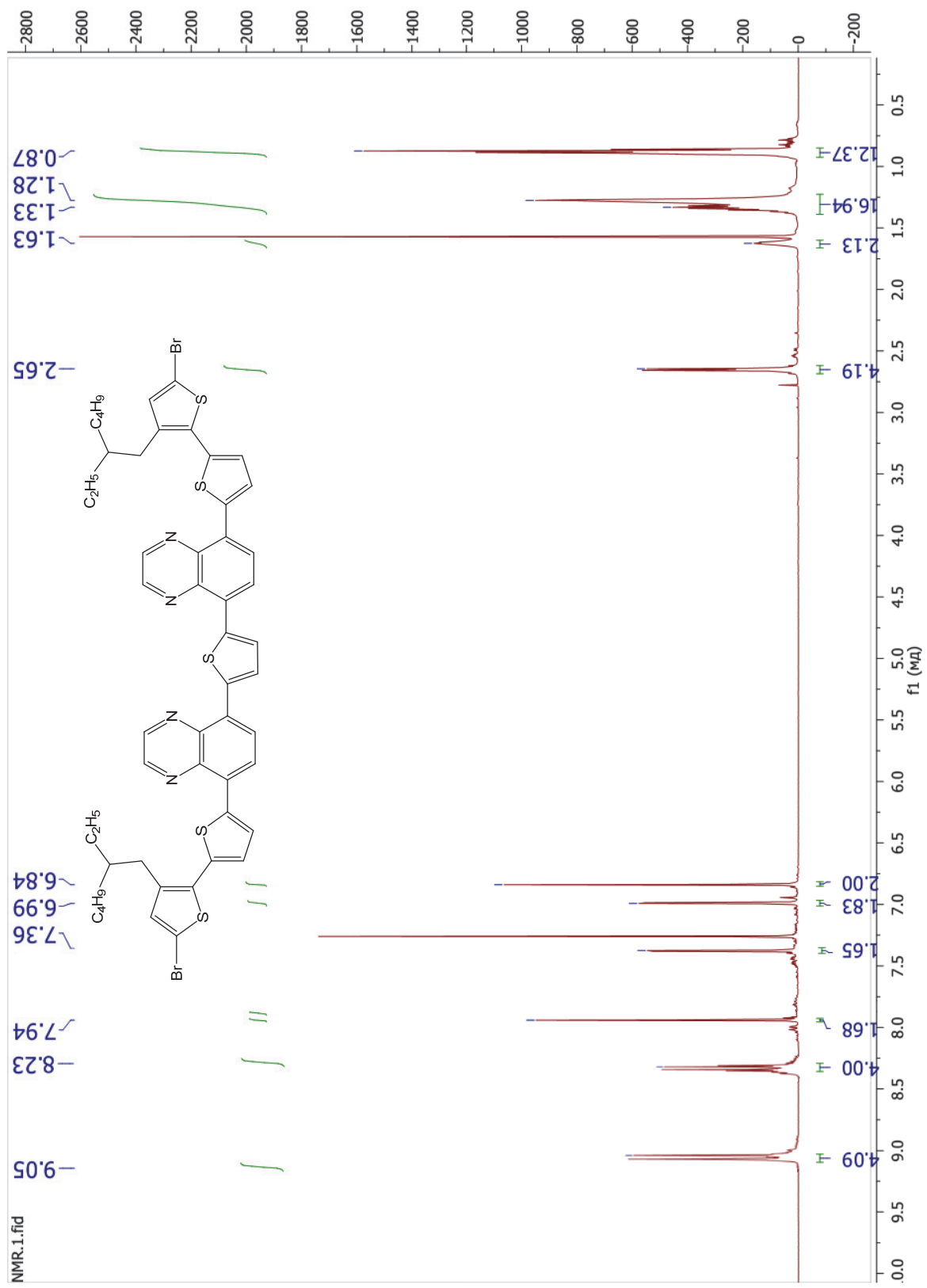


Figure S40. <sup>1</sup>H NMR spectrum of D6

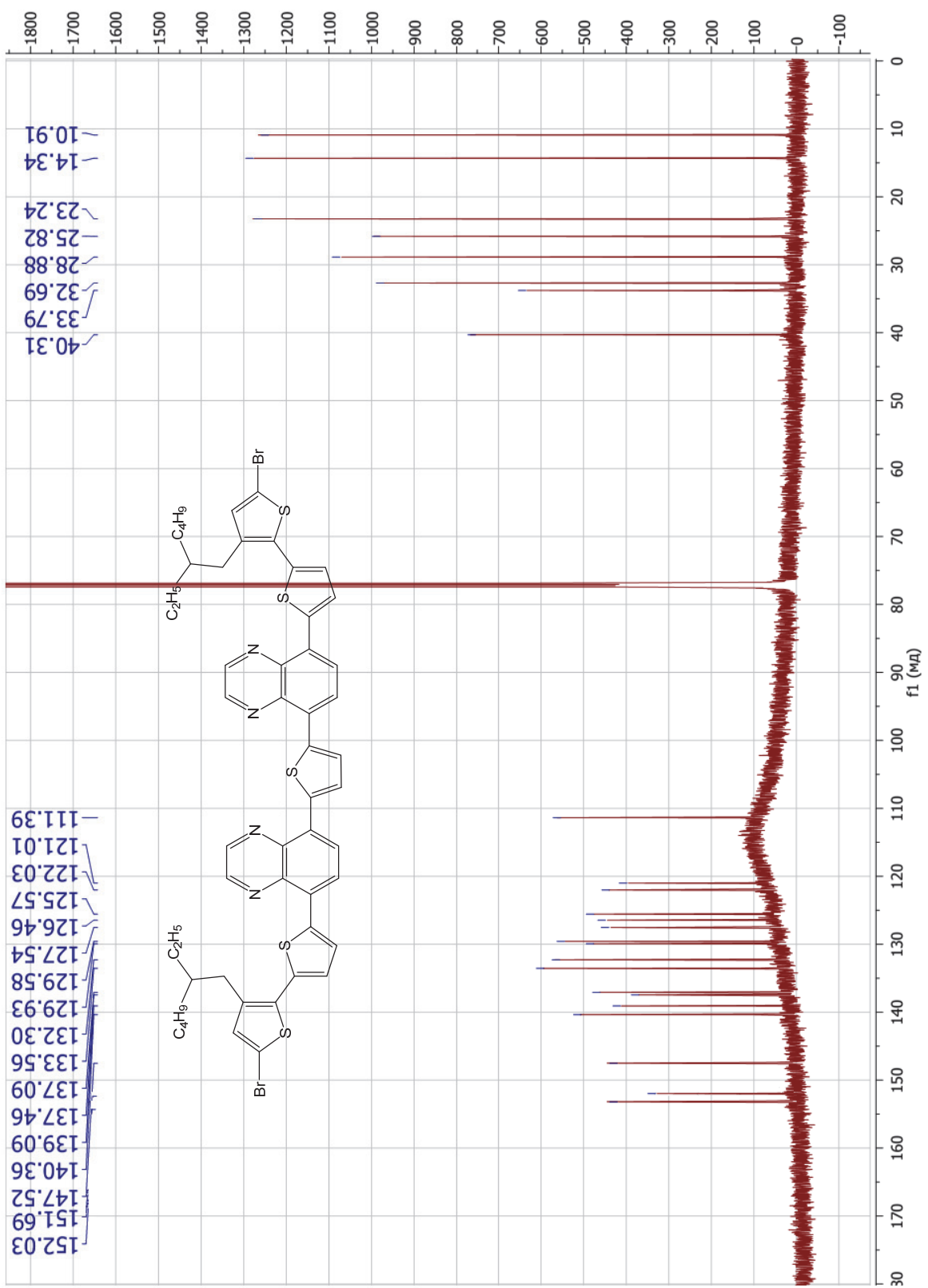


Figure S41.  $^{13}\text{C}$  NMR spectrum of D6

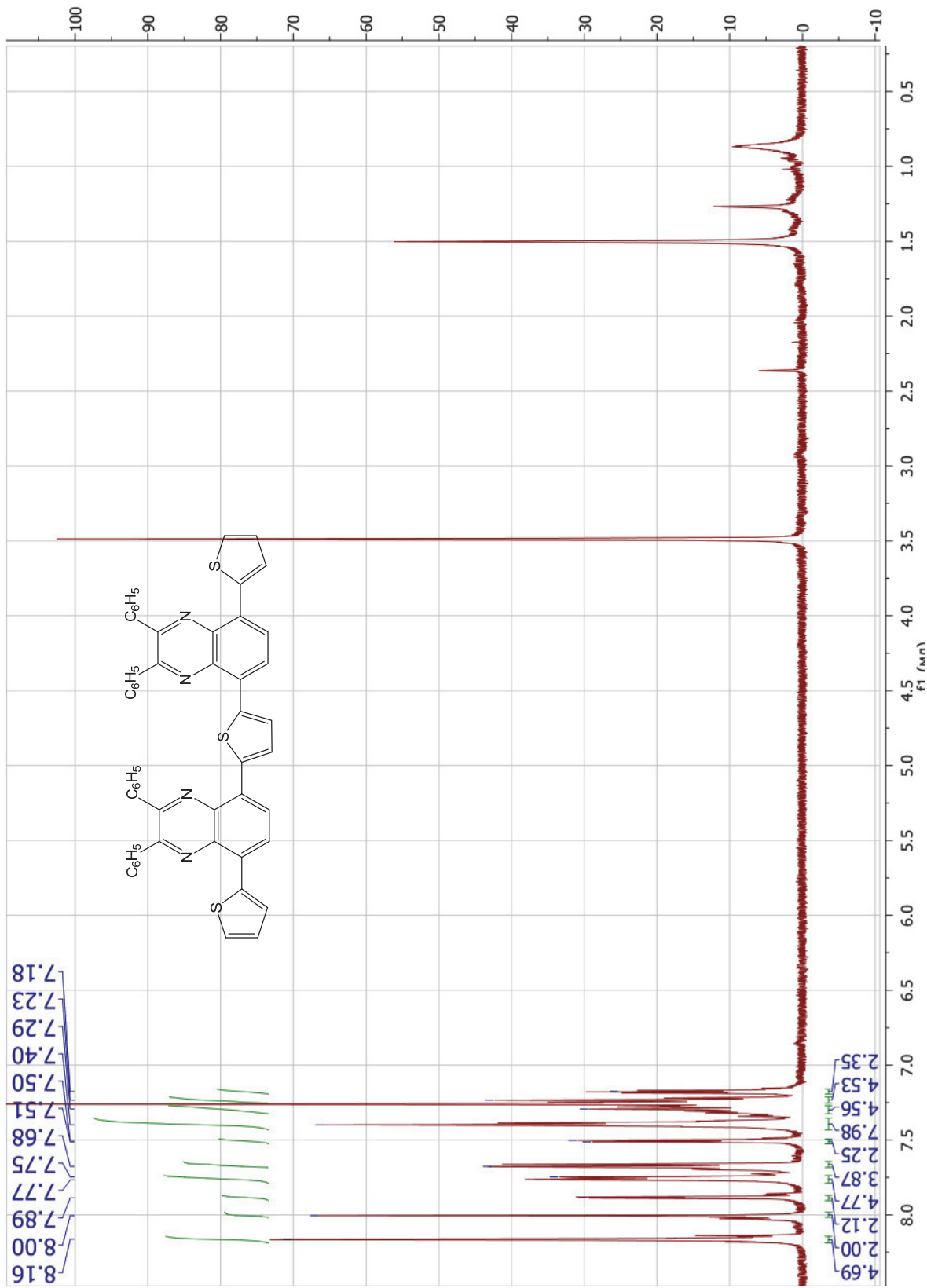


Figure S42.  $^1\text{H}$  NMR spectrum of A7

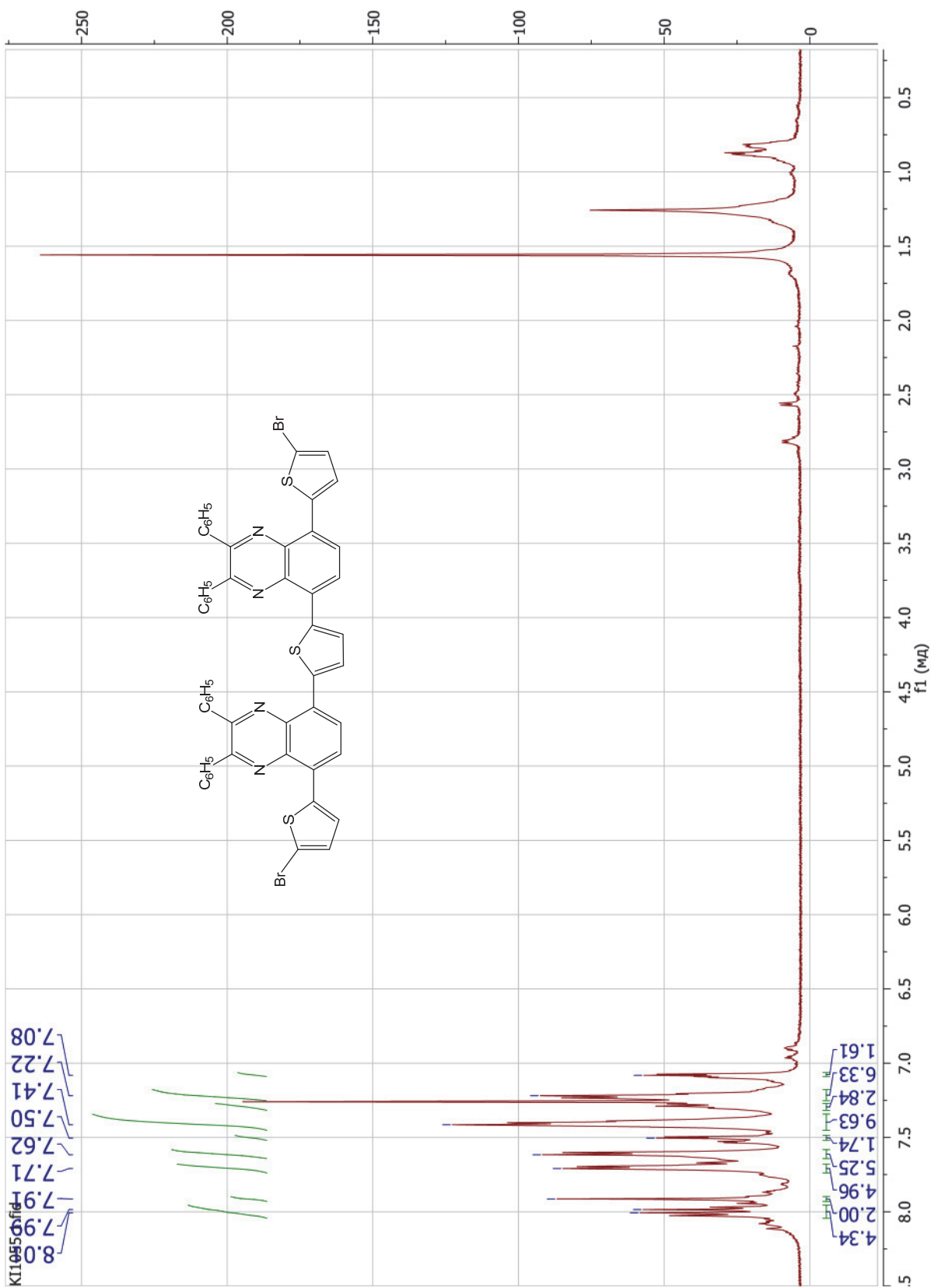


Figure S43.  $^1\text{H}$  NMR spectrum of B7

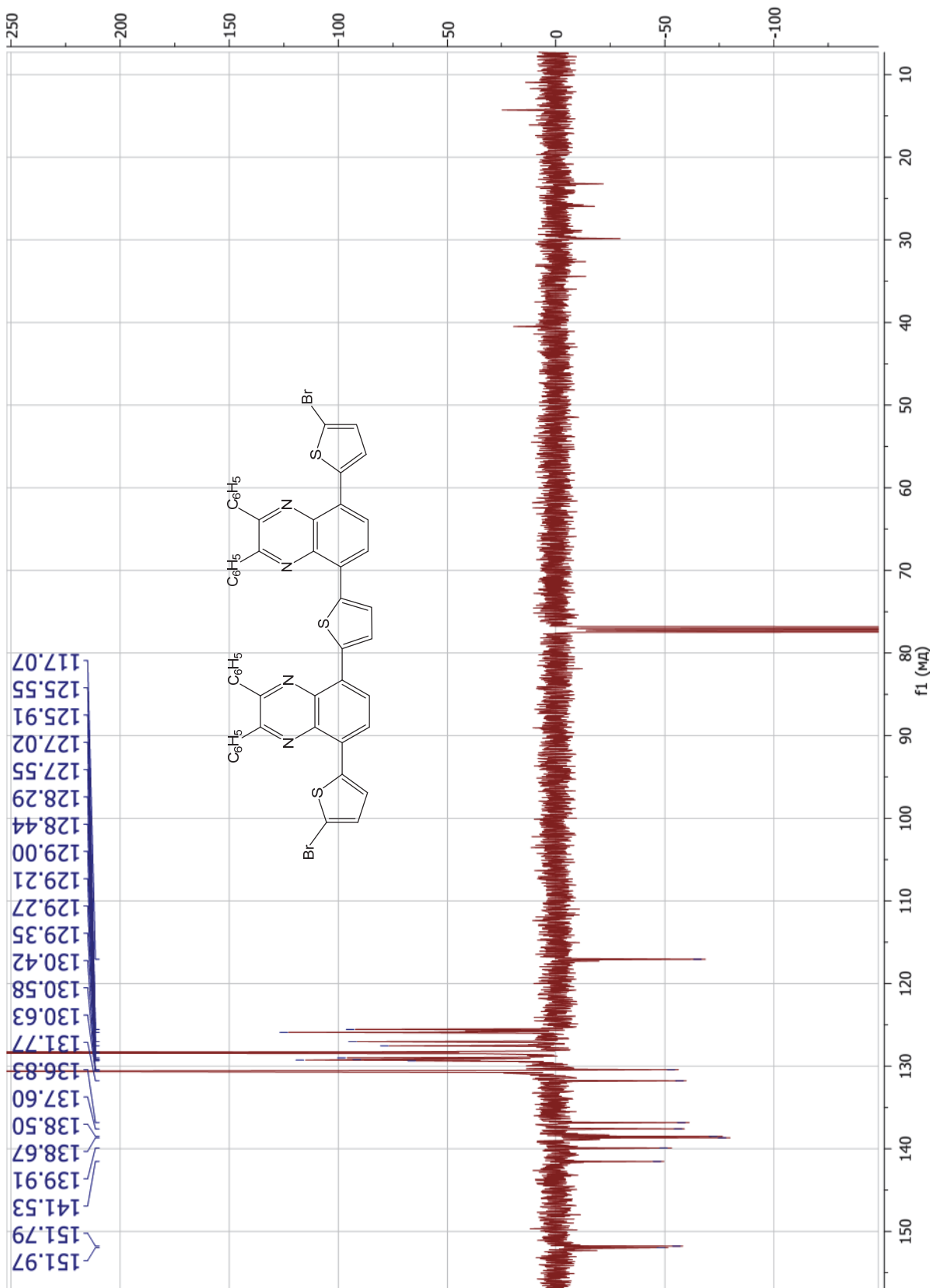


Figure S44.  $^{13}\text{C}$  NMR spectrum of B7

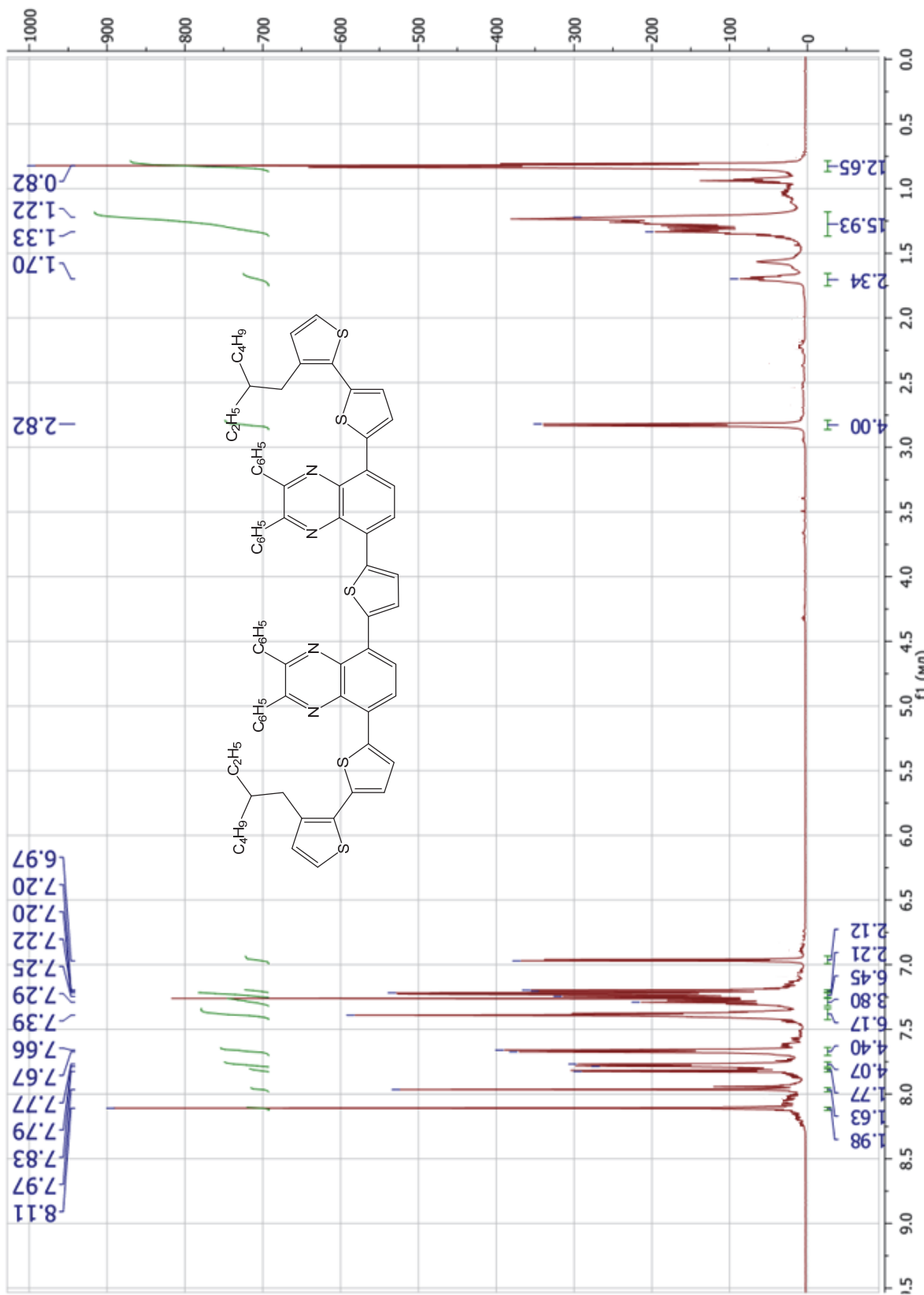


Figure S45.  $^1\text{H}$  NMR spectrum of C7

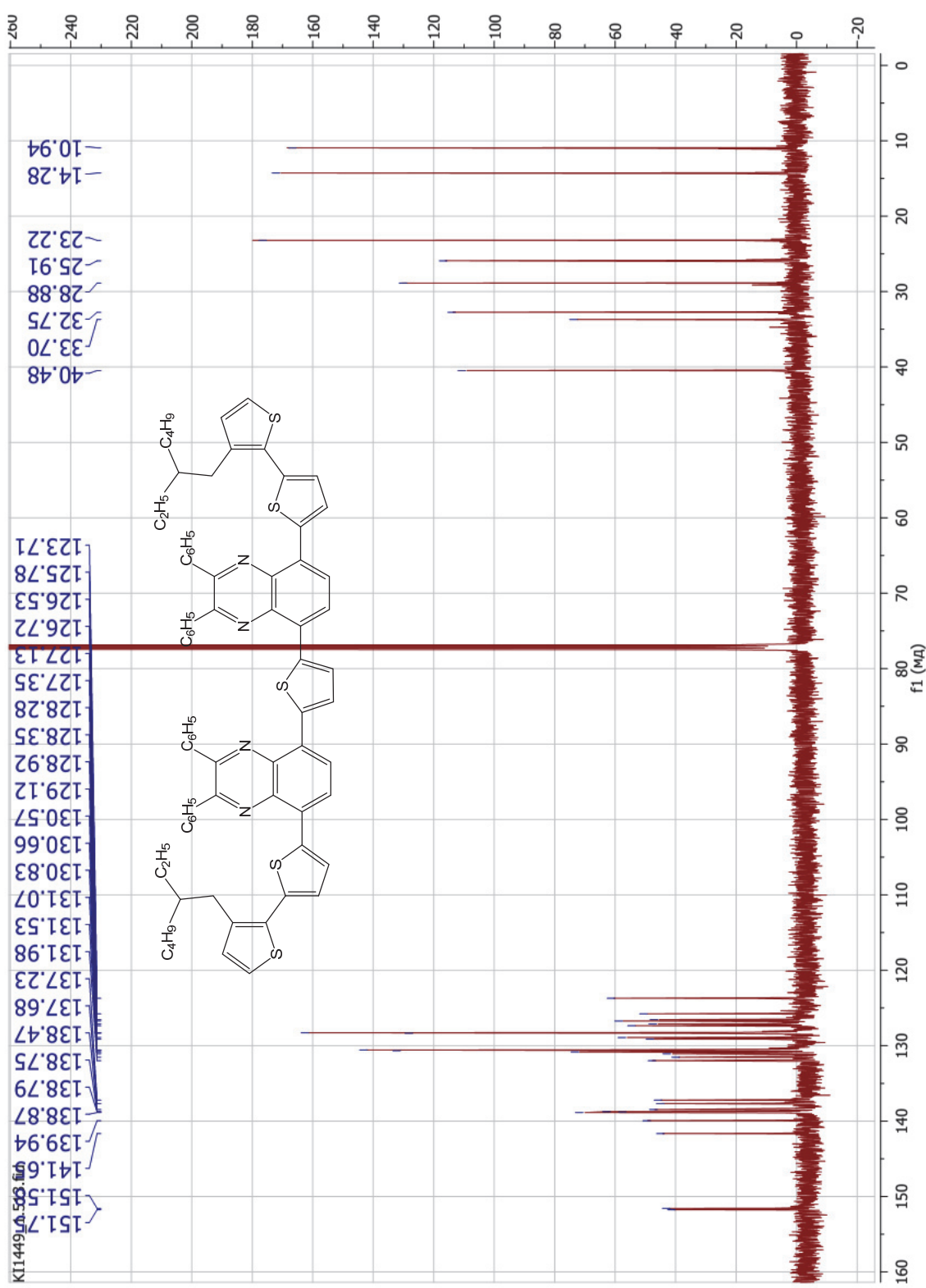


Figure S46.  $^{13}\text{C}$  NMR spectrum of C7

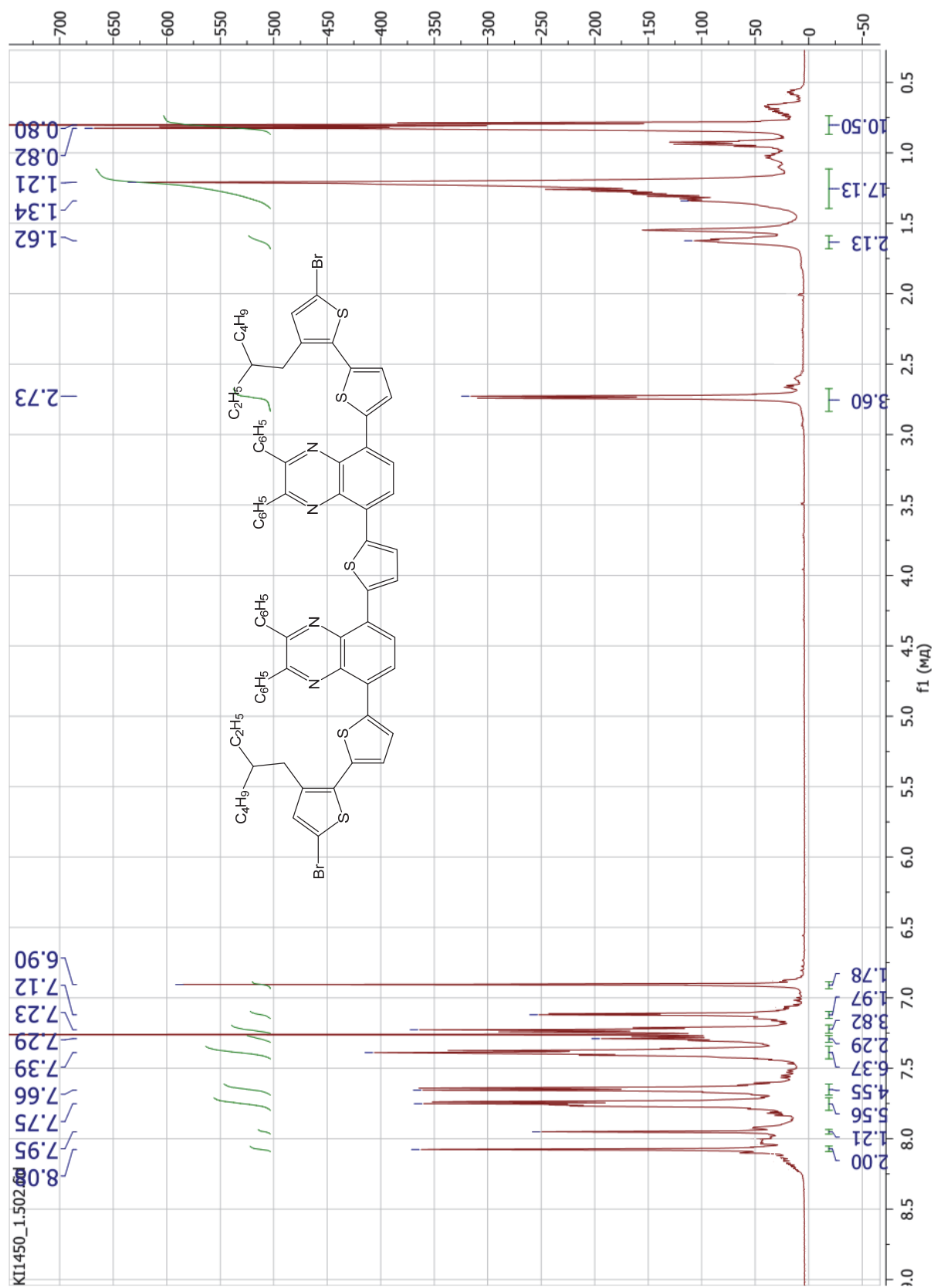


Figure S47. <sup>1</sup>H NMR spectrum of D7

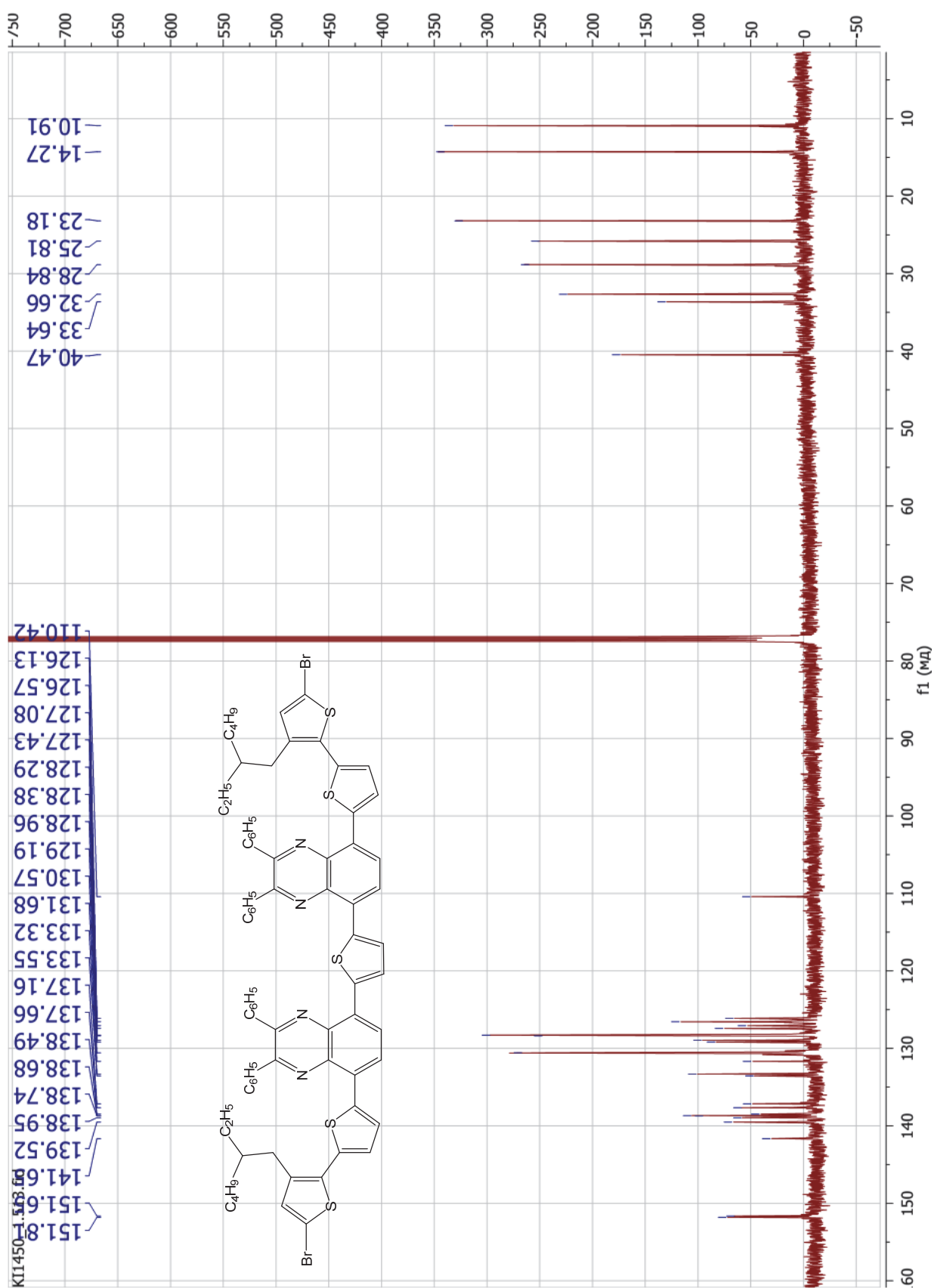


Figure S48.  $^{13}\text{C}$  NMR spectrum of D7

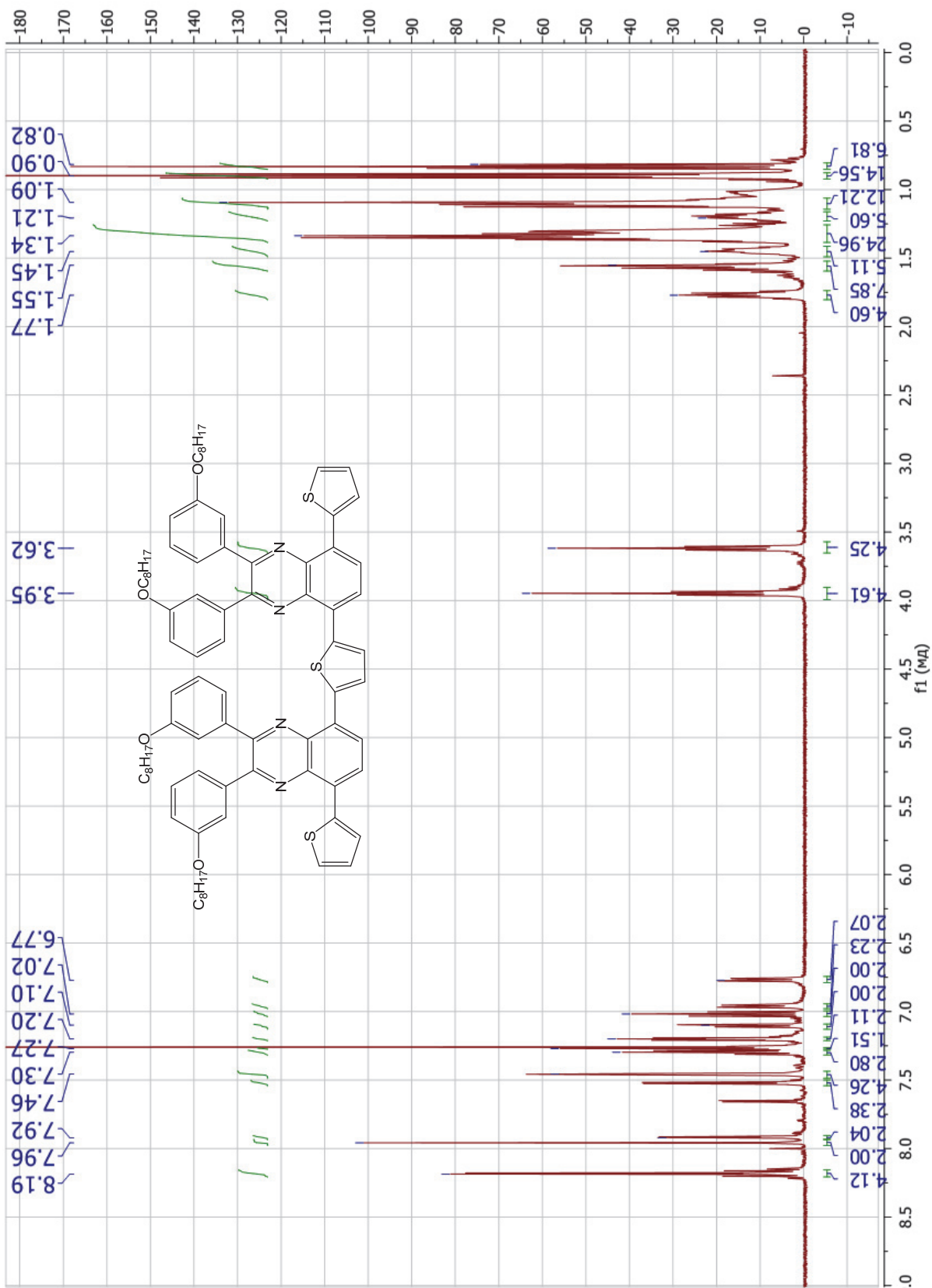


Figure S49.  $^1\text{H}$  NMR spectrum of A8

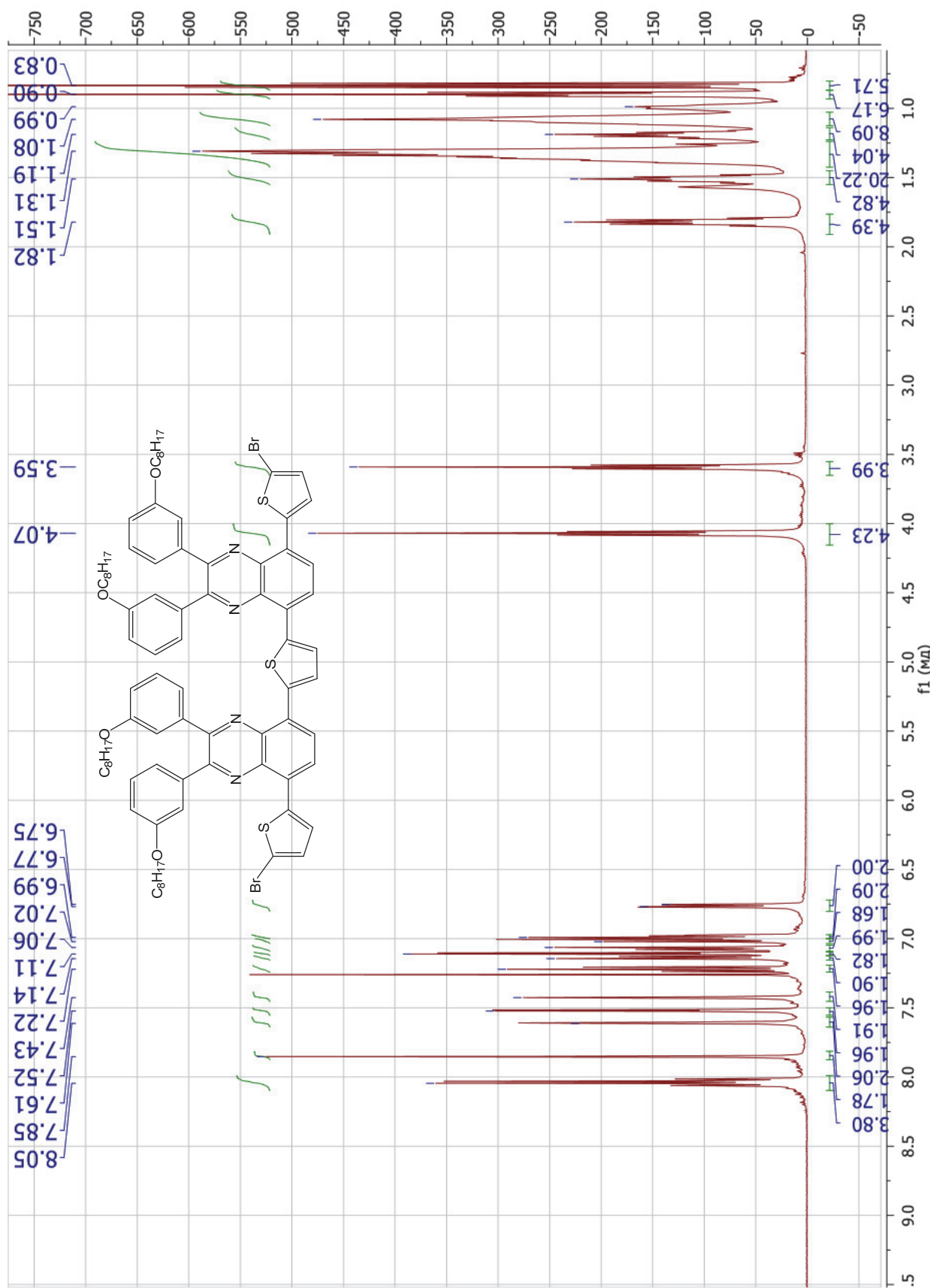


Figure S50.  $^1\text{H}$  NMR spectrum of B8

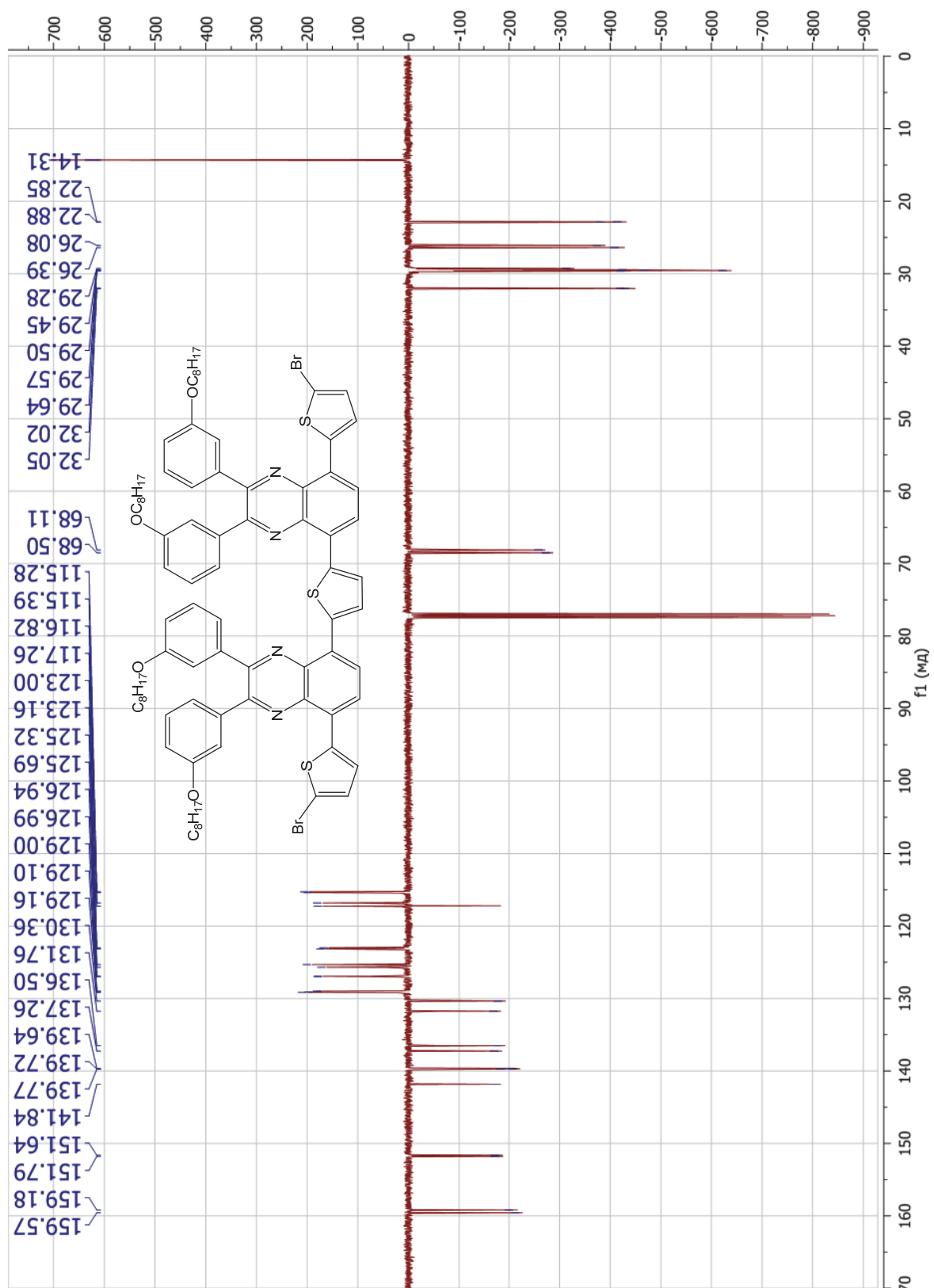


Figure S51.  $^{13}\text{C}$  NMR spectrum of B8

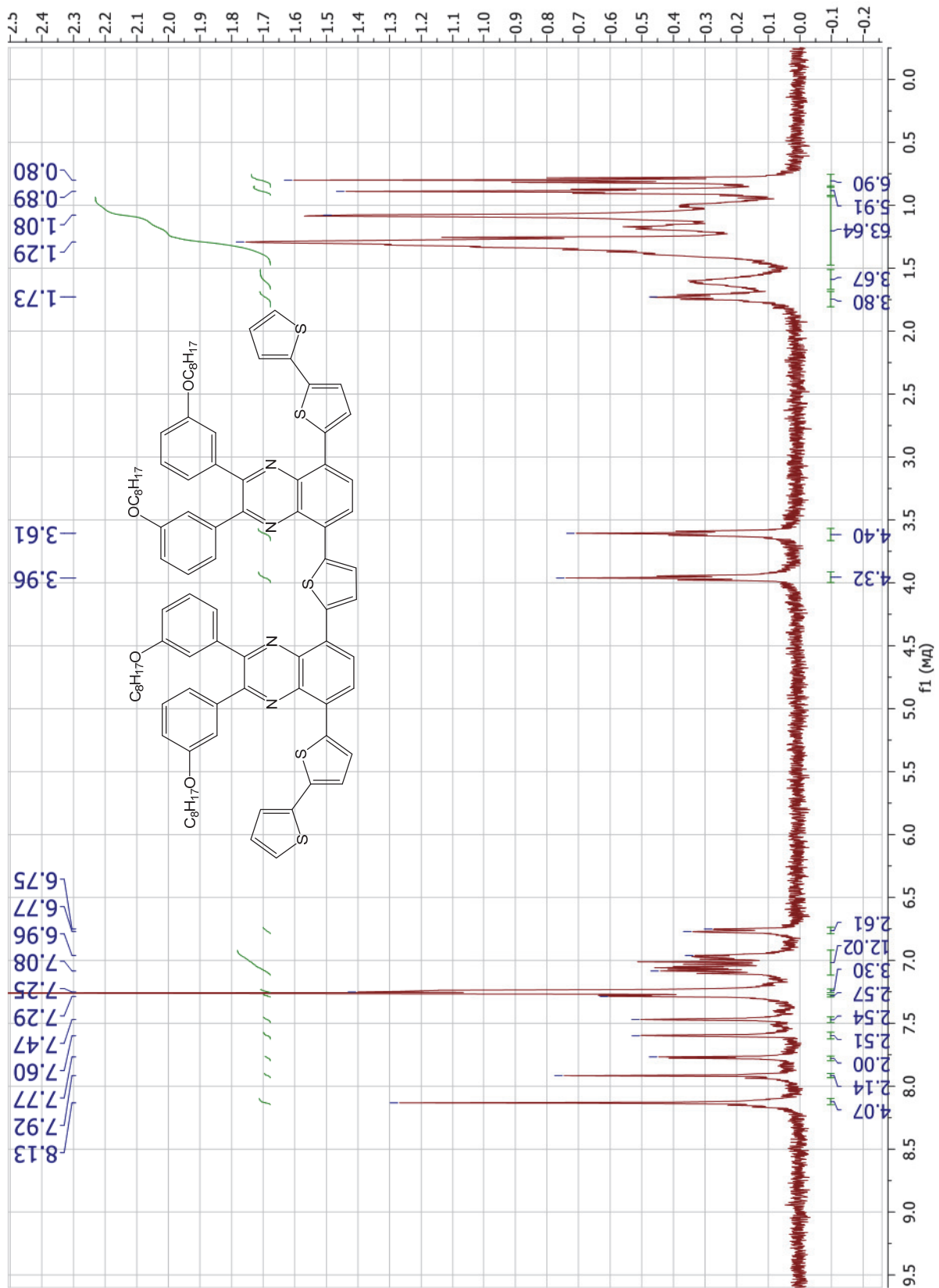


Figure S52.  $^1\text{H}$  NMR spectrum of C8

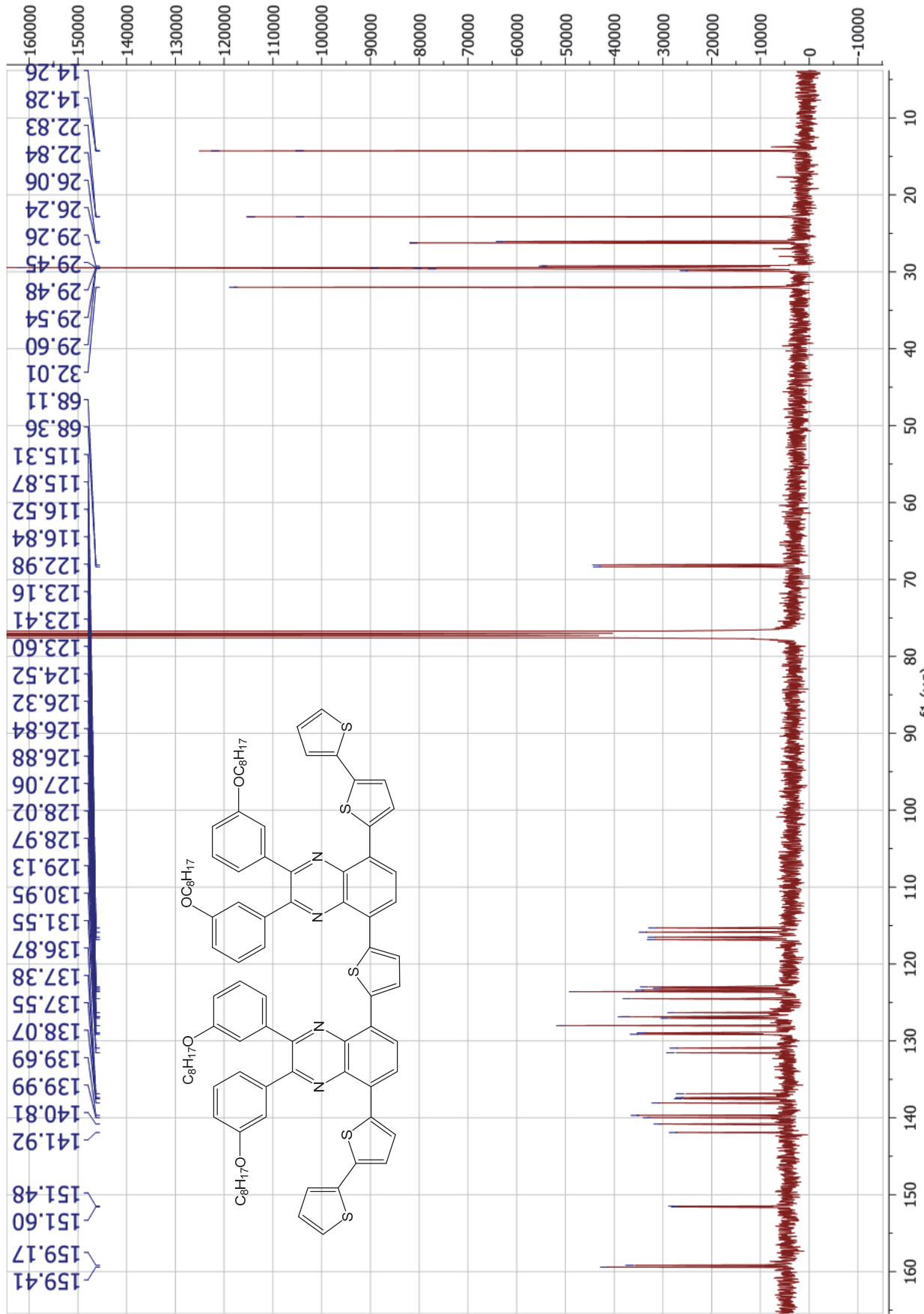


Figure S53.  $^{13}\text{C}$  NMR spectrum of C8

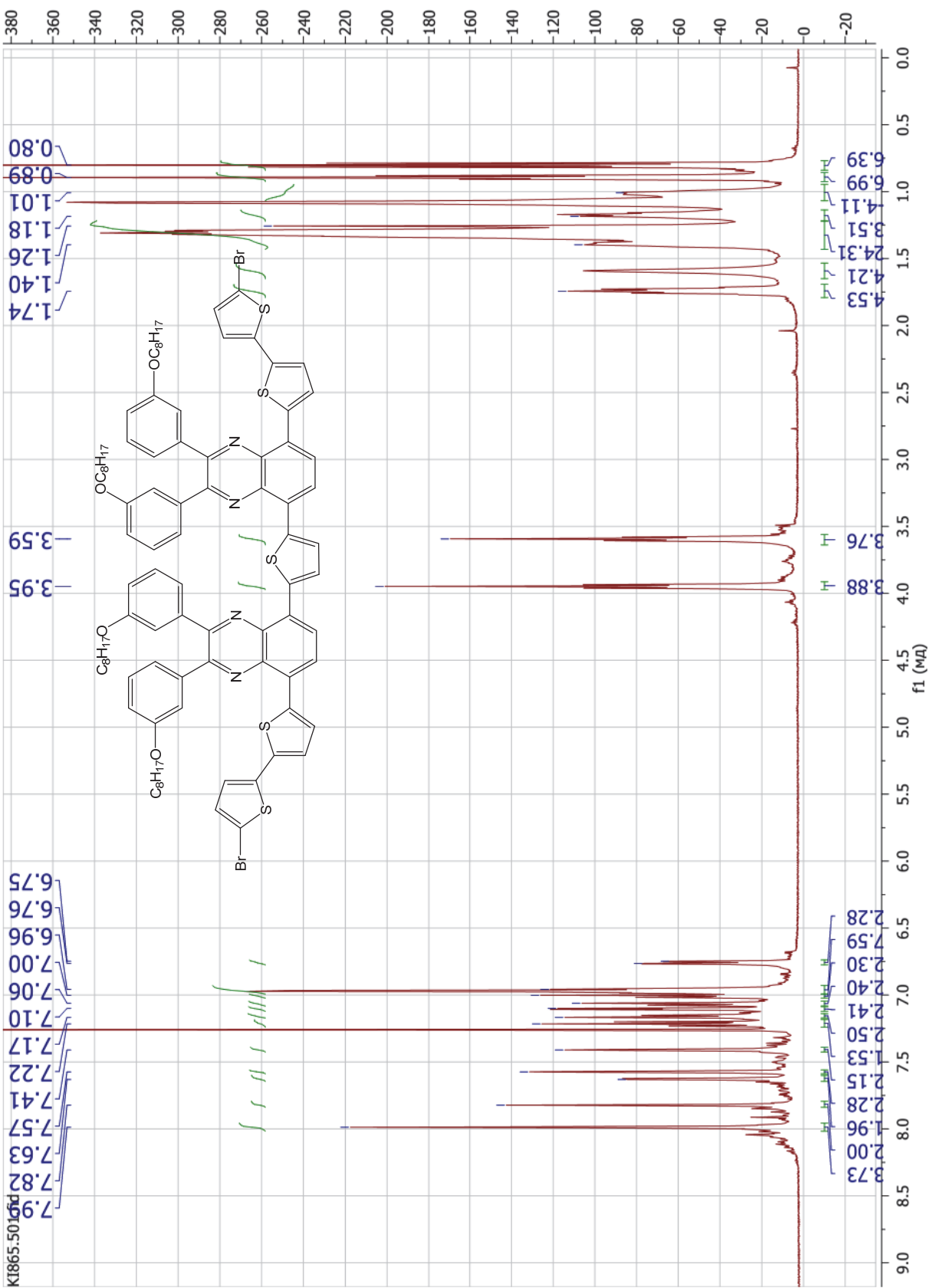


Figure S54.  $^1\text{H}$  NMR spectrum of D8

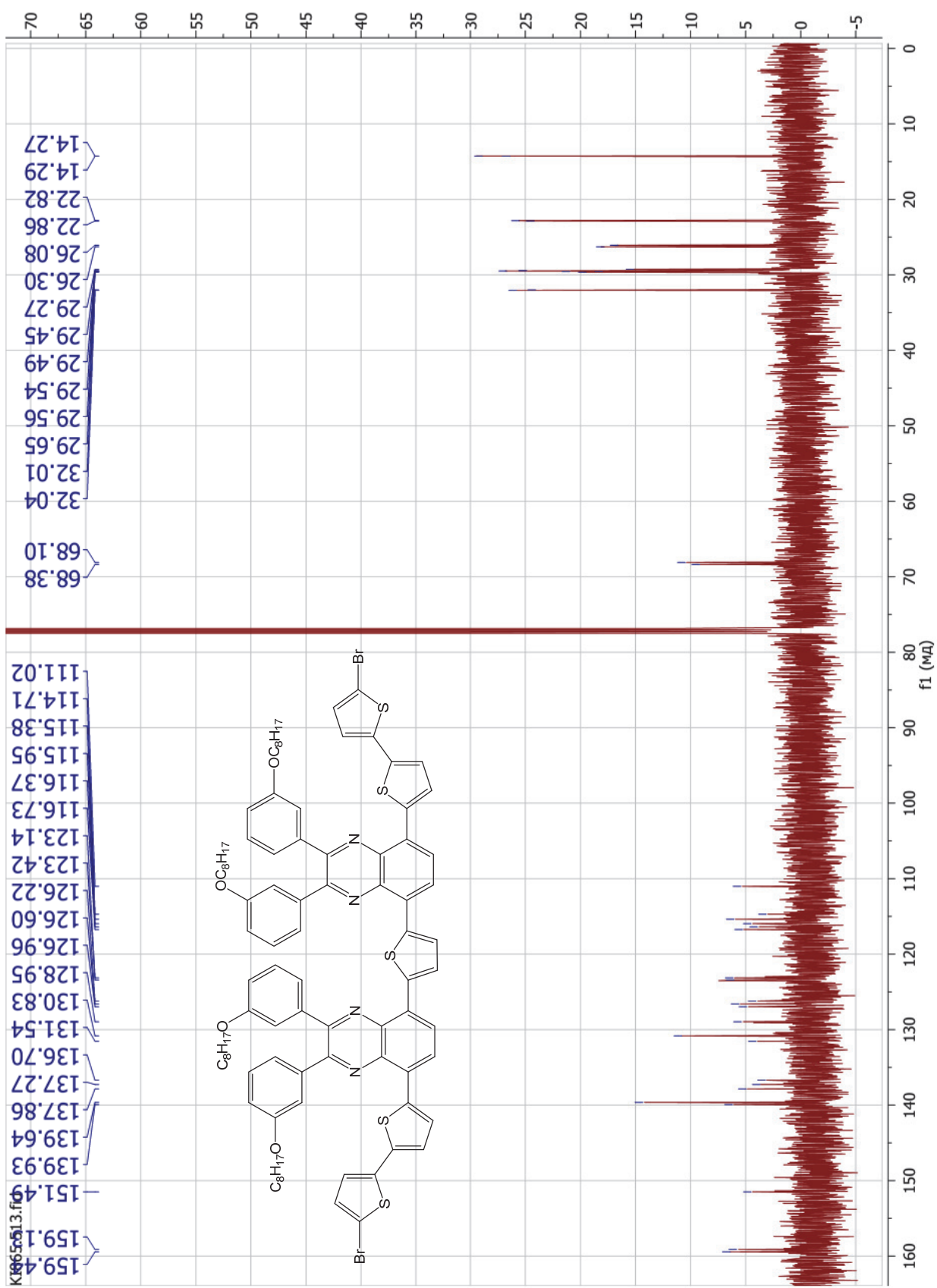


Figure S55.  $^{13}\text{C}$  NMR spectrum of D8

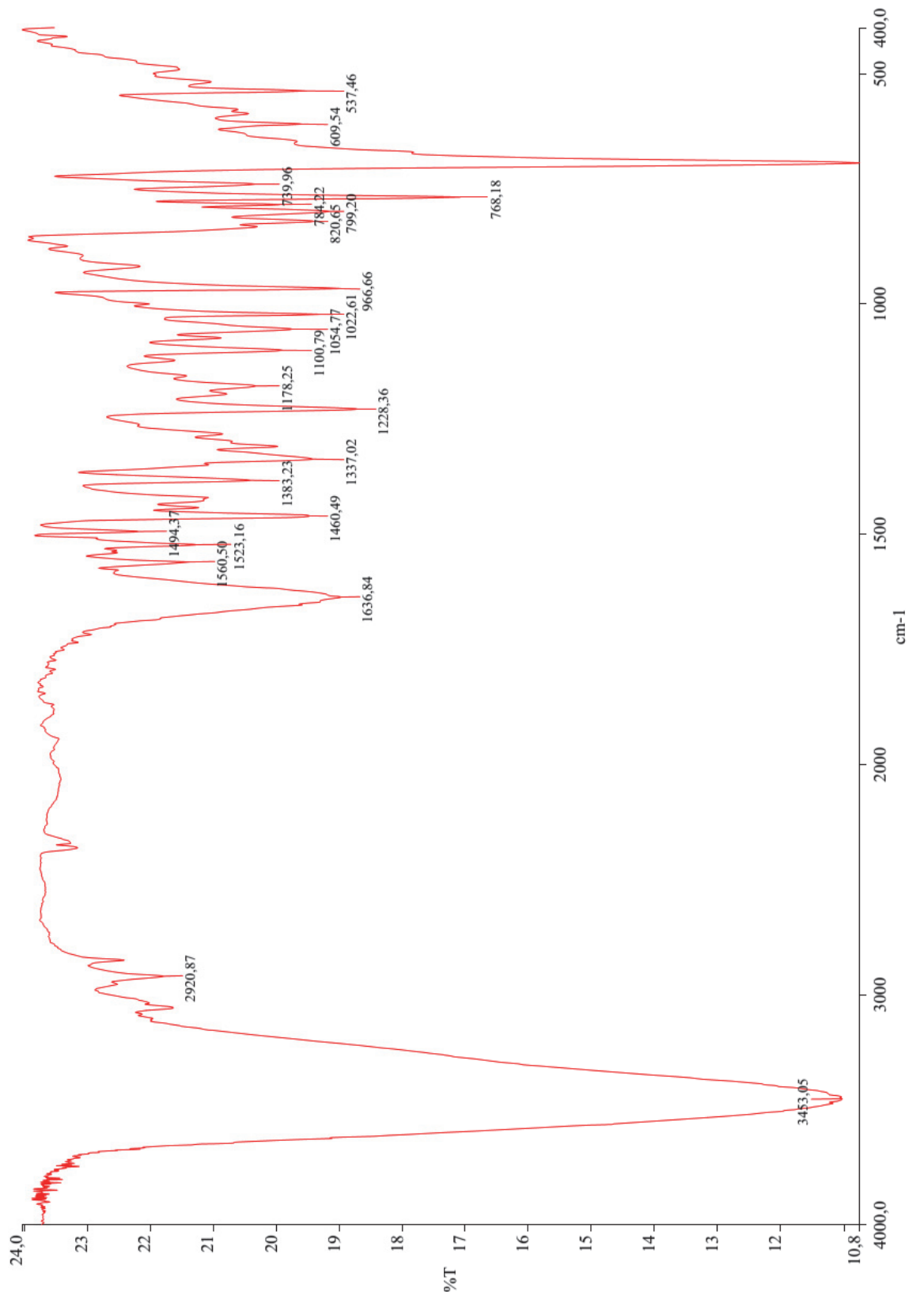
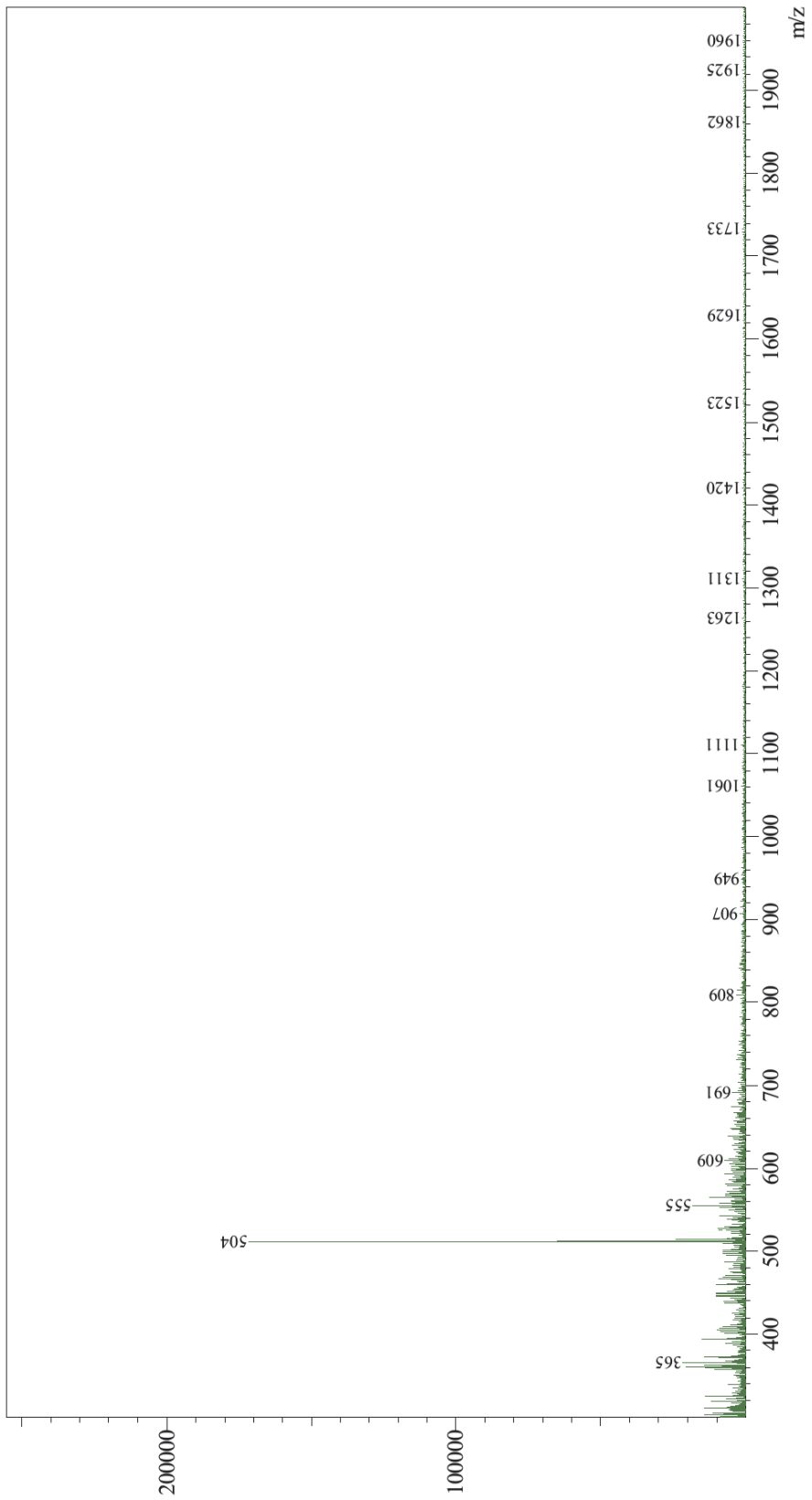


Figure S56. IR spectrum of A6



**Figure S57.** MS spectrum of A6

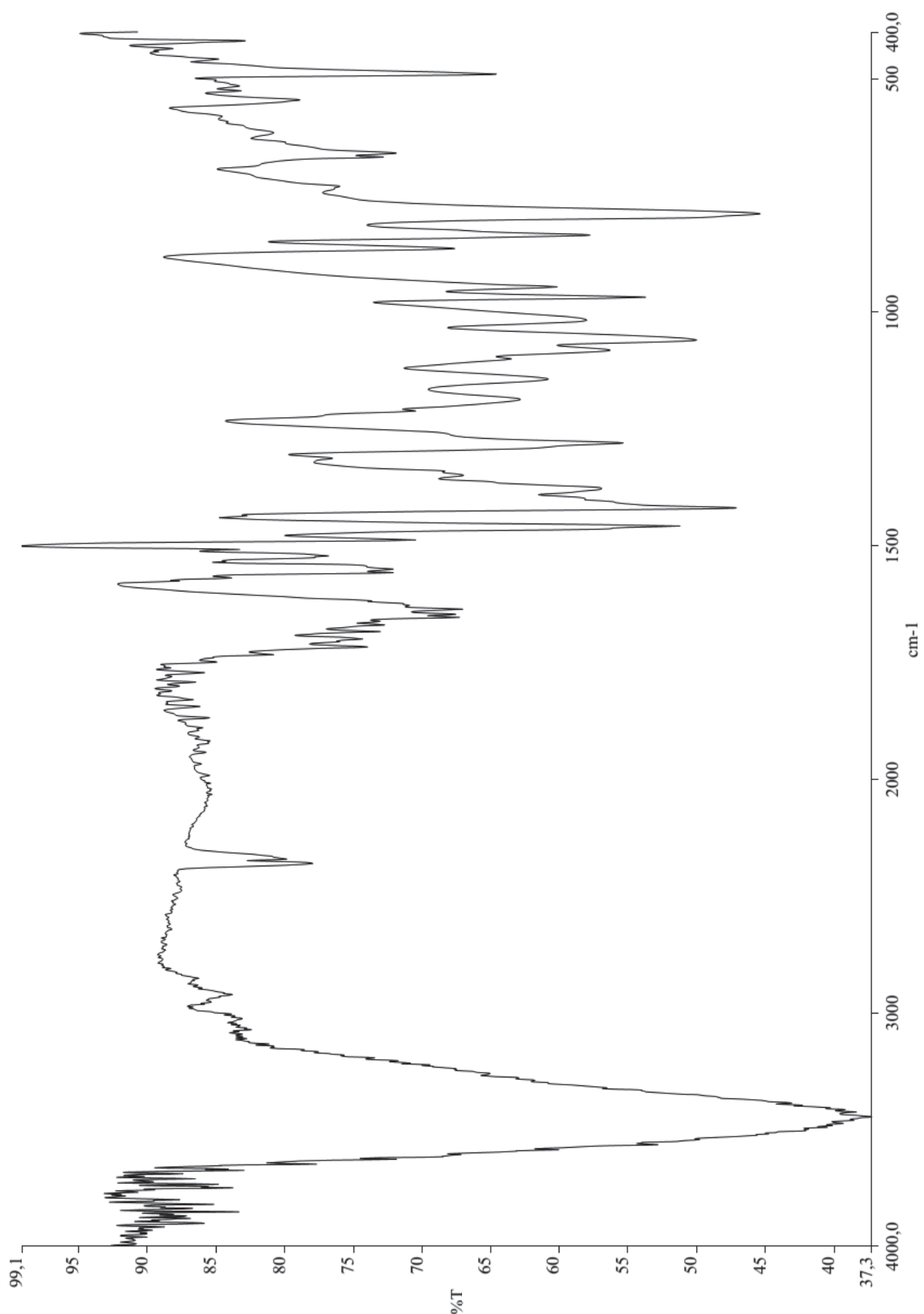


Figure S58. IR spectrum of A7

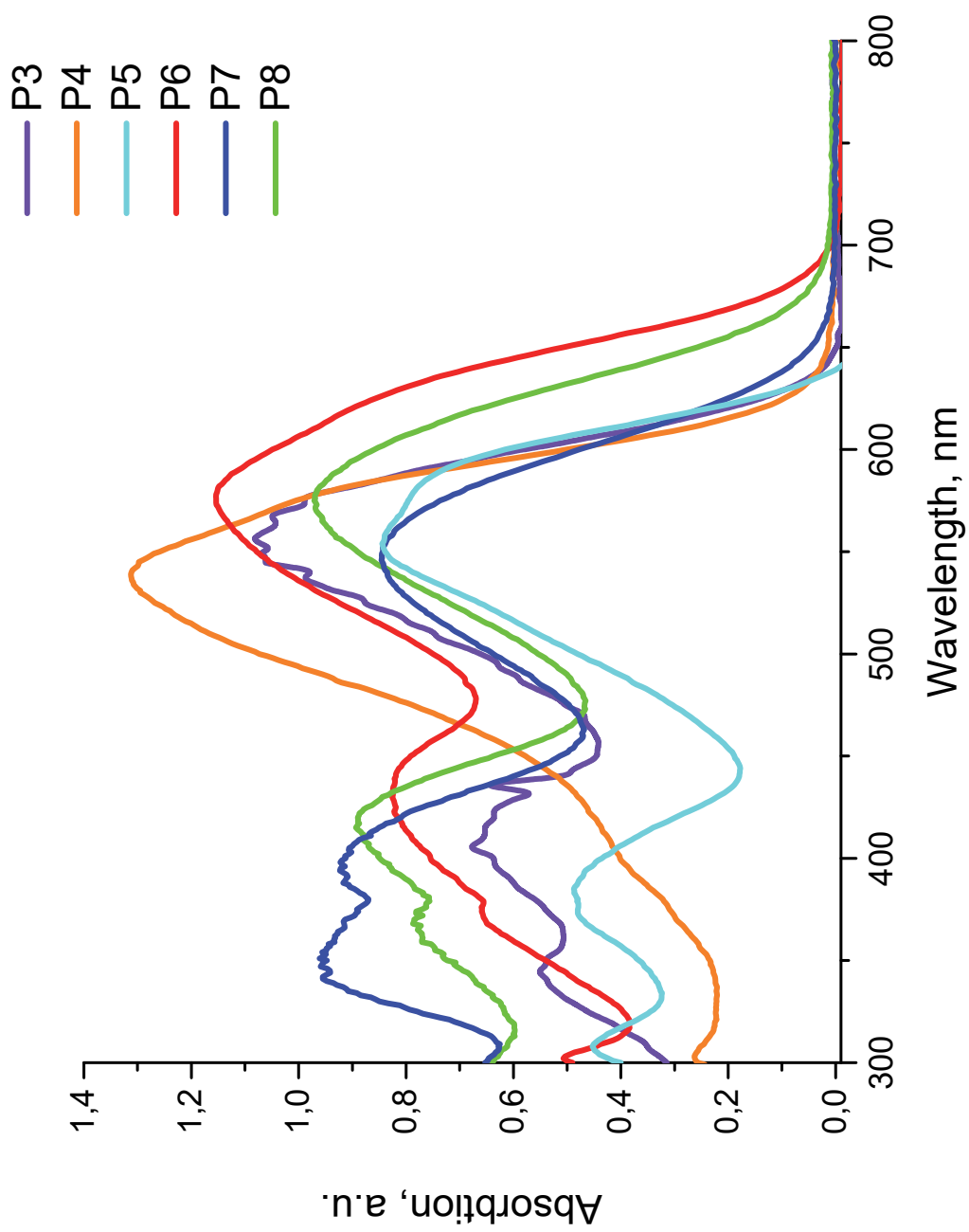


Figure S61. Absorption spectra of polymers **P3-P8** in 1,2-dichlorobenzene

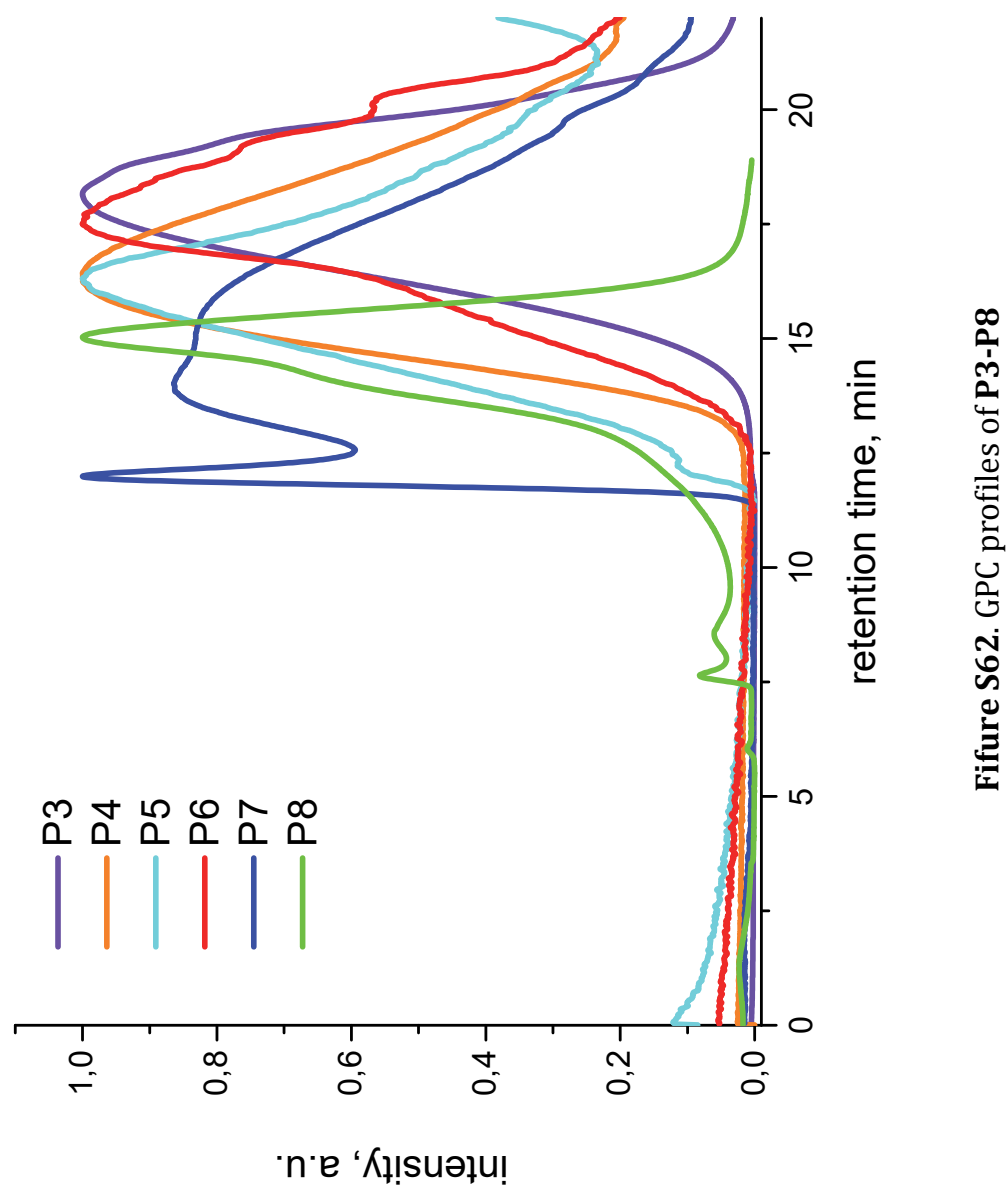


Figure S62. GPC profiles of P3-P8